

EARTHQUAKE EFFECT ANALYSIS OF BURIED PIPELINES IN GUJARAT, INDIA

SUBMITTED BY

INDRANIL GUHA

Under the guidance of

Dr. B.P. PANDEY

Mr. R.P.SHRIWAS

UNIVERSITY OF PEROLEUM AND ENERGY STUDIES
DEHRADUN

Prof. RAUL FLORES BERRONES

MEXICAN INSTITTUE OF WATER TECHNOLOGY
MEXICO

Mr. R.M.GANDHI

GUJARAT GAS COMPANY LIMITED
GUJARAT, INDIA

A REPORT SUBMITTED IN PARTIAL FULFILLMENT OF THE REQUIREMENTS
FOR M.Tech (PIPELINE ENGINEERING)

OF

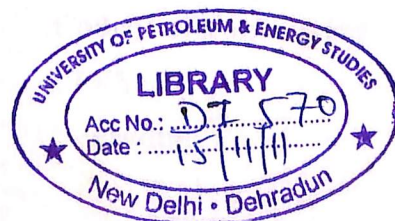
UNIVERSITY OF PETROLEUM AND ENERGY STUDIES

UPES - Library



D1570

GUH-2007MT




COLLEGE OF ENGINEERING
UNIVERSITY OF PETROLEUM AND ENERGY STUDIES
DEHARADUN, INDIA

Date: 16/05/07


18

CERTIFICATE

This is to certify that the project work entitled "EARTHQUAKE EFFECT ANALYSIS OF BURIED PIPELINES IN GUJARAT, INDIA" submitted by Mr. INDRANIL GUHA in partial fulfillment of the requirement for the award of degree of Masters of Technology (Pipeline Engineering), at College of Engineering, University of Petroleum & Energy Studies, Dehradun is a record of the work carried out by him under our supervision and guidance.


18/05/2007

R.P. Shriwas
Course Coordinator
Pipeline Engineering Department
UPES
Dehradun


18/05/07

Dr B.P. Pandey
Dean
College of Engineering
UPES
Dehradun

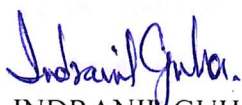
ACKNOWLEDGMENT

This is to acknowledge with thanks the help, guidance and support that I had received during the training.

I owe my deep gratitude and sincere thanks to my guide, **Mr. R.P. Shriwas**, Course Coordinator, Pipeline Engineering Department, UPES, Dehradun for his valuable guidance and continuous encouragement which gave me an opportunity to explore myself by taking his profound insights. I express my special indebtedness to them for their sustained interest during the preparation of this book.

I express my gratefulness to **Dr. B.P. Panday**, Dean, College of Engineering, UPES, Dehradun and **Prof Raul Flores Berrones** (Institute of Water Technology, Mexico) for their encouragement and valuable guidance during this project.

I have no words to express a deep sense of gratitude to the management of Gujarat Gas Company Limited for giving me an opportunity to pursue my project and in particular **Mr. R.M. Gandhi (Manager, Project)**, **Mr. B.R. Patel (ASSO. MGR.)**, for their able guidance and support.



INDRANIL GUHA
M.Tech (Pipeline Engineering)
University of Petroleum and Energy Studies
Dehradun.

ABSTRACT

Pipelines have been acknowledged as the most reliable, economic & efficient means for the transportation of water and other important commercial fluids such as oil and fuel gases. The designation of pipeline systems as “Lifelines” signifies that their operation is essential in maintaining the public safety and well being. A pipeline transmission system is a linear system which traverses a large geographical area, and soil conditions thus, is susceptible to a wide variety of seismic hazards. Ruptures or severe distortions of the pipeline are most often associated with relative motion arising from fault movements, landslides, liquefaction, loss of support, or differential motion at abrupt interfaces between rock and soil. Notably the most catastrophic damages are the ones resulting from faulting or ground rupture. Owing to these facts the performance of buried and aboveground pipeline structures subjected to faulting and other seismic hazards have become important subject of study. Soil-Pipeline interaction has always been a major consideration in such studies and analysis. The present dissertation report gives the details of attempt to study the behaviour of pipelines against major seismic hazard i.e. faulting (or ground rupture). The study is based on the Finite Element Analysis carried out using “ANSYS” software package. As a matter of fact, the study of affect of fault crossing is most crucial for the case of buried pipelines. Representative model of a buried pipeline along with the surrounding soil was modeled and fault rupture was simulated using appropriate boundary conditions. Herein soil was modeled using springs with an equivalent stiffness characteristics. Nonlinear behaviour of the soil was incorporated into the equivalent soil spring models. As most of the previous analyses have been carried out on models using elastic beam elements, initial model of the pipe was done using similar elements. The analysis was then extended to study the effect of various parameters such as magnitude of fault displacement, pipe diameter, thickness, material & cover depth. Many important aspects of the pipe behavior came to surface. It was observed that all of those could be explained by effect of the parameters on stiffness of pipe and/or soil. Behavior of pipeline under the soil liquefaction has also been tested and at the end few recommendations are made.

In the first two chapters the literature survey and the related works along with the basic theories have been discussed. Then from fourth chapter onwards effect of fault crossing on the pipeline, parametric analysis and effect of buoyant force on the buried pipelines have been analyzed.

CONTENTS

Page No

| | |
|--|----------|
| Chapter 1: Introduction | 7 to 9 |
| 1.1 Pipelines | |
| 1.2 Seismic Hazard | |
| 1.3 Indian Context | |
| 1.4 Objective & Scope of Seismic Analysis | |
| Chapter 2: Literature Review for Fault Crossing Covering: | 10 to 25 |
| 2.1 Faulting | |
| 2.2 Past Seismic Performance of Pipelines | |
| 2.3 Pipeline Behaviour under Fault Movement | |
| 2.4 Analytical Work So Far | |
| 2.5 Pipeline Soil Interaction | |
| Chapter 3: Literature Review for Buoyancy Force on Buried Pipelines Due to Soil Liquefaction Covering: | 26 to 39 |
| 3.1 How Does Soil Liquefaction occurs | |
| 3.2 Conditions of Soil Liquefaction | |
| 3.3 Soil Pipeline Interaction | |
| 3.4 Summary of Past Performance of Pipeline Under Soil Liquefaction | |
| 3.5 Gujarat Earthquake 2001 | |
| 3.6 Effect of Soil Liquefaction on Buried Pipelines | |
| <u>Project work details</u> | |
| Chapter 4: Modelling of Pipeline Under Fault Movement Covering | 40 to 53 |
| 4.1 Description of Representative Data | |
| 4.2 Finite Element Modelling | |
| 4.3 Results | |
| Chapter 5: Parametric Analysis Covering | 54 to 62 |
| 5.1 Data for Parametric Study | |
| 5.2 Finite Element Modelling | |
| 5.3 Results | |
| Chapter 6: Buoyancy Force Effect on Buried Pipelines Covering | 63 to 69 |
| 6.1 Design Criteria for Buoyancy due to liquefaction | |
| 6.2 Buoyant Force on Pipeline | |
| 6.3 Bending Strain in the Pipeline due to buoyancy | |

| | |
|---|-----------|
| Chapter 7: Discussion | 70 to 73 |
| 7.1 Discussion from Fault Crossing Modeling | |
| 7.2 Discussion from Parametric Modeling | |
| Chapter 8: Summary and Conclusions | 74 to 77 |
| Chapter 9: Recommendation | 78 to 81 |
| 9.1 Recommendation for Fault Crossing | |
| 9.2 Recommendation for Liquefaction | |
| References | 82 |
| APPENDIX | 83 to 113 |

1. INTRODUCTION

1.1 Pipelines

Pipeline system consists of buried and above ground pipelines, above ground facilities such as pumping stations, storage tanks and miscellaneous terminal facilities. However the term pipeline in general implies a relatively large pipe spanning a long distance. They generally have a minimum diameter of 0.1 m and a minimum length of 1.6 km. Few of the largest and longest pipelines may have a diameter of over 3.0 m and a length of over 1600 km. Pipelines have been acknowledged as the most reliable, economic & efficient means for the transportation of water and other important commercial fluids such as oil and fuel gases.

An extensive network of underground pipelines exists in every city, state, and nation to transport water, sewage, crude oil, petroleum products (such as gasoline, diesel or jet fuel), natural gas, and many other liquids and gases. Increasingly, pipelines are being used for transporting solids including minerals (such as coal, iron ore etc.); construction materials (sand, crushed rock, cement, and even wet concrete); radioactive materials; and hundreds of other products. As highways and streets become increasingly congested, and as the technology of transportation through pipelines continues to improve, they are becoming indispensable and the preferred mode for the transportation of products as outlined earlier. Underground transportation by pipelines not only reduces traffic on highways and streets, but also reduces noise and air pollution, apart from chances of accidents. It also minimizes the use of surface land. Thus pipelines perform vital functions as in a sense they serve as arteries, bringing life-dependent supplies such as water, petroleum products, and natural gas to consumers through a dense underground network of transmission and distribution lines. They also serve as veins, transporting life-threatening waste generated by households and industries to waste treatment plants for processing via network of sewers. The designation of pipeline systems as "*Lifelines*" signifies that their operation is essential in maintaining the public safety and well being.

1.2 Seismic Hazard

A pipeline transmission system being a linear system which traverses a large geographical area, and soil conditions thus, is susceptible to a wide variety of seismic hazards. The major seismic hazards which significantly affect a pipeline system are: i) ground failure, ii) ground motion and iii) others miscellaneous effects. While ground failure includes faulting, liquefaction and earthquake induced landslides, tsunamis, and other affect of supporting and surrounding structures are usually placed under miscellaneous hazards. Ruptures or severe distortions of the pipeline are most often associated with relative motion arising from fault movements, landslides, liquefaction, loss of support, or differential motion at abrupt interfaces between rock and soil. Notably the most catastrophic damages are the ones resulting from faulting or ground rupture. Owing to these facts the performance of buried and aboveground pipeline structures subjected to faulting and other seismic hazards have become important subject of study.

1.3 Indian Context

Currently, India has 7,000 km of pipelines. The oil and gas pipeline infrastructure is being accorded top priority by the nation's planners and a network of these pipelines criss-crossing the nation has been planned. The pipeline market itself is estimated to be around Rs 20,000 crore over a period of five-six years. The National Gas Grid being implemented by GAIL (India) Ltd, which is expected to take three-four years to reach completion, will lay a 17,000 km pipeline network. The proposed oil pipeline network, on the other hand, is expected to build a pipeline network spanning over more than 5,000 km. These projects will give an enormous boost to the pipeline demand in the country.

Notably, India has had more than five moderate earthquakes (Richter Magnitudes ~6.0-7.5) since 1988. As noted in IS 1893 Himalayan-Nagalushai region, Indo-Gangetic Plain, Western India, Kutch and Kathiawar regions are geologically unstable parts of the country, and some devastating earthquakes of the world have occurred there. A major part of the peninsular India has also been visited by strong earthquakes.

From the past seismic performance of pipelines in various other countries it can be noted that the consequences of pipeline failure due to earthquakes could be an exaggerated one, particularly so for India, both in terms of economic and social aspects. Thus implementing the seismic design considerations at the current phase of Indian pipeline scenario is absolutely essential.

1.4 Objective and Scope of Seismic Analysis

Noting the feeble possibilities, if any, of the experimental studies in the area of pipelines analytical seismic qualification studies of the pipeline systems such as one presented here will help in following ways:

- a) Better understanding of the behaviour of pipelines under varied seismic hazards.
- b) Outlining the basic approach of modeling and analysis for such systems.
- c) To carry out the analysis of existing systems and propose modifications for improved earthquake performance.
- d) In designing the proposed pipeline systems against possible earthquake hazards.

2. LITERATURE REVIEW

2.1 Faulting

Faulting is the deformation associated with the relative displacement of adjacent parts of earth's crust. Ground ruptures can occur over an extended length of the fault, the length and amount of surface rupture depends mainly on the magnitude of the earthquake and focal depth.

Faults are classified on the basis of slip (direction of movement) or their angle of dip with respect to the ground surface and their attitude relative to adjacent beds. In general, depending upon the predominant component of movement, faults are classified as being strike-slip, normal-slip, or reverse-slip. In many cases faults exhibit a combination of two types of movements and are termed as oblique slip.

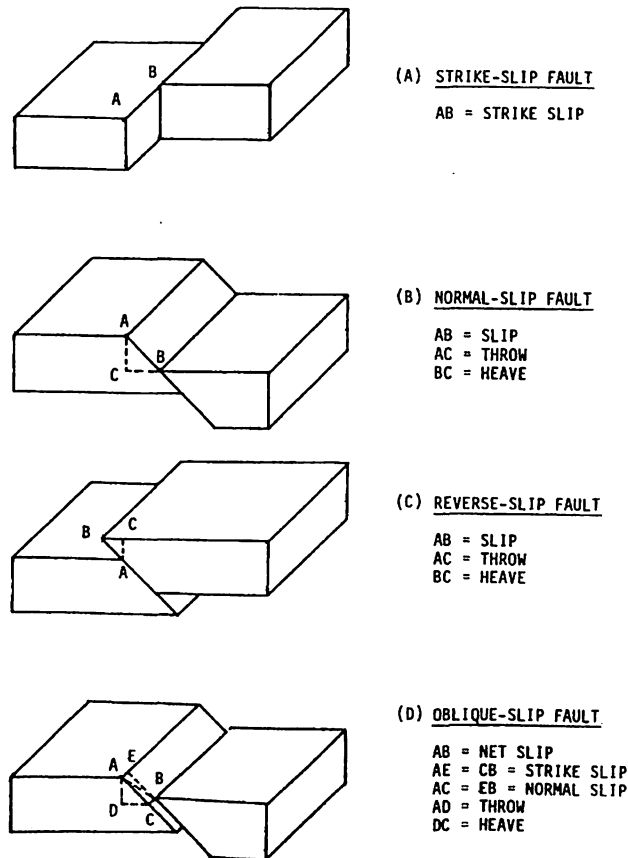


Fig. 2.1.1 Types of Faulting

Figure 2.1.1 illustrates the types of fault movement. For the purpose of illustration, the faults are represented as a single plane on which relative movement between each side of fault occurs. A strike slip fault is one in which the predominant component of movement is a horizontal displacement. If the movement of one side of the fault when viewed from the other side is to the right, the fault is called right lateral strike-slip fault. Conversely, when the movement is to the left, the fault is called a left lateral strike-slip fault. Normal-slip and reverse-slip faults are those in which the overlying side moves downward and upward, respectively, with respect to the underlying side of the fault. A low angle reverse-slip fault (whose plane of movement is oriented less than 45° with the horizontal) is often referred to as an oblique-slip fault. The amount of horizontal shortening or lengthening in the plane perpendicular to the fault is referred to as heave. The vertical offset measured in the same plane is referred to as throw.

Along with the type of fault amount of fault displacement is an important consideration for design. Many empirical formulas have been developed from past observations which predict the amount of ground displacement. The amount of surface displacement due to surface fault rupture can be estimated using models such as those provided by Wells and Coppersmith [1].

$$\log(MD) = -5.26 + 0.79M \quad (2.1a)$$

where, M is the moment magnitude and MD is the maximum displacement, in inches.

Most fault offset models provide a median estimate of the maximum displacement along the length of the fault for a given magnitude earthquake. A dispersion estimate of the amount of fault offset is usually provided with the model. But in general fault offset will vary along the length of the surface rupture from zero inches to the maximum amplitude. Given this variation, it is recommended that the maximum displacement from such models be varied along the length of the fault, from zero to the maximum, with an expected value of some percentage of the maximum displacement.

2.2 Past Seismic Performance of Pipelines

Understanding the behavior and possible failure mechanisms of a lifeline structure is important in the development of a design criterion for safe operation. Part of understanding the performance of a lifeline structure in earthquakes involves understanding the design from which the structure was constructed and the affect of different types of construction practice used in its erection. A summary of recent lifeline experiences during earthquakes follows.

2.2.1 Pipeline Performance during Past Earthquakes [2]

- a) *1971 San Fernando Earthquake*: It resulted in direct losses to the pipeline systems by damaging a 1.24 m diameter water pipeline at nine bend and welded joints. Ductile steel pipelines were able to withstand ground shaking but could not withstand ground deformation associated with faulting and lateral spread. Eleven transmission pipelines were damaged by liquefaction induced lateral spread and landslides. Eighty breaks occurred to the underground welded steel transmission pipeline located in the upper San Fernando Valley, the most serious in an old oxyacetylene-welded pipeline. Although located in an uplift zone the failure was caused by compressive forces wrinkling the pipe.
- b) *1983 Coalinga Earthquake*: It caused numerous breaks in the natural gas line but fires did not occur since the main valve was closed manually shortly after the earthquake. Several pipeline failures occurred in oil drilling and processing facilities. In general it was noted that most pipe breaks occurred at pipe connections.
- c) *1987 Whittier Narrows Earthquake*: Damages during this earthquake were usually limited to sections that were corroded or anchored at two locations which experienced large lateral relative displacement. Southern California Gas reported 1411 gas leaks were directly caused by the earthquake. Portions of the California State University, Los Angeles were without gas for 12 weeks. Five fires were reported; three of these were attributed to gas leaks.
- d) *1989 Loma Prieta Earthquake*: This Magnitude 7.1 earthquake caused failure of many pipelines. Damage consisted primarily of broken water lines. Broken waterlines occurred at the Ford plant from liquefaction and excessive soil pressures. At the Port of Oakland located on the east side of the San Francisco Bay on fill all water lines broke and fire lines ruptured eliminating fire fighting protection.
- e) *1992 Big Bear Earthquakes*: Two earthquakes occurred in San Bernadino County, California, a magnitude 7.5 another of magnitude 6.6. These two events were followed by numerous aftershocks. Horizontal fault rupture displacement associated with this event was from 5 to 9.5 feet. Most pipeline damage was associated with the rupture zone.

- f) *1994 Northridge Earthquake*: This event caused about 1,400 pipeline breaks in the San Fernando Valley area. Outside the zone of high liquefaction potential, the dispersed pattern of breaks is attributed to old brittle pipes damaged by ground movement. In the On Balboa Boulevard a 0.5588m pipe suffered two breaks, one in tensile failure and the other in compressive failure. These pipe failures were located in a ground rupture zone perpendicular to the pipeline. Leaking gas ignited at several locations. Some broken water and gas lines were found to have experienced 0.1524 to 0.3048 m of separation in extension. The area experienced widespread ground cracking and differential settlements. A 2.159 m sewage pipe ruptured in the Jensen Filtration.
- g) *1995 Hyogoken-Nanbu Earthquake*: Takarazuka City was also heavily damaged. The damage on the water supply pipelines was serious and 203 pipeline damages were reported. Although Sakasedai district has the area of almost 1km square, 30 pipeline damages (pipe material was DCIP) occurred in the 1995 Hyogoken-nanbu earthquake. Almost 50% of damages were occurred in unliquefied ground.
- h) *1999 (Mw 7.4) Kocaeli, Turkey Earthquake*: Substantial water supply damage occurred in many cities. For example, the entire water distribution system in Adapazari was damaged. One of them, a water pipe made of steel with a diameter of 2.4 m, damaged at Kullar due to right-lateral strike-slip. A butt-welded Thames raw water steel pipeline 2.2 m in diameter crosses the Sapanca Segment of the North Anatolian fault and was damaged at the fault crossing. Damage was observed at three locations where a small surface leak was observed in the pipe at point near the fault crossing; a significant leak occurred at yet another point and a minor leak happened at the bend of pipe.
- i) *1999, the Chichi Earthquake*: In Taiwan many buried water and gas pipelines were damaged at many sites. It was reported that buried gas pipelines underwent bending deformation due to ground displacement at a reverse fault near the Wushi Bridge about 10 km south of Taichung. The bending deformation in a 100A-size pipeline was Vshaped, with the pipeline being bent at three points. The deformation of a 200A-size pipeline was Z-shaped, with the pipeline being bent at two points. There have been virtually no cases of substantial deformation comparable to this case in gas pipelines comprised of welded steel pipes.

2.2.2 Summary of Past Performance of Pipelines under Fault Crossing

Localized permanent ground deformations occur in surface fault rupture areas. Pipeline damage tends to concentrate at discontinuities such as pipe elbows, tees, in-line valves, reaction blocks and service connections, especially if permanent ground deformations develop compression strains. Such features create anchor points or rigid locations that promote force/stress concentrations. Damage to segmented pipes (e.g., cast iron pipe having caulked bell-and-spigot joints) is heavy when crossing surface ruptured faults. Butt-welded continuous steel pipes may sometimes be able to accommodate fault crossing displacements, up to a few feet. Continuous butt-welded steel pipelines are less prone to damage if they are oriented such that tensile strains result from the fault displacement. Tensile deformation takes advantage of the inherent ductility and strength of the steel, while compressive deformation promotes pipe wall wrinkling and the accumulation of high local strain. For both segmented and continuous pipelines, it is advantageous to avoid bends, tie-ins and local constraints close to the fault. This allows the pipeline that crosses the fault additional length over which to distribute the imposed strains resulting from the fault offset.

The angle of the pipeline-fault crossing has a major impact on pipeline response for orientations that promote tension. For segmented pipelines subject to tension, the optimal angle of the fault crossing depends on joint characteristics. This angle depends upon taking maximum advantage of both the pullout and joint rotational capacities of the joints. Leaded joint couplings appear to be able to take only 2.5 to 5.0 cm of fault displacement before failure. Extra-long restrained couplings can take up to about 0.3 m of fault displacement [3]. Burial depth is also a factor at fault crossings. For example, a pipeline with 1 m of overburden can sustain about four times more fault displacement than a pipeline with 3m of overburden.

Two failure modes occur when a pipeline is deformed in compression. The pipeline may buckle as a beam or it may deform by local warping and wrinkling of its wall. Buckling can occur across fault crossings, either due to fault creep or sudden fault offset. Beam buckling was observed in areas of mining subsidence and at fault crossings for cases in which the soil covering the pipeline was loose and limited in depth. Pipe wrinkling failure occurs in thinner walled pipes in high frictionally restraint soil conditions.

2.3 Pipeline Behaviour under Fault Movement

Loads are induced in a buried pipeline when the soil restricts the free motion of the pipeline or when the pipeline attempts to resist the motion of the surrounding soil. Lateral fault movement causes the pipeline to displace laterally with respect to the soil. This results in the soil applying a lateral pressure on the pipeline and the pipeline in turn pushing away the soil. This loading imparts tensile strains and curvature to the pipeline on both sides of the fault.

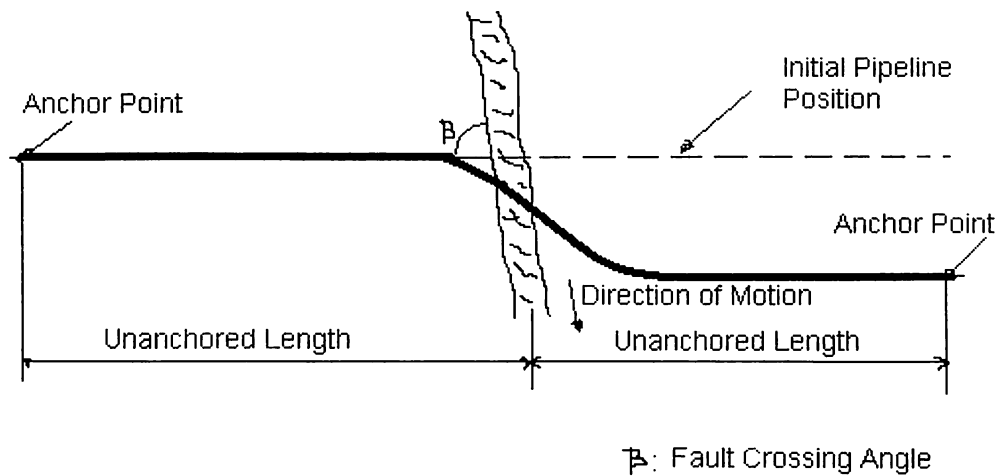


Fig. 2.3.1 Plan of Pipeline Subjected to Both Normal and Strike Slip Movement at a Fault Crossing

Vertical fault movement is resisted by a pipeline in a different manner. For a shallow buried pipeline, the uplift resistance of the soil typically is much lower than the downward bearing resistance. Thus, the pipeline may be able to lift upward with relative freedom to accommodate the vertical fault movement, and the maximum pressure between the pipeline and the soil will occur predominantly on the up thrown side of the fault. The corresponding curvature and bending strains will generally be lower than those caused by strike-slip movements of equal magnitude.

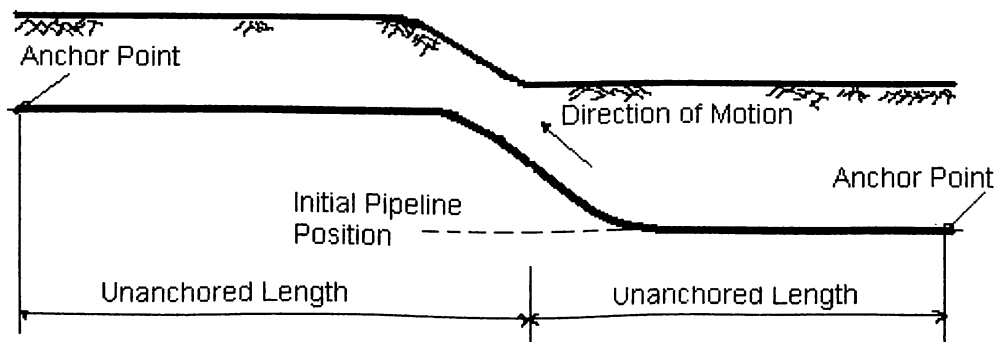


Fig. 2.3.2 Elevation of Pipeline Subjected to Both Normal and Strike Slip Movement at a Fault Crossing

The axial component of fault movement is resisted by friction forces at the soil-pipeline interface. For a given pipeline axial force, there is a length of pipeline required to develop opposing soil frictional forces. Beyond this length, the pipeline is not affected by the fault movement such that the pipeline is considered to be effectively anchored. Hence, the frictional resistance provided by soil-pipeline interaction governs the length of pipeline available to accommodate fault-generated strains.

It is noteworthy to understand that fault crossing is most crucial for the case of buried pipelines. This is so because in case of aboveground pipelines crossing a fault line the fault displacement can be accommodated via number of ways. One of the classical ways to do so is by using various kinds of flexible joints. Recent methods of placing the pipeline at low height bearings in set configurations have proved their efficacy. Further it is the surrounding soil and the interface friction and reaction which worsen the behaviour of pipelines to fault movements. Loads are induced in a pipeline by relative motion between the pipeline and the surrounding soil i.e. when the soil restricts the free motion of the pipeline or when the pipeline attempts to resist the motion of the surrounding soil. The entire fault displacement in that sense is dictated to the pipeline by soil over its entire length. Aboveground pipeline is completely free to move and unrestrained in this respect.

2.4 Analytical Work So Far

The prominent analysis procedures for analyzing buried pipelines under faulting have been cable model proposed by i) Newmark-Hall [9], ii) Kennedy [10], beam model by iii) Wang [11] and iv) Liu-Hu [12] and finally the shell model proposed by Takada *et al.* [8].

Newmark & Hall [9] considered a pipeline in tension, deformed laterally, longitudinally and vertically between the anchor points due to a statically applied ground displacement. Elongations of the line were computed by handling the elastic and plastic sections independently. Iterative approach was used with the deformed length based upon an assumed pipeline stress condition being compared with the known fault-induced deformed length (the method does not consider the displacement profile between anchor points).

Kennedy et al. [10] considered lateral soil forces on the pipeline and the resulting associated bending strains. It offered improved modeling of longitudinal soil friction forces by recognizing different values of frictional resistance for the straight and curved portions of the pipeline. Thus it was conservative in most cases as it overestimated the effects of lateral and vertical soil resistance on the bending strain. The treatment of the problem in this procedure generally followed trial and error approach to determine an axial stress that produces an axial elongation equal to a required elongation calculated on the basis of the known fault movement. Results obtained using this method are reasonably accurate as long as the estimate of the bending strains are such that the deformation can be considered to arise from axial elongation only.

Wang [11] and *Liu-Hu* [12] additionally considered the bending stiffness supported by field observation by modeling the pipeline as beam. The case was investigated using the theory of beam on elastic foundation and cantilever analogy for pipe.

Takada et al. [8] further considered section deformation and local buckling of pipe. They used *Kennedy et al.* model used for finding the pipe longitudinal geometry and thus the pipe bending angle. The relation between pipe bending angle and the maximum strain considering the sectional deformation was found through a set of FE shell analyses. Finally maximum strain was predicted using pipe bending angle from a simplified formula based on results of the analysis.

Ivanov et al. [14] studied the vulnerability of underground jointed pipelines to fault displacements using numerical modeling. The pipe was modeled by line elements and plastic hinges were considered. Only normal (vertical) and drag (axial) soil springs were used. The performance so obtained was verified by test data by an experimental set up. They obtained joint pullout forces under different conditions.

Guo et al. [15] conducted a parametric analysis using 3-D shell spring model and simulated pipeline soil performance under fault crossing. Pipe material, site soil stiffness, pipe diameter and fault dip were the parameters which were considered. They used the site data for initial modeling from Qinghai-Xinjiang border and have carried out the parametric study directly for feasible values of soil stiffness etc. Soil stiffness formulations weren't used for accounting for the influence of varying the parameter on the soil resistance to pipeline movement. Further only maximum pipe strain was studied for different values of the parameter.

Barros et al. [16] also conducted parametric analysis and studied only the moments for different values of soil friction angles, diameters and cover depths. Stiffness values for the soil springs used in the model were determined by experiments and other geotechnical studies. Material nonlinearity of pipeline material weren't considered.

2.5 Soil-Pipeline Interaction

One of the major factors that come into play in each of the seismic hazards is the soil interaction with the pipeline. The reaction offered by surrounding soil can generally be resolved into equivalent stiffness components in the axial (or longitudinal), transverse (horizontal or lateral), and vertical directions.

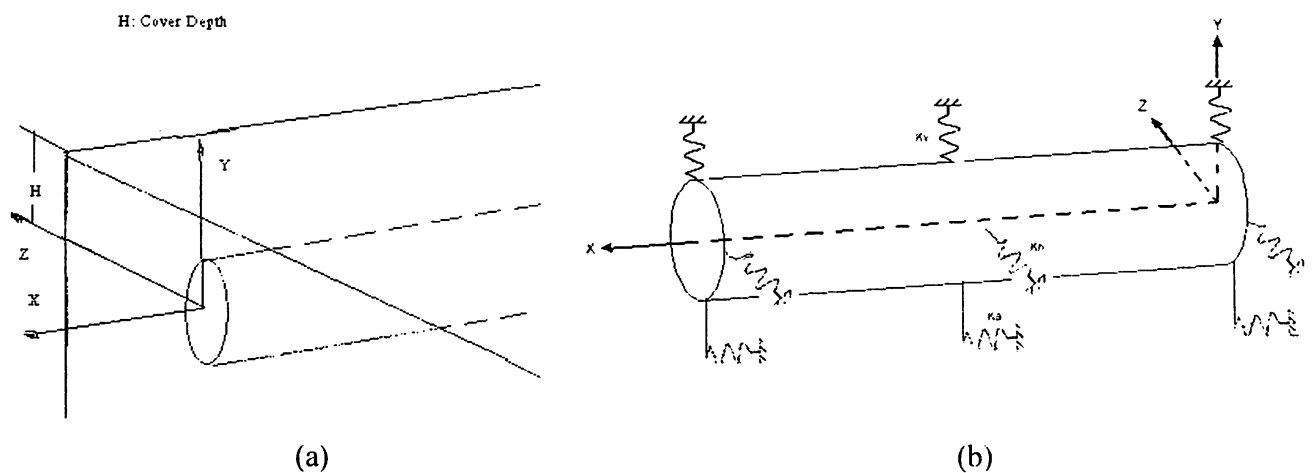


Fig. 2.5.1 (a) Actual and (b) Equivalent Pipe with Surrounding Soil Conditions

This concept, known as subgrade reaction, has been used for more than a century and is usually characterized by coefficients of subgrade reaction. For the sake of mathematical convenience, the coefficients of subgrade reaction are generally considered to be constant. Simple linear elastic relations (constant coefficients of subgrade reaction) do not allow for a limiting soil restraint to be reached and generally lead to overly conservative results (i.e., the restraint induced by the soil on the pipeline is overpredicted).

2.5.1 Soil Spring Representation [17]

The three-dimensional soil restraint can thus be schematically represented by a series of discrete nonlinear springs (e.g., elastic-plastic, multi-linear) whose load-deformation characteristics are denoted as t-x, p-y, and q-z curves (Fig.2.5.2). The maximum soil spring forces and associated relative displacements necessary to develop these forces are computed using the equations given in the following sections.

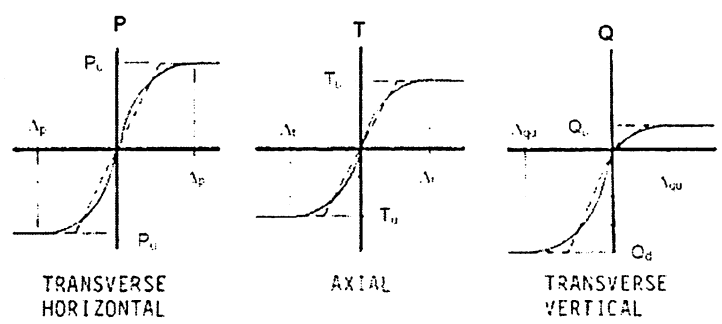


Fig. 2.5.2 Force Deflection Curves of Bi-Linear Soil Springs used to Represent Soil Force on Pipe

Although tests have indicated that the maximum soil force on the pipeline decreases at large relative displacements, the formulations used herein are based on the assumption that the soil force is constant once it reaches the maximum value. The dimension for the maximum soil spring force is force per unit length of pipeline. The equations in this section are only for buried pipelines in uniform soil conditions. For deeply buried pipelines with variable soil properties between the ground surface and the pipeline depth, the equations as used here may not be representative of true soil loading conditions.

The expressions for maximum soil spring force are based on laboratory and field experimental investigations on pipeline response, as well as general geotechnical approaches for related structures such as piles, embedded anchor plates, and strip footings. Several of the equations have been derived to fit published curves to facilitate their use in spreadsheets or other computer based applications.

2.5.2 Axial Soil Springs

The maximum axial soil force per unit length of pipe that can be transmitted to the pipe is:

$$T_t = \pi D \alpha c + \pi D H \bar{\gamma} \frac{(1 + K_0)}{2} \tan \delta \quad (2.1)$$

where, D is the pipe outside diameter, c is soil cohesion representative of the soil backfill, H is the depth to pipe centerline from the ground surface, $\bar{\gamma}$ is the effective unit weight of soil, K_0 is the coefficient of pressure at rest, α is the adhesion factor (curve fit to plots of recommended values in Fig. 2.5.3) given by

$$\alpha = 0.608 - 0.123c - \frac{0.274}{c^2 + 1} + \frac{0.695}{c^3 + 1} \quad (2.2)$$

where c is in kPa/100

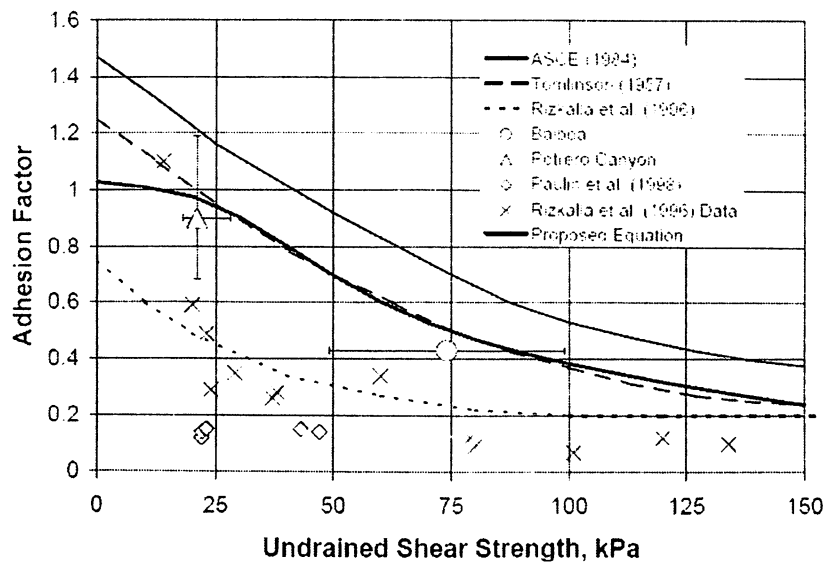


Fig. 2.5.3 Plotted Values for the Adhesion Factor [17]

δ is the interface angle of friction for pipe and soil given by

$$\delta = f\phi \quad (2.3)$$

here, ϕ is the internal friction angle of the soil & f is the coating dependent factor relating the internal friction angle of the soil to the friction angle at the soil-pipe interface. Representative values of f for various types of external pipe coatings are provided in Table 2.1

Table 2.5.1 Friction factor f for various external coatings [17]

| Pipe Coating | f |
|---------------------|-----|
| Concrete | 1.0 |
| Coal Tar | 0.9 |
| Rough Steel | 0.8 |
| Smooth Steel | 0.7 |
| Fusion Bonded Epoxy | 0.6 |
| Polyethylene | 0.6 |

Δ_r is the displacement at T_r and is given by

$$\Delta_r = \begin{cases} 0.1 \text{ inches (3 mm) for dense sand} \\ 0.2 \text{ inches (5 mm) for loose sand} \\ 0.3 \text{ inches (8 mm) for stiff clay} \\ 0.4 \text{ inches (10 mm) for soft clay} \end{cases} \quad (2.4)$$

2.5.3 Lateral Soil Springs

The maximum lateral soil force per unit length of pipe that can be transmitted to the pipe is:

$$P_u = N_{ch}cD + N_{qh}\bar{\gamma}HD \quad (2.5)$$

where, N_{ch} is the horizontal bearing capacity factor for clay (0 for $c = 0$) given by

$$N_{ch} = a + bx + \frac{c}{(x+1)^2} + \frac{d}{(x+1)^3} \leq 9 \quad (2.6)$$

N_{qh} is the horizontal bearing capacity factor (0 for $\phi = 0^\circ$) given by

$$N_{qh} = a + bx + cx^2 + dx^3 + ex^4 \quad (2.7)$$

and $x = \frac{H}{D}$

The expressions for N_{ch} and N_{qh} are closed form fits to published empirical (plotted) results such as those illustrated in Fig. 2.5.4.

N_{qh} can be interpolated for intermediate values of ϕ between 20° and 45° .

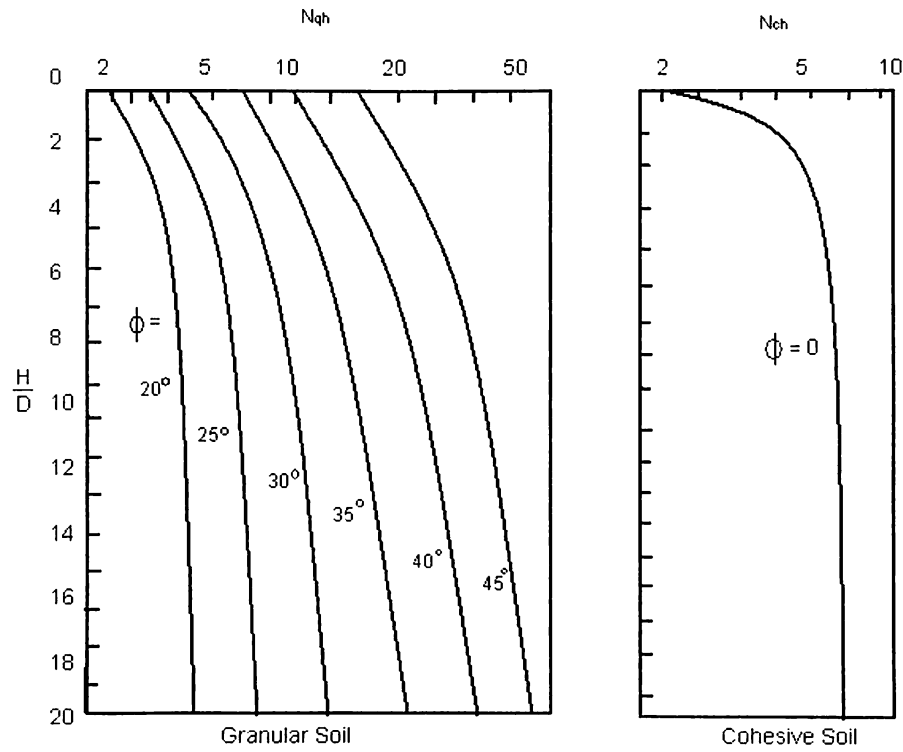


Fig. 2.5.4 Values of N_{qh} and N_{ch} of Hansen [17]

Table 2.5.2 Values of constants a , b , c , d & e [14]

| Factor | ϕ | x | a | b | c | d | e |
|----------|--------|-------|--------|-------|---------|-------------------|-------------------|
| N_{ch} | 0° | H/D | 6.752 | 0.065 | -11.063 | 7.119 | -- |
| N_{qh} | 20° | H/D | 2.399 | 0.439 | -0.03 | $1.059(10)^{-3}$ | $-1.754(10)^{-5}$ |
| N_{qh} | 25° | H/D | 3.332 | 0.839 | -0.090 | $5.606(10)^{-3}$ | $-1.319(10)^{-4}$ |
| N_{ch} | 30° | H/D | 4.565 | 1.234 | -0.089 | $4.275(10)^{-3}$ | $-9.159(10)^{-5}$ |
| N_{qh} | 35° | H/D | 6.816 | 2.019 | 0.146 | $7.651(10)^{-3}$ | $-1.683(10)^{-4}$ |
| N_{qh} | 40° | H/D | 10.959 | 1.783 | 0.045 | $-5.425(10)^{-3}$ | $-1.153(10)^{-4}$ |
| N_{ch} | 45° | H/D | 17.658 | 3.309 | 0.048 | $-6.443(10)^{-3}$ | $-1.299(10)^{-4}$ |

Δ_p is the displacement at P_u and is given by

$$\Delta_p = 0.04 \left(H + \frac{D}{2} \right) \leq 0.10D \text{ to } 0.15D \quad (2.8)$$

2.5.4 Vertical Uplift Soil Springs

The equations for determining upward vertical soil spring forces are based on small-scale laboratory tests and theoretical models. For this reason, the applicability of the equations is limited to relatively shallow burial depths, as expressed as the ratio of the depth to pipe centerline to the pipe diameter (H/D). Conditions in which the H/D ratio is greater than the limit provided below require case-specific geotechnical guidance on the magnitude of soil spring force and the relative displacement necessary to develop this force.

$$Q_u = N_{cv}cD + N_{qv}\bar{\gamma}HD \quad (2.9)$$

where N_{cv} is vertical uplift factor for clay (0 for $c = 0$) and is given by

$$N_c = 2\left(\frac{H}{D}\right) \leq 10 \quad (2.10)$$

N_{qv} is vertical uplift factor for sand (0 for $\phi = 0^\circ$) and is given by

$$N_{qv} = \left(\frac{\phi H}{44D}\right) \leq N_q \quad (N_q \text{ is defined in next section}) \quad (2.11)$$

The above equations represent an approximation to published results as those in Fig. 2.5.5

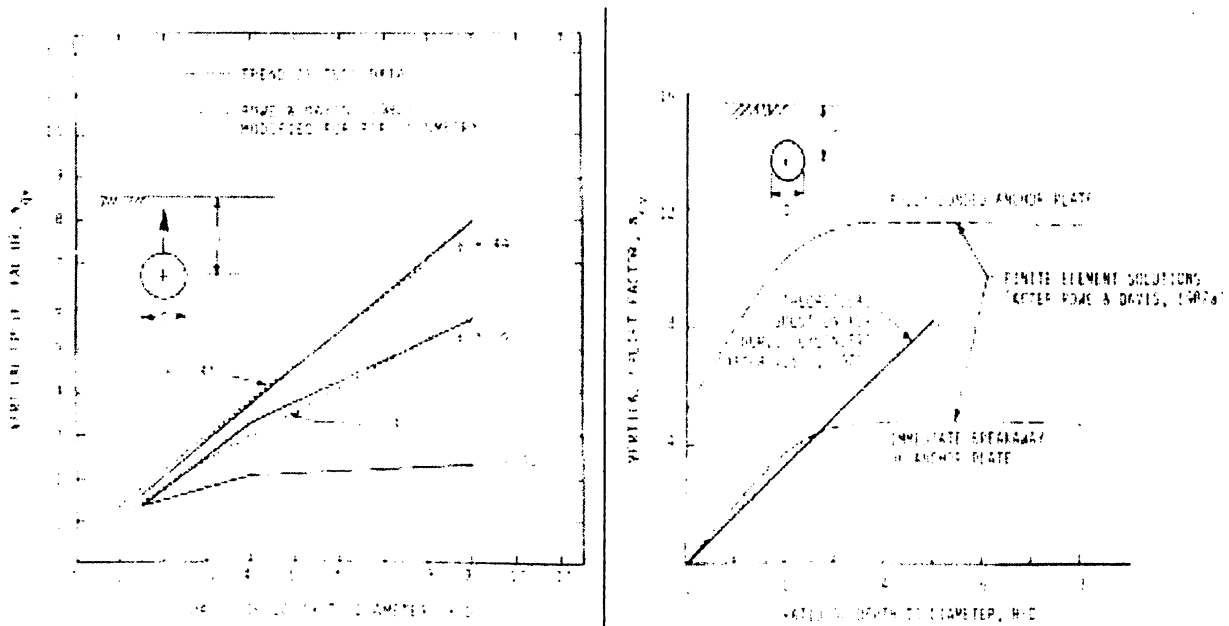


Fig. 2.5.5 Ranges for Values of N_{qv} and N_{cv} [17]

Δ_{qu} is the displacement at Q_u and is given by

$$\Delta_{qu} = \begin{cases} 0.01H \text{ to } 0.02H & \text{for dense to loose sands } < 0.1D \\ 0.1H \text{ to } 0.2H & \text{for stiff to soft clays } < 0.2D \end{cases} \quad (2.12)$$

2.5.5 Vertical Bearing Soil Springs

Maximum bearing force that can be exerted by the per unit length is given by

$$Q_d = N_c cD + N_q \bar{\gamma}HD + N_\gamma \gamma \frac{D^2}{2}$$

where, γ is total unit weight of soil & N_c , N_q , N_γ are bearing capacity factors given by

$$N_c = [\cot(\phi + 0.001)] \left\{ \exp[\pi \tan(\phi + 0.001)] \tan^2 \left(45 + \frac{\phi + 0.001}{2} \right) - 1 \right\} \quad (2.13)$$

$$N_q = \exp(\pi \tan \phi) \tan^2 \left(45 + \frac{\phi}{2} \right) \quad (2.14)$$

$$N_\gamma = e^{(0.18e - 2.5)} \quad (2.15)$$

(This is a curve fit to plotted values of N_γ in Fig. 2.5.6)

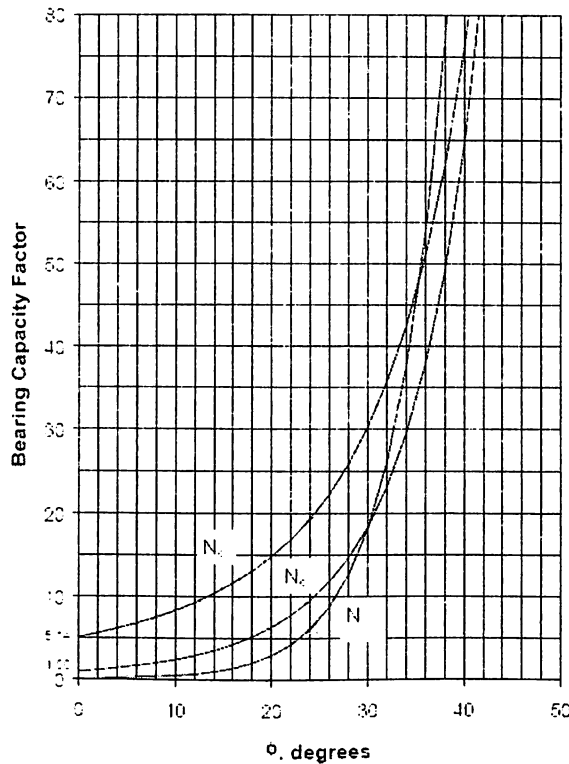


Fig. 2.5.6 Plotted Values of Bearing Capacity Factors (N_q , N_c , and N_γ) [17]

Δ_{qd} , displacement at Q_d is given by

$$\Delta_{qd} = \begin{cases} 0.1D & \text{for granular soils} \\ 0.2D & \text{for cohesive soils} \end{cases} \quad (2.16)$$

3. What is Liquefaction

Liquefaction is a common earthquake hazard related to ground shaking that accompanies earthquakes, typically magnitude 5.0 or greater. The term *liquefaction* refers to the physical change that occurs when certain soils are shaken and transformed from solid ground capable of supporting a structure to a quicksand-like liquid with a greatly reduced ability to bear the weight of a building.

3.1 How does Liquefaction occur

Liquefaction occurs when seismic waves generated by a large earthquake pass through unconsolidated sediments near the ground surface. When a structure is built, the weight of the structure and its contents are transferred through the foundation into underlying soils. If you were to closely examine soil in the ground, you would see it is composed of many sediment particles which form a framework of grains in contact with one another with a small amount of void space (or pore space) between them, similar to a bucket filled with marbles.

As seismic waves pass through an area, the ground undergoes oscillatory straining (shaking) which can cause the individual soil particles to shift into a tighter framework. If the space between the grains is filled with groundwater, as the particles readjust into a closer packing arrangement, the pressure in the pores between the grains is increased. If the pore pressure increases enough and the water cannot easily drain away, gravity loads are transferred from the sediment framework to the pore water. This process of sediment losing load carrying ability to the pore water is called *liquefaction*. Liquefaction results in a greatly diminished capacity for the ground to support the weight of overlying structures. In dry, unsaturated sediments where the void spaces are filled with air, liquefaction does not occur because the air in the pore space is easily compressed and the sediment framework sustains the load. Although any source of strong ground motion, such as an explosion, can trigger liquefaction, only moderate to large earthquakes generally create the intensity and duration of shaking needed to cause liquefaction-induced damage in areas with susceptible soils. Because liquefaction occurs beneath the ground surface, there is often no apparent evidence to indicate where liquefaction has occurred in the past.

Sometimes construction excavations will reveal disturbed, convoluted sedimentary layers that suggest prehistoric earthquake-induced liquefaction. In some cases, surficial evidence of liquefaction will appear in the form of sand boils (or sand *volcanoes*), ground settlement, and fissures (FIGURE). These surface features are not always created during liquefaction, and when formed, they can be quite easily eroded and seldom preserved. Therefore their absence from a site does not indicate that liquefaction has not occurred in the past.

3.2 Conditions for Liquefaction

Three critical factors must be present for sediments to be prone to liquefaction. The sediment must be 1) saturated with ground water, 2) composed of sand or silt-sized particles, and 3) compacted fairly loose. For liquefaction to occur, all three factors must be present at the same time; for example, neither a loosely compacted, dry sand, or a saturated, densely compacted sand would be prone to liquefaction because one of the three critical liquefaction elements is missing. The Liquefaction Potential Map for Salt Lake County shows that the most liquefaction-prone areas (the *High* and *Moderate* areas) are located along the valley floor, tributary stream channels, and near the Great Salt Lake. Soils in foothill areas are generally less susceptible to liquefaction because they are coarser, and not saturated by shallow groundwater.

Ground Water - Sediments must be saturated with ground water in order to liquefy during an earthquake. A shallow perched water table will contribute to liquefaction conditions and should not be disregarded or confused with deeper water levels recorded in culinary water well logs. Fluctuations in the shallow ground water level will also affect liquefaction conditions. Seasonal or cyclical wet periods often cause ground water levels to rise, saturating shallower sediments, and perhaps increasing the liquefaction potential in an area.

Grain Size - The size of the sediment particles controls the size of the porespaces. This is critical in clay and fine silt grains (those less than 1/32 of an inch in diameter) because, although water can fill the small pore spaces, the flow of water between pores becomes so restricted that liquefaction becomes difficult. Gravel particles (larger than 1/5 of an inch in diameter) pose a different situation. Due to the much larger mass of the grains and generally higher porosity, the great intensity and duration of ground shaking that is required to induce liquefaction rarely occurs, except in the largest earthquakes. Generally, only sands and coarse silts combine the optimum grain mass and pore-space geometry to liquefy, given the intensity of shaking expected in a moderate to large Wasatch Front

earthquake. The sands and silts must also be relatively clean for liquefaction to occur. This means that liquefaction is most likely to occur in sands and coarse silts with a uniform grain size. A clayey-sand, for example, would have a reduced liquefaction potential because the clay-sized particles fit between the sand grains, tightening up the framework and increasing soil cohesion.

Soil Density - Loose compaction of the soil also contributes to the liquefaction potential. The more densely the grains are compacted in the framework, the greater the earthquake-shaking intensity, or acceleration, needed to raise pore pressures enough to shift the grains. It is unlikely that a typical Wasatch Front earthquake could provide sufficient shaking to induce liquefaction in very densely compacted soils. Soil density generally increases with the age and depth of deposits. Sediments tend to compact over time and with burial, increasing their density. Historically, liquefaction has been observed mainly in sediments less than 45 feet below the ground surface.

3.3 Soil-pipeline interaction:

The soil around the pipeline plays a very important role in relation to its seismic behavior, if it is cohesive soil, the softer it is, the greater differential settlement there will be due to consolidation and higher amplification effects; if it is granular material, the probability of liquefaction becomes higher the looser it is. In case of soil pipeline interaction, the soil will not fail, but the soil displacement will produce friction-like forces at the soil-pipeline interface.

An elasto-plastic model is often adopted for the force-deformation behavior at soil-pipeline interface (O'Rourke et al, 1995). This model is fully defined by two parameters: the maximum axial force per unit length at the soil pipe interface, f_m , and the relative displacement at which slippage between pipe and soil occurs. The slippage displacement is small and conservatively neglected here.

The maximum axial force per unit of length f_m depends on the type of soil surrounding the pipe and the method of pipe installation (i.e., the compaction control of the backfill). For cohesionless soil f_m depends on the effective normal stress at the soil-pipe interface, the coefficient of friction and the effective friction angle ϕ between the soil and the pipe material, and the pipe diameter F_p . Considering that we have plane strain, and that the coefficient of lateral pressure k_o for compacted soil is approximately equal to unity, the effective normal stress s'_v is simply equal to the product of the effective unit weight of soil γ'_m , and the depth H , to the pipe's centerline. Thus, for cohesionless backfill, the friction force per unit length becomes

$$f_m = s'_v \tan \phi F_p$$

For cohesive soil, f_m depends on the undrained shear strength S_u of the soil. For normally consolidated clay, S_u gives a good estimation of the adhesion to the pipe. For overconsolidated soils Lambe and Whitman (1969) recommended the use, as adhesion, of the undrained shear strength of an equivalent normally consolidated soil. So for cohesive soil,

$$f_m = S_u \rho F_p$$

For the most general soil condition, when the soil surrounding the pipe has both friction and cohesive characteristics, f_m will be given by

$$f_m = (c + s' \tan \phi) \rho F_p$$

where c = shear strength of the soil corresponding to zero-effective vertical stress on the shear-strength curve.

3.4 Summary of past performance of Pipelines under Liquefaction:

Liquefaction is usually associated with strong ground motion with long duration, and always occurs in areas of young, soft and cohesionless soils, in poorly constructed fills and in the presence of shallow water table. The effect of liquefaction on lifelines can be classified into three types, the first of which is generation of buoyancy that leads to pipelines damaged at boundary between pipelines and buildings, abutments, and manholes, etc. The second is permanent ground deformation due to liquefaction-induced lateral spread, and the third is the differential dynamic response effect from liquefied and nonliquefied areas, which usually damages pipelines at the boundary between liquefied and nonliquefied area.

Post-earthquake investigations showed that pipelines were seriously damaged by liquefaction during strong earthquakes, e.g., the 1964 Niigata earthquake, the 1971 San Fernando earthquake, the 1975 Haicheng earthquake, the 1976 Tangshan earthquake, the 1989 Loma Prieta earthquake, the 1994 Northridge earthquake, and the 1995 Kobe earthquake, etc. For example, O'Rourke and Tawfik reported that during the San Fernando earthquake, eleven transmission pipelines were affected by liquefaction-induced landslide and lateral spread, and five of which were damaged substantially, and the most severe damage occurred in gas pipelines due to lateral spread. The pipelines were subjected to a maximum differential movement of 1.7 m over a distance of about 70 m. There were a lot of liquefaction occurred in backfill areas in Haicheng City during the 1975 Haicheng earthquake, and most pipelines in these areas were damaged. In Tianjin City, there were many alluvial valleys, and pipelines through these areas were heavily damaged due to liquefaction

during the 1976 Tangshan earthquake . During the 1989 Loma Prieta earthquake, there were more than 123 failures to the water distribution pipelines in Marina in San Francisco, all of which were resulted from liquefaction-induced settlement or lateral spread of ground .

Hamada et al. investigated the failure process of a gas pipeline during the 1983 Nihonkai-Chubu earthquake, and found that the permanent ground displacement was the main cause of the failure, more than the dynamic relative displacement such as by wave propagation and non-uniform characteristics of the surrounding ground along the pipeline. Nishio examined twelve damage failures of gas pipelines due to liquefaction in the 1983 Nihonkai-Chubu Earthquake, and based on the failure modes he concluded that the damages were caused by dynamic compression and tension, rather than by static ~or permanent! ground deformation. He attributed the damage mechanism of the pipelines to dynamic ground motion associated with soil liquefaction.

Due to the difficulty in theoretical solution for liquefaction problem, seismic behavior of pipelines in liquefaction areas was mainly studied by experiments. The early experimental studies were done by Katada and Hakono , and then by Kitaura and Miyajima . Kuribayashi et al., Nishio et al. , Hamada et al., and Takada et al., etc. Based on the damage investigation of pipelines due to liquefaction during the 1983 Nihonkai-Chubu earthquake, Nishio et al. conducted a model experiment on seismic behavior of pipeline in partially liquefied ground. The observed behavior of the pipeline was proved by a simple mathematical model of ground motion combining with a conventional model of soil-pipe interaction. They concluded that partially liquefied ground was one of the most possible, but unfavorable, conditions associated with seismic liquefaction Seismic response of pipelines during liquefaction was studied analytically by Yeh and Wang , in which, they considered pipes to be partially supported by assuming that soil within liquefaction area loses all the strength and behaves like a viscous fluid, and finite difference method was used for the solution. However, in the model dynamic motion of the ground which supported the pipe was not taken into consideration, and the soil restriction against the pipe in the axial direction was neglected inappropriately. With these considerations, Nishio et al. proposed an analytical model, and the analytical solution was derived. The numerical results were verified by the model experiment, and the model was applied to an existing ground and pipelines. Analytical studies have also been conducted in recent years by many researchers, Hamada 1994, Takada 1985.

3.5 Gujarat Earthquake, 2001:

An earthquake measuring 7.9 on the Richter Scale (7.6 Moment Magnitude), hit the Kachchh region, located in the northwest region of the State of Gujarat at 8:46 am on January 26, 2001. It was felt in most parts of India. The earthquake caused substantial loss of life and property. According to the estimates available from the government sources at the time of this report, 18,253 people lost their lives, and another 166,836 suffered injuries of various degrees. 7,904 villages in 182 talukas of 21 districts in Gujarat were affected. 332,188 houses were destroyed while 725,802 houses were damaged to varying degrees. The strong motion records obtained from the Passport Office Building under construction in Ahmedabad, about 230 kms from the epicenter, indicated a peak ground acceleration of about 0.11g.

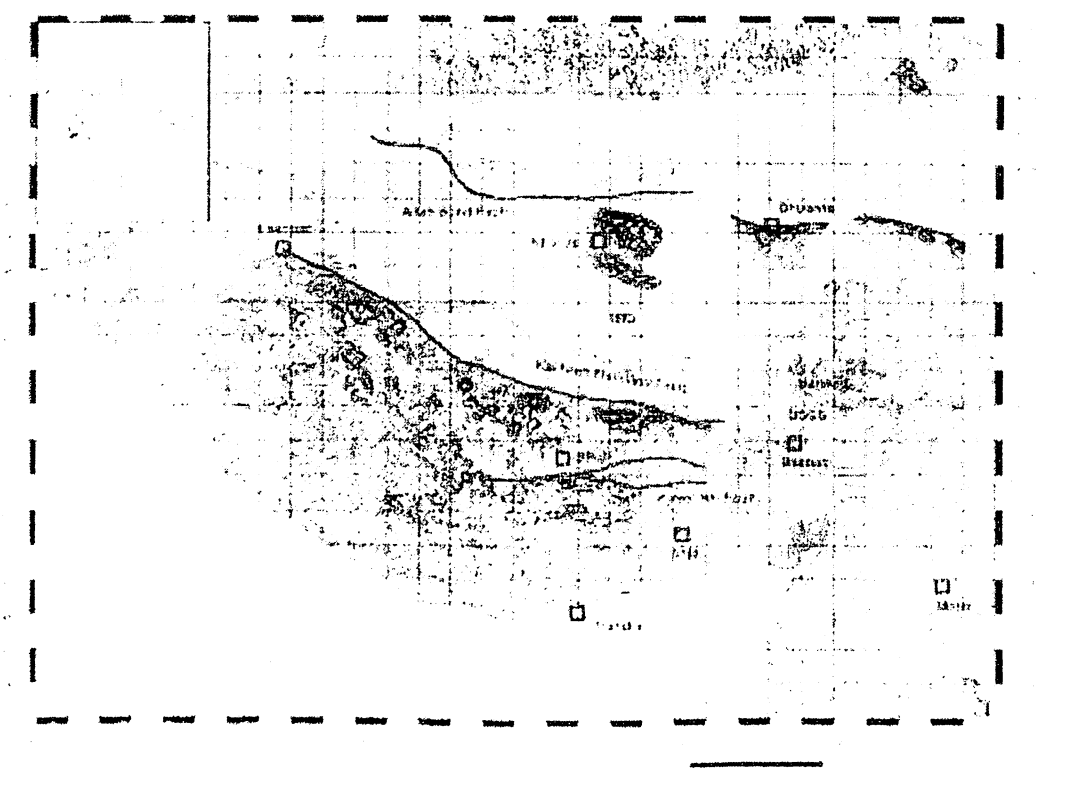


Figure 3.5. . Map showing locations of epicenters of the Bhuj earthquake according to various sources viz. Indian Meteorological Department, New Delhi; United State Geological Survey and Harvard.

(Topographic map is prepared by Prof. Koji Okumura, Hiroshima University, Japan, and is based on DEM GTOPP30, GMT; contour interval 10 m).

3.5.1 Technical Issues

Many teams investigated technical issues as they related to buildings, and lifelines (electrical, communications, water, and transportation). The lifelines were all affected to some extent. The reported magnitude of the Bhuj earthquake varies from Mw 7.6 (Earthquake Research Institute, University of Tokyo) to Mw 7.7 (United States Geological Survey). The body-wave magnitude was reported to be mb 6.9. The United States Geological Survey (USGS) has located the epicenter at 23.36°N, 70.34°E, placing it at approximately 100km NNE of Jamnagar India and 290km SE of Hyderabad Pakistan:

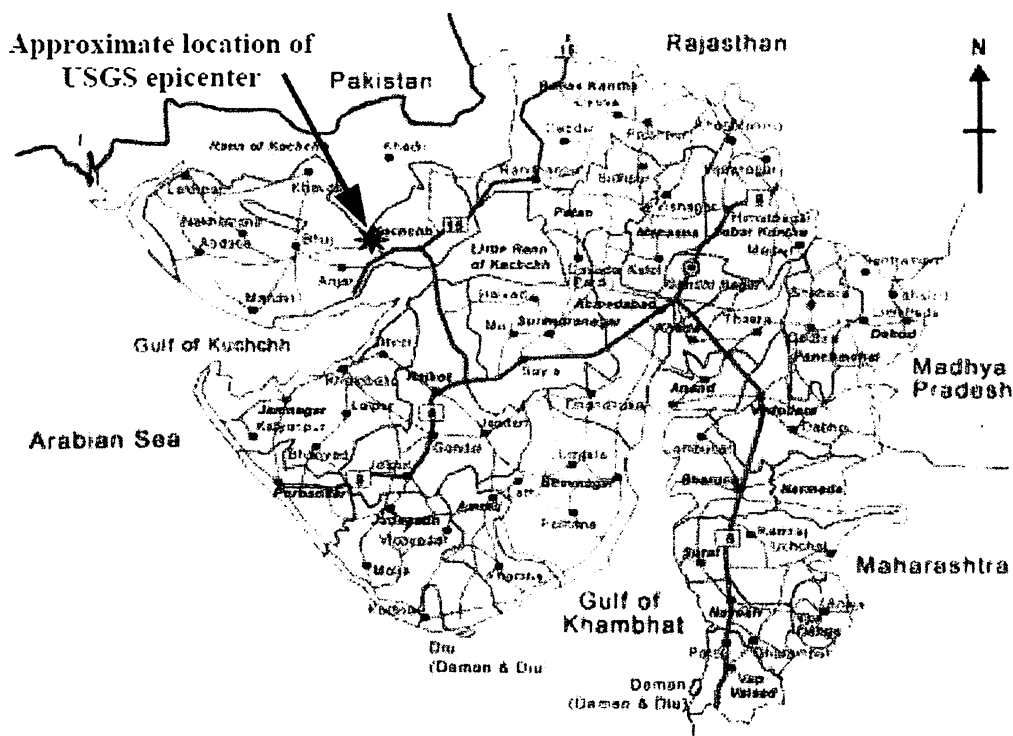


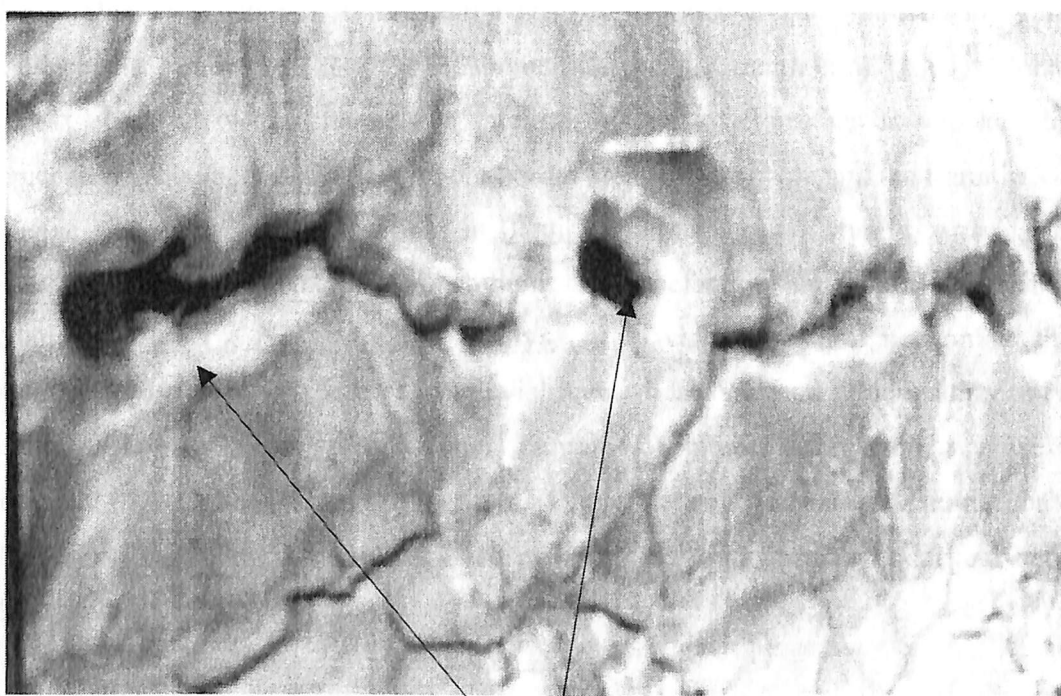
Fig: 3.5.1 Approximate location of USGS epicenter of 2001 earthquake

Epicenter location determined by the United States Geological Survey for the January 26, 2001 Gujarat earthquake. (R. Mistry, Weimin Dong, Hareesh Shah, April 2001)

The rupture propagated approximately 40 km from east to west. The source duration was approximately 20s. Estimates of the depth of the hypocenter range from 18km (Earthquake Research Institute, University of Tokyo) to 22km (USGS). The mechanism of the earthquake was pure dip slip due to north-south compressive stress.

3.5.2 Liquefaction in 2001 Gujarat earthquake:

During the 2001 Bhuj earthquake maximum intensity and extent of damage was around Bhuj, Bachau and Anjar, but Ahmedabad, 250 km east-south east of the epicenter also suffered collapse of multistoried buildings with a loss of about 1500 lives. Strong motion and minor damage were reported as far south as Surat. Ground cracking due to liquefaction and liquefaction features like sand blows were observed in the epicenter area. Liquefaction has been recorded on an extensive scale in several parts of the state . It has been profusely recorded in the little Rann of Kutch, Ran of Kutch as well as the coastal areas of the Gulf near Gandhidham , Kandla and between Malya and Samakhiali .



Fissure

Fig:3.5.2 Observed damage at Gujarat due to lateral soil displacement due to liquefaction.

3.5.3 Liquefaction and fluidization

The earthquake resulted into large-scale liquefaction and fluidization in an area of 6000 km², covering the Great Rann, Little Rann, Banni Plain and coastal areas. Numerous hidden river channels show emergence of water in satellite imageries. Shallow ground water at these places provide most favorable environment for liquefaction in areas of intensity VIII or more. Manifestations of liquefaction are fluidization, sand blows or dykes, craters, ground fissures, subsidence and lateral spreads. Water that emerged is saline and was seen as wet ground or pools of water even after three months of the main earthquake. White patches are formed near craters due to salt deposition. The amount of fluidization is intense but ejection of sand is less, maximum being 10 cm height. The sand dykes are extremely narrow with maximum of a few cm height and mostly less than a cm. Isolated cases of liquefaction have been observed up to 275 km like Rupen River bed in Patan District, Tharad in Banaskantha District, Dholka in Sabarmati basin, Vataman and Nada village near Jambusar (22N–72.5E, Bharuch District) (Karanth et al., 2001). Mohanti et al. (2001) report observing water channels in satellite imagery of Rajasthan at 450 km distance from the epicenter. Liquefaction has occurred at border areas of Mesozoic and the Rann in Manfara, Chobari, Vejpar and Amarsar. The locations in Banni region are Lodai, Dhrang, Amrapar and Bhirandiala. The coastal regions where large amounts of liquefaction and lateral spread occurred include Mandvi, **Mundra**, **Navlakhi** and **Maliya**. At Navlakhi, a small portion of the railway track submerged in seawater. Further in alluvial areas of Halvad and Dhrangadhra railway tracks were damaged due to lateral spread. Water fountains or sprouts along with sand were reported from Katwant, Desalpar, Lodai, Budharmora, Dhora, Khengarpar and Mandvi. For example Water fountains are reported as high as 2–10 m lasting for over 2 hr at Lodai and between Rapar and Dholavira.

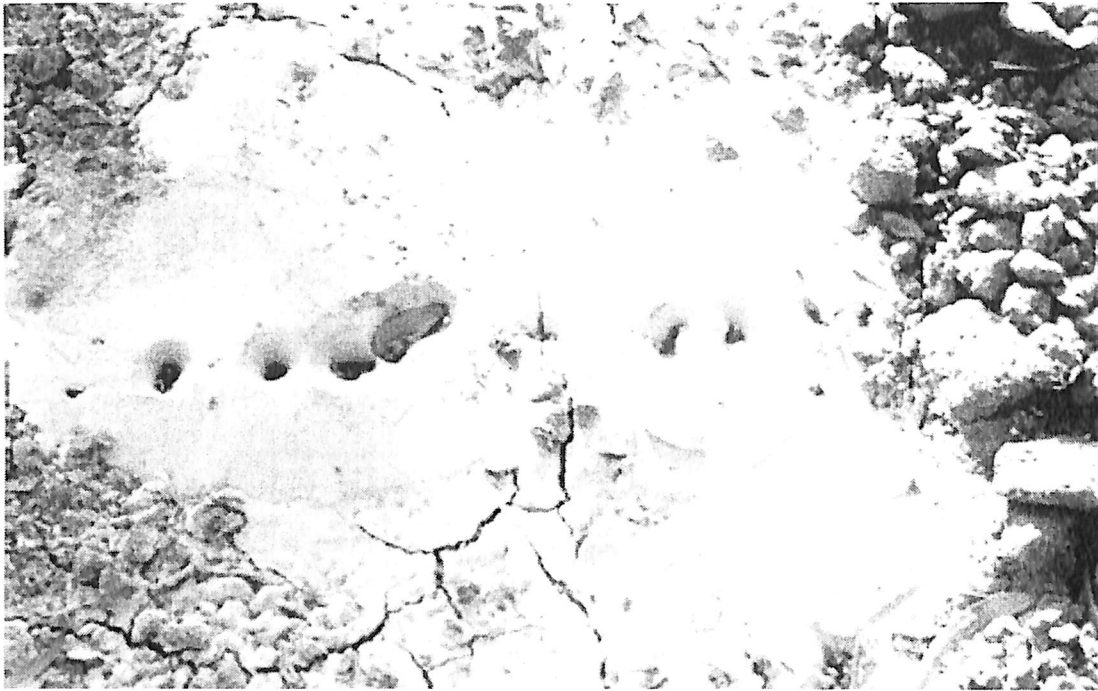


Fig: 3.5.3 Small sand craters formed by liquefaction of soil

3.6 Effect on buried pipelines :

Damages to buried pipelines in liquefied ground have been observed in many major earthquakes. Causes of these damages are considered to be buoyancy and sinking of ground as well as lateral flow of soil. A lot of researches have been conducted experimentally and theoretically to explore the possible damage mechanism. It becomes known that soil liquefaction resistance is highly related with the standard penetration resistance of soil. Consequently, in engineering practice for evaluating liquefaction potential, it is rather popular to use the standard penetration resistance as an index of soil liquefaction resistance during earthquake shaking.

The potential of liquefaction can be evaluated to be the safety factor of liquefaction resistance. This factor is the ratio of shear strength of soil to the shear induced during an earthquake. It is more appropriate to express such a factor in terms of soil penetration resistance, since several previous investigations have shown that there is a good correlation between soil liquefaction resistance to earthquake excitation and soil penetration resistance.

The shear stress ratio , which represents the shear strength of the soil, can be determined conveniently from the relationship (Tokimatsu and Yoshimi, 1983) .

$$\left(\frac{\tau}{\sigma_v} \right)_R = a \times C_r \times \left[\frac{16\sqrt{N_a}}{100} + \left(\frac{16\sqrt{N_a}}{C_r} \right) \right] \dots\dots\dots(1)$$

$$N_1 = \frac{1.7 N_{60}}{\sigma_v + 0.7} \dots\dots\dots(2)$$

$$\Delta N_f = \begin{cases} 0 \dots\dots\dots \text{When } FC \leq 5\% \\ FC - 5 \dots\dots\dots \text{When } 5\% < FC \leq 10\% \dots\dots\dots(3) \\ 0.1FC + 4 \dots\dots\dots \text{When } FC > 10\% \end{cases}$$

Where t= average shear stress and s_v = total overburden pressure at depth under consideration (kg/cm²). In addition , a= 0.45, C_r=0.57, n = 14, C_t= 80~ 90 and N_a=N₁+? N_f

In the above equation , s_v' is effective overburden pressure , FC is fines content, and N60 is corrected SPT N value at 100 kpa effective overburden stress and 60% energy obtained from adjacent soundings.

On the other hand , a comprehensive approach to estimate the potential for cyclic softening due to earthquake loading was developed first by Seed in 1985 and modified by others (Roberson & Wride 1997). The approach requires the determination in the lab, with undisturbed or restituted soil samples, of the cyclic stress ratio caused by an earthquake. A simplified method to estimate the ratio is based on the maximum ground acceleration , A_{max} , at site and is expressed as ,

$$\left(\frac{\tau}{\sigma_v'} \right) = 0.1(M - 1) \frac{A_{max}}{g} \frac{\sigma_v}{\sigma_v'} r_d \dots\dots\dots(4)$$

Where,

g = acceleration due to gravity, s_v' = effective overburden pressure

M = magnitude of earthquake,

r_d = stress reduction factor , which is dependent on soil depth z in meter
= 1-0.015z

The safety factor of liquefaction resistance, F_L is obtained as

$$F_L = \frac{\left(\begin{matrix} \tau \\ \sigma'_v \end{matrix} \right)_R}{\left(\begin{matrix} \tau \\ \sigma'_v \end{matrix} \right)_L} \dots \dots \dots (5)$$

F_L is a function of depth, therefore, a liquefaction potential index, P_L , is suggested as follows

$$P_L = \int_0^z F(z)W(z)dz \dots \dots \dots (6)$$

where

$$F(z) = \begin{cases} 1 - F_L(z) & \dots \dots \dots F_L(z) < 1 \\ 0 & \dots \dots \dots F_L(z) > 1 \end{cases} \dots \dots \dots (7)$$

$$W(z) = 10 - 0.5z$$

It is understood that $PL=15$ indicates high potential of liquefaction while $5 > PL > 0$ implies low possibility of liquefaction.

3.6.1 Design criteria for buoyancy due to liquefaction :

When the liquefaction of the soil around the pipeline occurs, buoyancy forces are exerted upon pipeline and must be resisted by anchors and the drag forces imposed by the liquefied soil as the pipeline begins to elevate.

Buoyancy effects are probably of greatest concern in areas such as flood plains and estuaries where massive liquefaction could take place in a large earthquake. When the surface liquefies, the pipe keeps uplifting at most to a position where a portion of pipe is at ground surface near the centre of the liquefied zone. However, when a non-liquefied soil layer is present as a cover over liquefied layer, the pipe come to rest at the interface of the non-liquefied and liquefied layer.

3.6.2 Buoyant force on pipeline :

The net upward force on unit length of pipeline is:

$$F_b = \frac{\pi D^2}{4} (\gamma_{sat} - \gamma_{content}) - \pi D t \gamma_{pipe} \quad (8)$$

Where

F_b = Upward force due to buoyancy per unit length of pipe

γ_{sat} = Saturated unit weight of soil

$\gamma_{content}$ = Unit weight of pipe content

γ_{pipe} = unit weight of pipe material

D = Diameter of the pipe

t = Thickness of the pipe

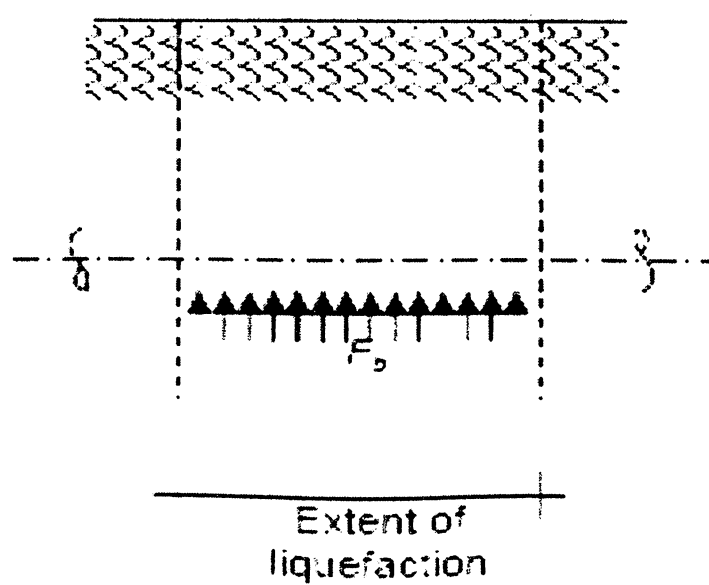


FIG 3.6.2 Longitudinal section of the pipeline showing the force upon it due to buoyancy (ALA, 2001)

3.6.3 Bending strain in the pipe due to buoyancy:

The bending strain in the pipeline due to uplift force may be approximated as:

$$\varepsilon_b = \pm \frac{F_b L_l^2}{3\pi E t D^2} \dots\dots\dots(9)$$

Where,

E = Modulus of elasticity of pipe material

t = Thickness of the pipeline

Ll= Length of the pipe subjected to liquefaction

While calculating the bending strain, the pipe is considered as a stiff beam restrained due to non-liquefied soil beyond the margins of liquefied zone.

Project Work Detail

Name of the Project : *EARTHQUAKE EFFECT ANALYSIS OF BURIED PIPELINES IN GUJARAT, INDIA.*

Aim of the Project: To analyze the buried pipelines in various condition of earthquake namely

- 1> Analysis of the buried pipeline under fault movement
- 2> Parametric analysis of the buried pipeline
- 3> Buoyancy force effect on buried pipelines

at the same time few recommendations were made at the end based on the data generated by software and manual calculations.

Basic inputs are taken from various organizations namely,

- 1> GSPL (Gujarat State Petronet limited)
- 2> GGCL (Gujarat Gas Company Limited)

4. PIPELINE UNDER FAULT MOVEMENT

4.1 Description of Representative Data

As can be expected there are variety of pipelines with wide range of specifications available for transport of fluids like water, oil & natural gases etc. The range of diameter extends from few centimeters to even 3m. Accordingly the thickness ranges from few mm to 2 cm. Still from the survey of pipelines in use in India it can be seen that most of the pipeline diameter ranges from 0.25m to 1.5m with thickness 0.001m to 0.02m. Similarly the cover depth i.e. the height of soil cover above the pipeline centre ranges from 0.5m to 3.0m. Usually the long buried pipelines which are planned to be commissioned or those in use are steel pipelines for the most and are meant for transportation of crude oil or natural gases. Now as far as soil is concerned it can show a natural variation throughout the span of the pipeline. Typically the pipeline may pass through rivers, desert, and tropical area or even under sea and thus encountering severe extremes of soil properties. Concerning the fault displacement values, scrap heights as much as 6.0m were measured on the Hebgen fault after the 1959 Hebgen Lake earthquake of magnitude 7.1, and a single strike-slip displacement of 8.8m was measured after the 1957 Gobi-Altai earthquake of magnitude 8.3. From the review of past earthquakes and literatures available, normally the value of fault displacement ranges from few centimeters up to a maximum value of 7.0m.

Length of the pipeline to be modeled is an essentially important factor to be decided upon. This is so because pipelines are in general very long structures which may not be so straight in their layout. Thus, modeling the entire length is not very feasible. Now, if we model only a finite segment of the entire pipe run then necessary boundary conditions must be applied especially at the ends to simulate the real situation. This is a very complex issue to take care in its entirety. Thus an easy way adopted usually, is to model sufficient length of the pipeline, such that any affect of the fault movement vanishes or dies out before the end conditions can have any affect on them. Although for a free end the moments and other forces will always become negligible care has to be taken to ensure that sufficient portion of the pipeline is in the undisturbed region. This in turn will ensure that the model is well capable of representing the actual conditions.

Considering the above factors the following set of data was chosen for the analysis planned.

Pipe Diameter: 1m

Pipe thickness: 0.01m

Length of Pipe Modeled: 400m

Pipe Material: Steel with E (Young's Modulus) 2.01×10^{11} Pa & Poisson's ratio 0.3. The material was assumed to behave as Linear Elastic. The density of the material was taken as 7800 Kg/m^3 .

Cover Depth: 0.9144m (3 feet)

Unit weight of Soil: 1700 Kg/m^3

Soil Friction Angle: 35°

Soil Cohesion: 5000 Pa

Fault displacement: 1m Vertical with 1m Lateral.

4.2 Finite Element Modelling

Any of the general purpose 3D finite element programs (e.g., ANSYS or ABAQUS) and special purpose 2D pipeline deformation analysis programs (e.g., PIPLIN) can be used for the analysis. Herein, the 3D finite element program ANSYS was chosen in light of the ease in modeling and incorporation of varied nonlinearities into the model.

4.2.1 Modelling of Pipe

ANSYS offers various modified beam elements which are especially meant for analysis relating to pipelines. 'Pipe Element 16' a uniaxial elastic beam element with tension-compression, torsion, and bending capabilities was chosen for the current study. This element is based on the three-dimensional beam element, and includes simplifications due to symmetry and standard pipe geometry. The reason for choosing an elastic element is that most of the available results so far are the ones obtained using similar elastic elements. The model with these elements would account for the pipe axial and bending resistance. The element has six degrees of freedom at two nodes: translations in the nodal x, y, and z directions and rotations about the nodal x, y, and z axes. [13] The geometry, node locations, and the coordinate system for this element are shown in Fig. 3.2.1

For simplicity, the pipe is assumed to be initially straight with a uniform depth of soil cover. The pipe element lengths can be varied to insure adequate mesh refinement in regions of high transverse soil forces and significant bending. Progressively longer element lengths can be used in sections of the model where there is no significant pipe or soil deformation. But such a model would demand for variety of soil springs to model soil interaction. Thus elements of equal length of 1m were used to model the entire span of 400m of pipeline.

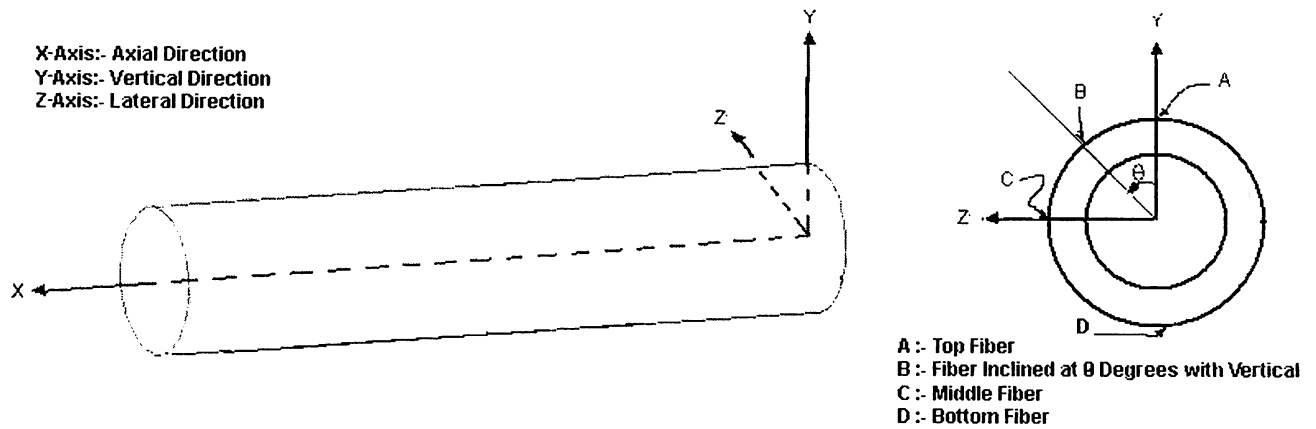


Fig. 4.2.1 Pipe Element Terms and Definitions

For making the interpretation of results easier modelling was done in a way such that the elemental coordinate system matches with the Global coordinate system. Thus longitudinal axis of the pipeline is along the X-axis, vertical direction is along the Y-axis & lateral direction is along Z-axis. Further all angles are measured positive in an anticlockwise sense from positive direction of Y-axis. Total mass of the element m_e is calculated as

$$m_e = m_w + (\rho_f A^i) L \quad (3.1)$$

where

$$m_w = \begin{cases} \rho A L & \text{if } m_w = 0.0 \\ m_w & \text{if } m_w > 0.0 \end{cases} \quad (3.2)$$

m_w is the alternate pipe mass if input by user, L is the length of the pipeline, ρ_f is the internal fluid density, ρ is the pipe material density, A is the pipe cross sectional area given by

$$A = \pi \frac{(D_o^2 - D_i^2)}{4} \quad (3.3)$$

and A^i is the pipe internal area given by

$$A^i = \frac{\pi D_i^2}{4} \quad (3.4)$$

D_o and D_i are outer and inner diameters respectively. If pipe thickness is given by t_w then

$$D_i = D_o - 2t_w \quad (3.5)$$

4.2.2 Modelling of Soil

The distributed soil resistance is modeled as a Winkler foundation, i.e., the soil support is modeled as a series of discrete springs which provide a specified resistance per unit length of pipe. For a rigorous analysis and design approach for buried pipelines the model involves a nonlinear pipe-soil interaction analysis. The soil resistance is typically idealized as an elastic-perfectly-plastic springs.

Axial spring restraints account for resistance of the soil caused by adhesion and friction along the pipeline wall which resists movement of the pipeline in the soil. Transverse spring restraints are used to simulate horizontal and vertical soil resistance perpendicular to the axis of the pipeline. For analysis in the horizontal plane, transverse springs generally are assigned the same properties for displacement to the left or right of the pipeline centerline. The same is true for longitudinal springs as the pipe will behave in symmetrical fashion along its axis. In the vertical plane, however, transverse springs have different upward and downward characteristics to simulate the effect of downward bearing of the pipeline or upward breakout resistance of the soil.

Soil properties representative of the backfill should be used to compute axial soil spring forces. Other soil spring forces should generally be based on the native soil properties. Backfill soil properties are appropriate for computing horizontal and upward vertical soil spring forces only when it can be demonstrated that the extent of pipeline movement relative to the surrounding backfill soil is not influenced by the soils outside the pipe trench.

Expressions for obtaining the values of limiting value of forces and the corresponding slip for each of these springs have been already outlined in Sec. 2.3. These were used to arrive at the value of spring stiffness taking into account the element size. e.g. if ' F_u ' is the maximum force that can be imposed by the soil on the pipeline per unit length in an arbitrary direction and D_u is the corresponding value of slip or displacement, then stiffness K_u in that direction for an element edge length L_e will be given by

$$K_u = \frac{F_u \times L_e}{D_u} \quad (3.6)$$

The values so obtained for 1m element length using equations of Sec. 2.4 are given in Table 3.1. (Until unless stated, all the spring stiffness values in this report are for unit element length)

Table 3.2.1 *Equivalent Soil Spring Stiffness*

| Spring | Maximum Force (N/m) | Slip/Yielding (m) | Stiffness (MN/m) |
|---------|---------------------|-------------------|------------------|
| Axial | 18291.3 | 0.004 | 4.572 |
| Lateral | 37313.6 | 0.056 | 0.659 |
| Bearing | 326291.0 | 0.150 | 2.117 |
| Uplift | 10274.7 | 0.013 | 7.491 |

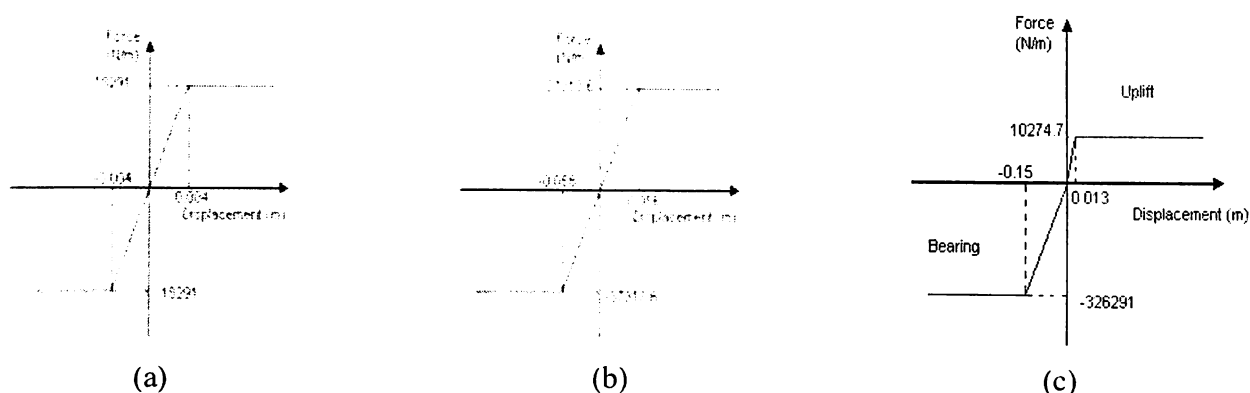


Fig. 4.2.2 *Bilinear Soil Spring Characteristics in (a) Axial, (b) Lateral and (c) Vertical Direction*

Two types of spring elements were chosen from ANSYS elemental library to model the nonlinear spring behaviour. Element COMBIN 40 was used for modeling transverse and longitudinal springs which show symmetric behaviour and COMBIN 39 was used for modeling vertical springs with different uplift and bearing behaviour. COMBIN 40 has an added advantage that at any stage springs can be modified to represent multilinear stiffness if required. Further it has an in built provision of lumping the mass eliminating the need of using any mass element separately. The element numbers and their connectivity is given in Table 3.2. Further the mass of the soil above the cover i.e. 1.5548 kN/m was lumped in between the nodes used for the springs.

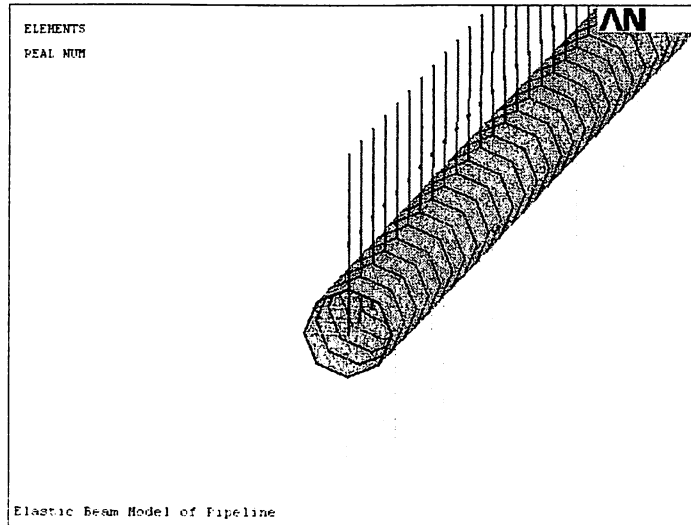


Fig. 4.2.3 *Elastic Beam Model of Pipeline with equivalent Soil Springs in ANSYS*

A noteworthy point is that the node connectivity of elements should be such that it simulates the real conditions of different uplift and bearing stiffness of soil for imposed fault movement. Further it is to be born in mind that the way fault displacement will be induced is through guillotine type of movement at the base of the soil springs. The soil reaction forces resulting from such imposed displacement dictates the pipe movement. Hence for modelling the vertical springs with its base above the pipe, its compression stiffness will model the uplift behaviour of the soil and stiffness in tension will represent the bearing resistance characteristics of the soil. Thus a great care should be taken to model the proper behaviour of vertical springs. Figure 3.3 shows the final full model of the pipeline along with the soil springs in 3 directions as modeled in ANSYS.

4.2.3 Boundary Conditions

If the pipe and burial conditions are symmetric about the fault region, symmetric boundary condition (i.e., zero rotation and zero longitudinal translation) can be imposed at the end of the model corresponding to the center of the section, in order to reduce the required size of the model. Since the behaviour of the pipeline is itself the objective of the study it was thought better to model the fault at the centre line and not exploit the seeming symmetric nature of the problem. The set of imposed boundary conditions are enlisted in Table 3.3. The model length should be long enough that the boundary condition specified at the remote end of the model has no influence on the analysis results, with zero axial strains at the ends of the model. The details have already been explained in Sec. 3.1.

For each analysis, a ground displacement profile is imposed at the base of the pipe-soil springs. The displacement profile is increased in small increments and the resulting pipe and soil deformation state is established at each increment. This is carried out in ANSYS by invoking the nonlinear solution approach.

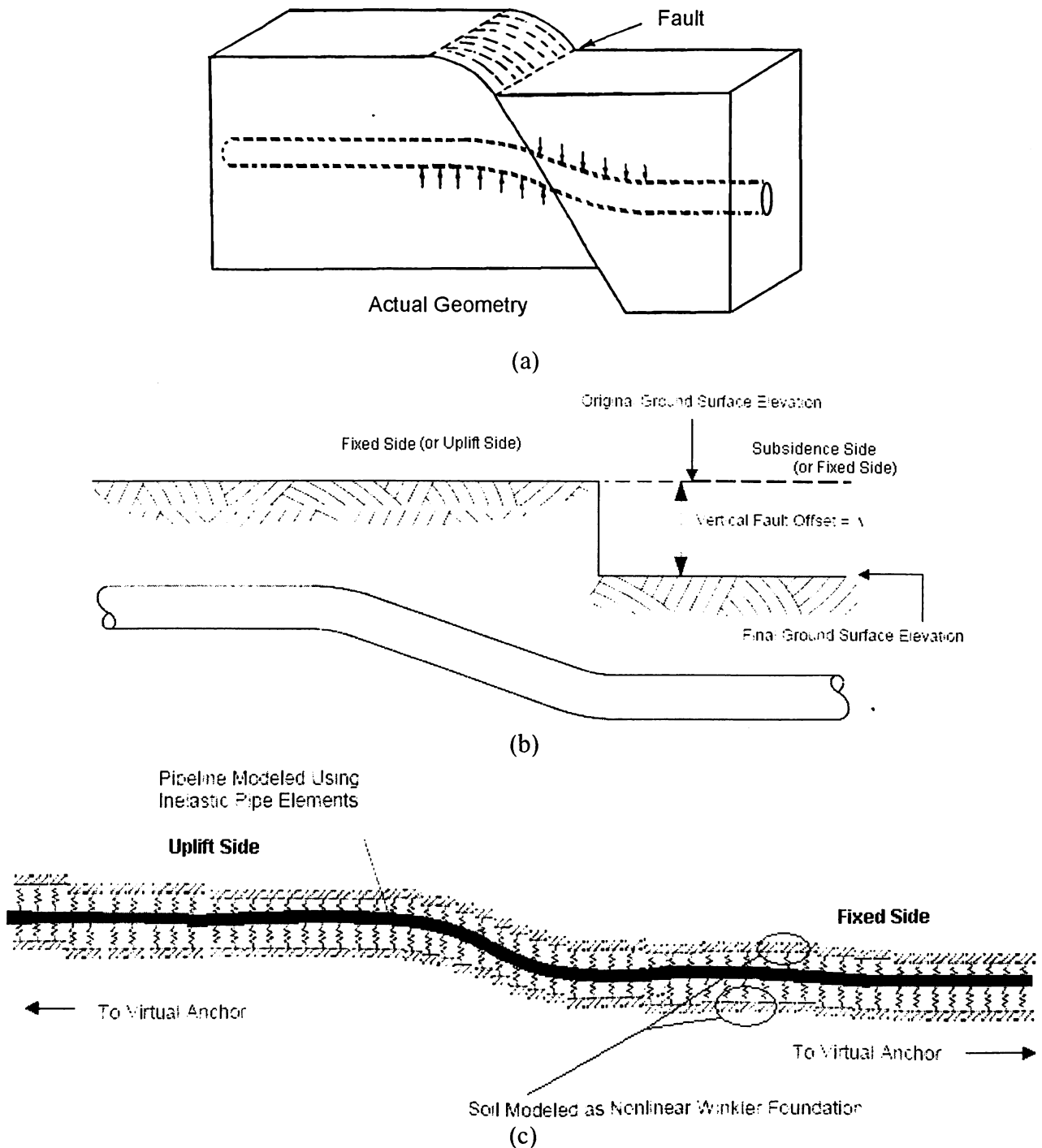


Fig. 4.2.4 (a) Actual Fault Geometry (b) Assumed Guillotine Type of Fault Displacement (c) Model of Pipeline under Fault Crossing in ANSYS.

4.3 Results

For the assumed set of data the analyses was carried out and following results were obtained:

- 1) Displacement profiles in vertical (along Y-Axis) and lateral (along Z-Axis) directions. The displacement and node definitions are illustrated in Fig. 3.5.

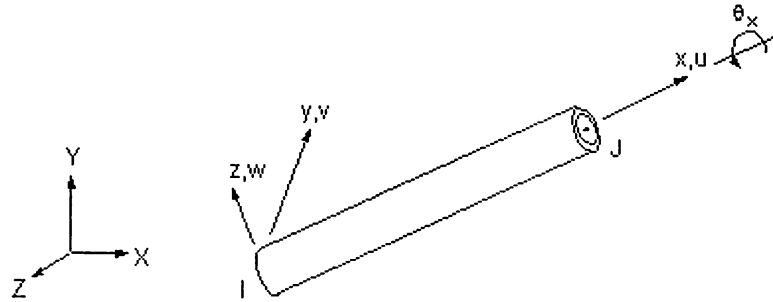


Fig. 4.3.1 Pipe Element Coordinate Axes, and Displacement Definitions

- 2) Once the pipe is forced by the surrounding soil across the fault crossing as described in Sec.2.3 the pipe will try to adjust to it. But owing to its stiffness and continuity the pipe will develop strains and will in turn resist the imposed forces by the surrounding soil. At an equilibrium where the resistance of the pipeline to move becomes equal to the forces imposed by the surrounding soil there will still be a reaction force at the pipeline-soil interface. This soil reaction force has also been studied in both vertical and lateral directions.
- 3) Bending stress σ_{bend} were calculated as

$$\sigma_{bend} = \frac{M_b D_o}{2I} \quad (3.7)$$

where, M_b is given as

$$M_b = \sqrt{M_y^2 + M_z^2} \quad (3.8)$$

M_y and M_z are moments about Y-axis and Z-Axis respectively.

I is given as

$$I_y = I_z = I = \pi \frac{(D_o^4 - D_i^4)}{64} \quad (3.9)$$

D_o and D_i are outer and inner diameters respectively. If pipe thickness is given by t_w , then

$$D_i = D_o - 2t_w \quad (3.10)$$

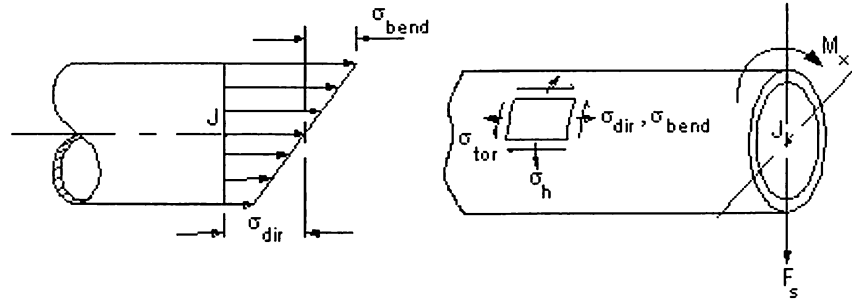


Fig. 4.3.2 Pipeline Stress Definitions

4) Bending Moments in both the directions were plotted.

5) When a model has only one functional direction of strains and stress, comparison with an allowable value is straightforward. But when there is more than one component, the components are normally combined into one number to allow a comparison with an allowable value. Thus, Von Mises Equivalent stresses at different circumferential locations of the pipe were studied. Further a plot of maximum Von Mises stress was compared with bending Stress distribution along the pipeline. The stresses were obtained from following equations.

The principal stresses ($\sigma_1, \sigma_2, \sigma_3$) are calculated from the strain components by the cubic equation:

$$\begin{vmatrix} \sigma_x - \sigma_o & \sigma_{xy} & \sigma_{xz} \\ \sigma_{xy} & \sigma_y - \sigma_o & \sigma_{yz} \\ \sigma_{xz} & \sigma_{yz} & \sigma_z - \sigma_o \end{vmatrix} = 0 \quad (3.11)$$

where, σ_o gives the values of these three principle stresses σ_1, σ_2 & σ_3 , arranged in descending positive magnitudes.

The Von Mises or equivalent stress σ_e is computed as

$$\sigma_e = \left(\frac{1}{2} \left[(\sigma_1 - \sigma_2)^2 + (\sigma_2 - \sigma_3)^2 + (\sigma_3 - \sigma_1)^2 \right] \right)^{\frac{1}{2}} \quad (3.12)$$

or

$$\sigma_e = \left(\frac{1}{2} \left[(\sigma_x - \sigma_y)^2 + (\sigma_y - \sigma_z)^2 + (\sigma_z - \sigma_x)^2 + 6(\sigma_{xy}^2 + \sigma_{yz}^2 + \sigma_{zx}^2) \right] \right)^{\frac{1}{2}} \quad (3.13)$$

where σ_x, σ_y & σ_z are direct stresses along the three coordinate axes respectively and σ_{xy}, σ_{yz} & σ_{zx} are shear stresses respectively.

- 6) Most of the available results are in terms of axial strain plots. This is so because buried pipeline failures are generally governed by strains. Thus, axial strains at different circumferential locations were plotted.

Axial stiffness K_l is given by

$$K_l = \begin{cases} \frac{AE}{L} & \text{if } k = 0.0 \\ k & \text{if } k > 0.0 \end{cases} \quad (3.14)$$

where, k is user specified stiffness value, A is the cross sectional area as defined earlier, L is the length of the pipeline.

Direct (axial) stress σ_{dir} is given by

$$\sigma_{dir} = \frac{F_x}{A} \quad (3.15)$$

where, F_x is the axial force & A is the cross sectional area.

Then, total stress σ_x in axial direction would be given by

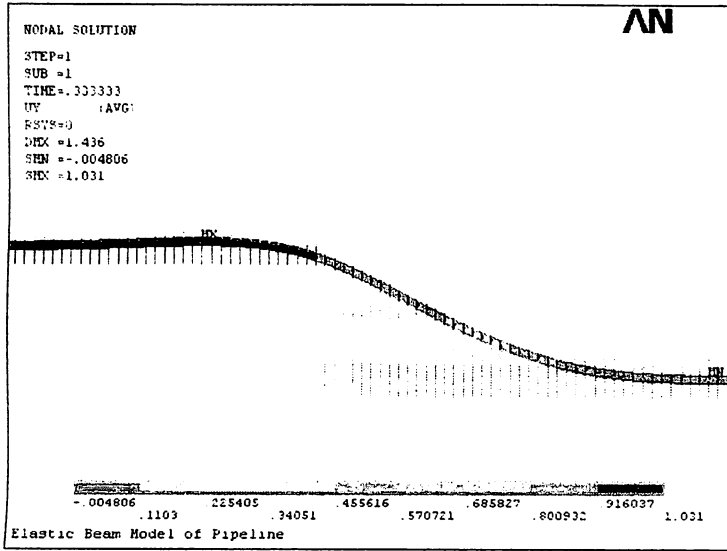
$$\sigma_x = \sigma_{dir} + A\sigma_{bend} \quad (3.16)$$

Axial stress σ_x could be related with the axial strain ϵ_x by the equation

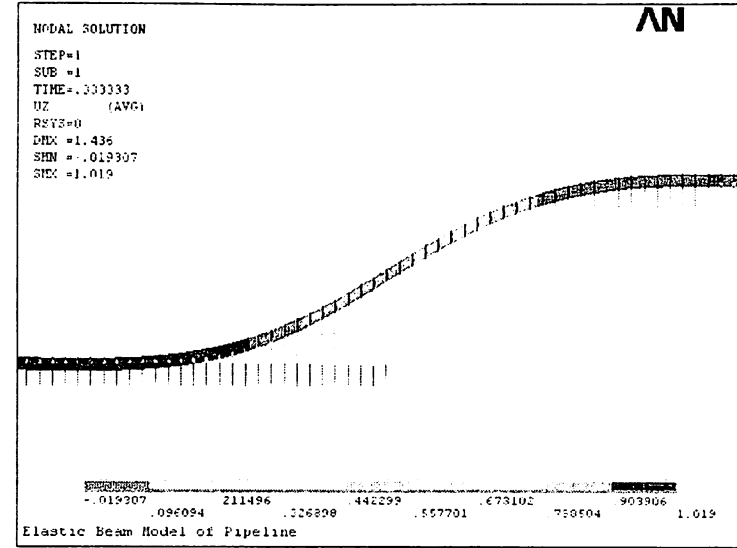
$$\sigma_x = E\epsilon_x \quad (3.17)$$

where, E is the Young's modulus of the pipe material.

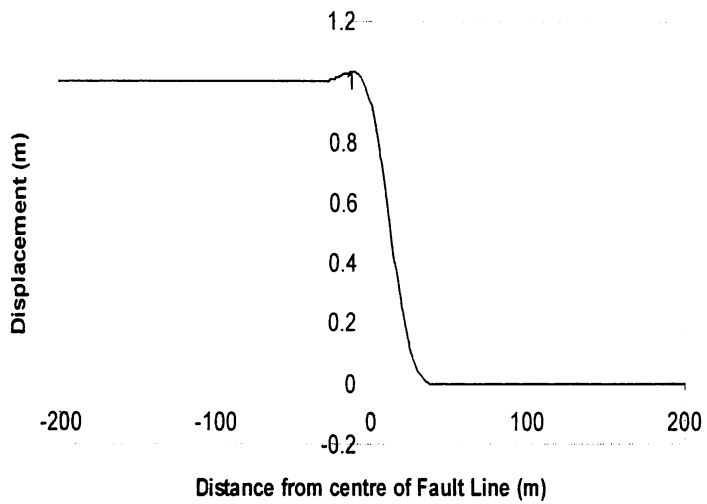
The definitions of the various locations have been illustrated in Sec.4.2.1 & Fig. 4.2.1



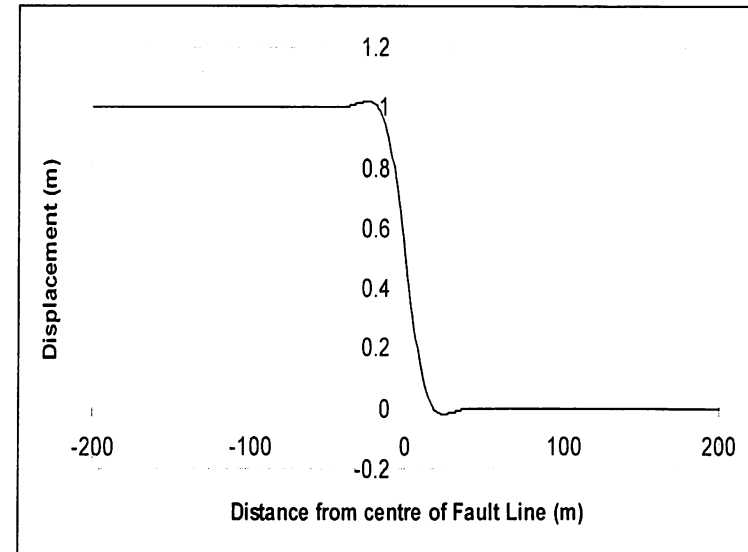
(a) Elevation (Vertical Deformation)



(b) Plan (Lateral Deformation)



(c) Pipe Displacement in Vertical direction



(d) Pipe Displacement in Lateral Direction

Fig. 4.3.3 Displacement Profiles

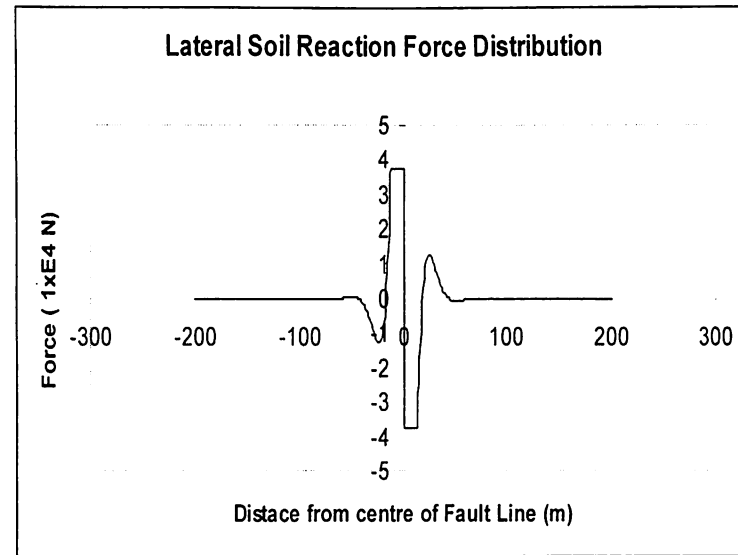
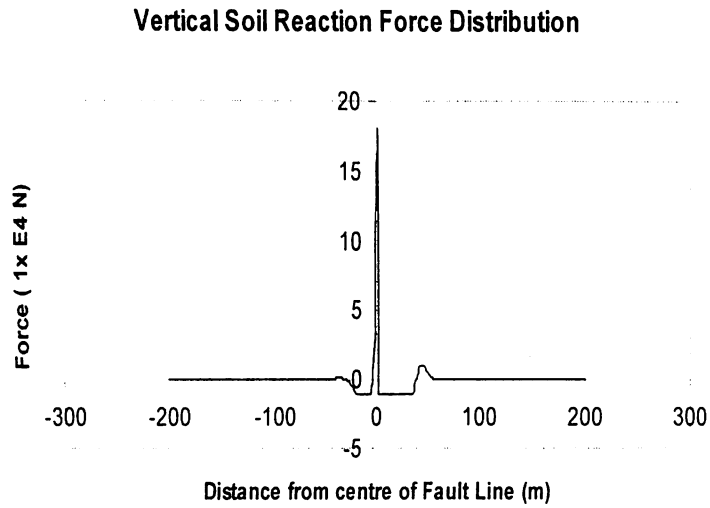


Fig. 4.3.4 Soil Reaction Force Profile in Vertical and Lateral Directions

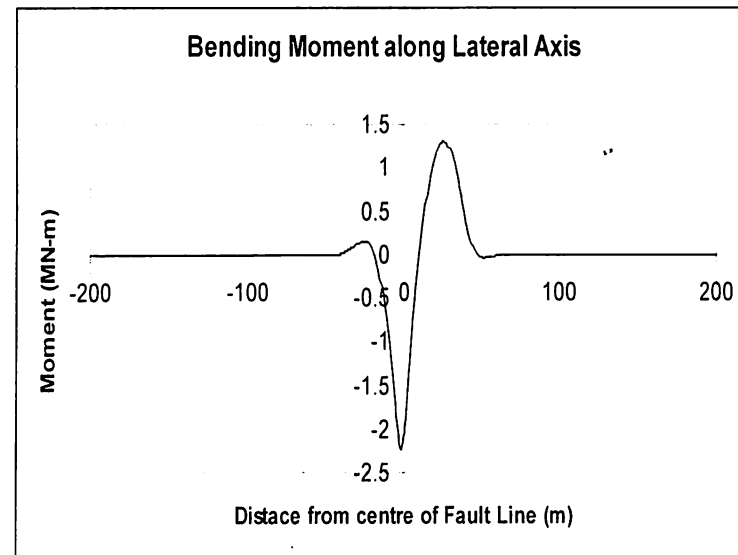
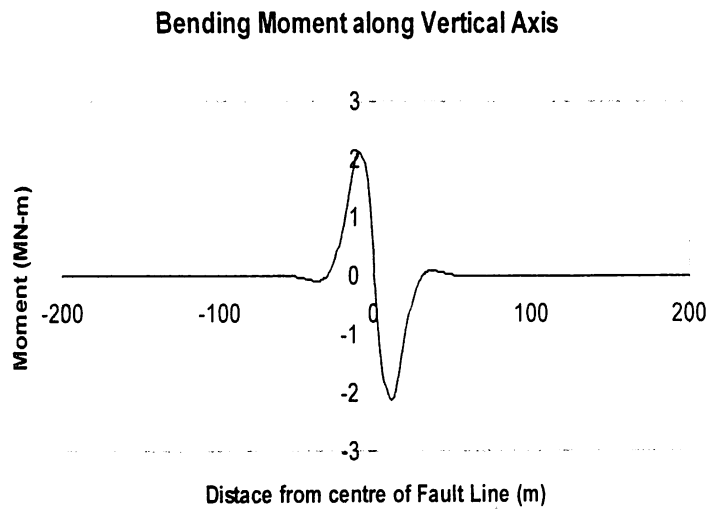


Fig. 4.3.5 Bending Moment Distribution along the Pipeline in Vertical and Lateral Directions

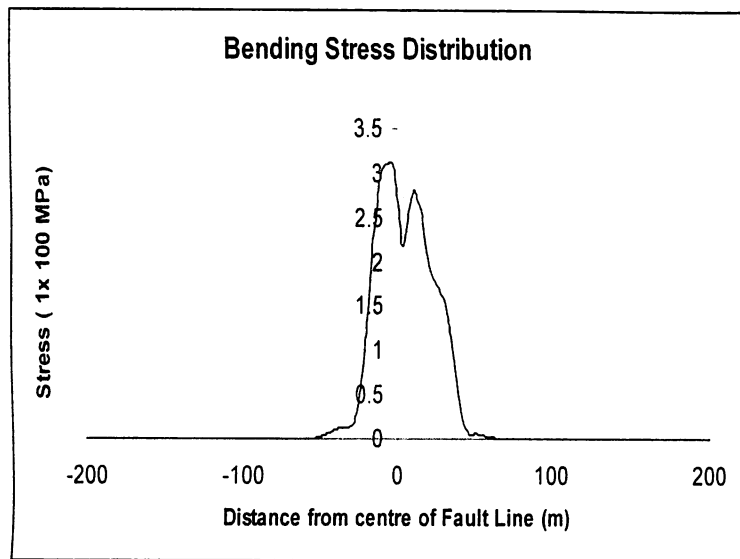


Fig. 4.3.6 *Bending Stress Distribution*

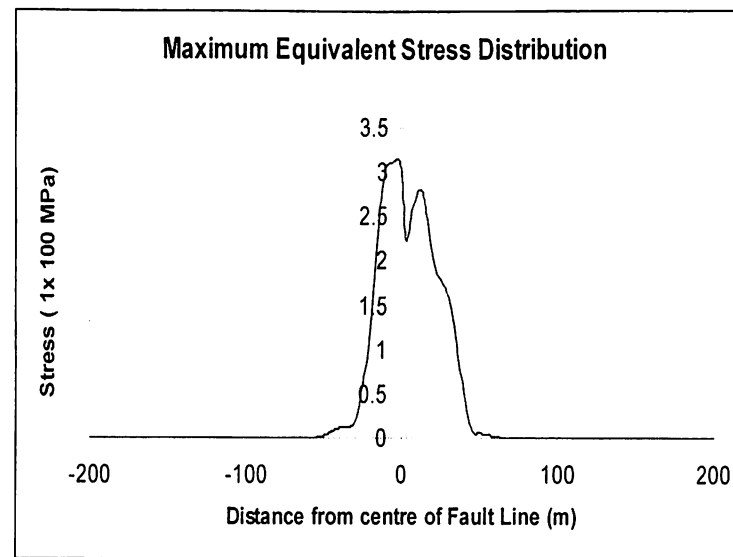


Fig. 4.3.7 *Maximum Equivalent Stress Distribution*

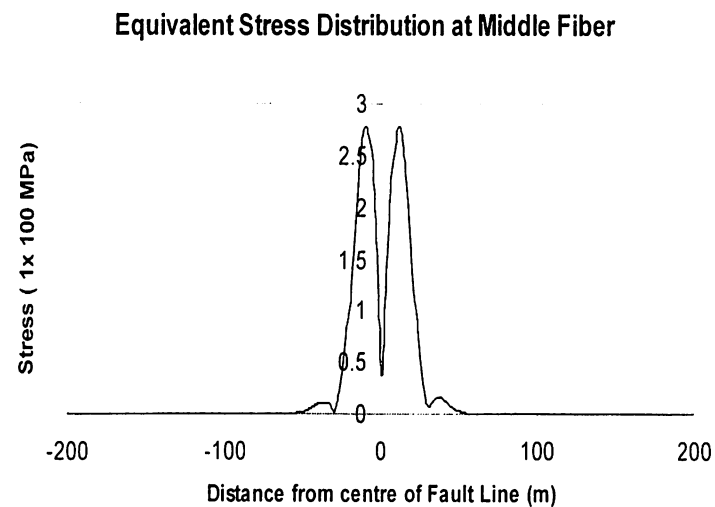
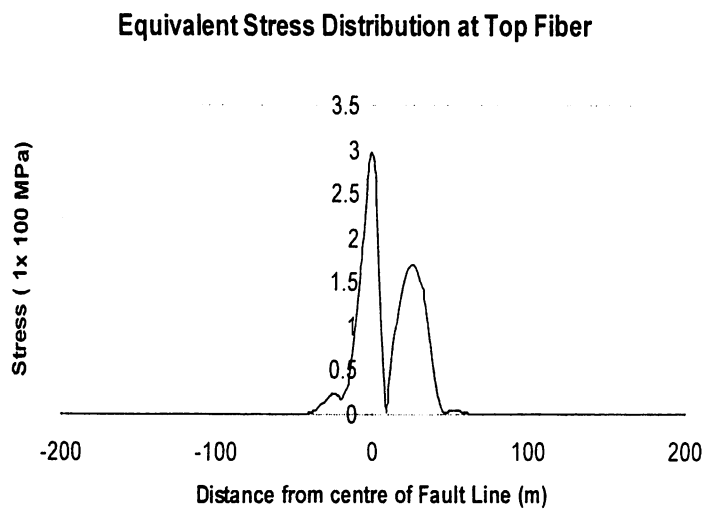
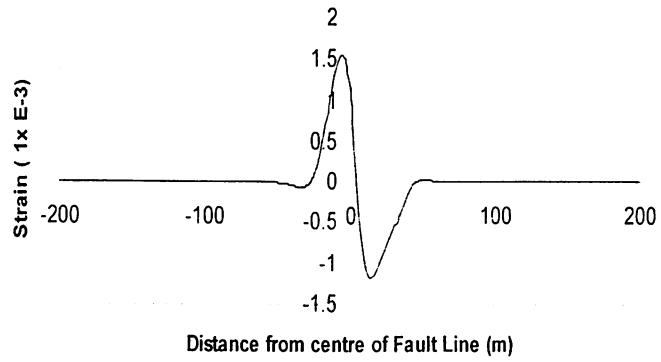


Fig. 4.3.8 *Equivalent Stress Distribution in Vertical and Lateral Directions*

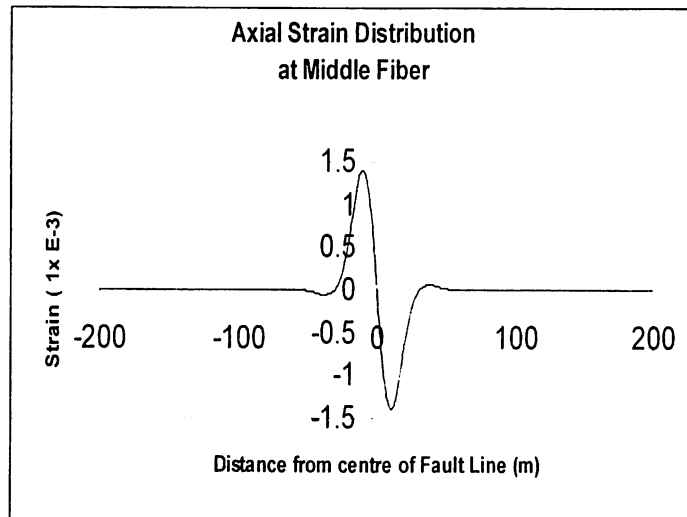
(a)

**Axial Strain Distribution
at Fiber Inclined at 45 Degrees**



(b)

**Axial Strain Distribution
at Middle Fiber**



(c)

**Fig. 4.3.9 Strain Distribution along the pipeline at
(a) Top Fiber, (b) Fiber inclined at 45° to horizontal & (c) Middle Fiber of the Pipeline**

5. PARAMETRIC ANALYSIS

For a typical ground displacement configuration, a range of analyses can be performed to investigate various model parameters, such as pipe thickness, pipe steel grade, span length, cover depth, soil strength, etc.

5.1 Data for Parametric Study

Based upon Sec. 3.1 the following 7 major parameters were studied to get a better understanding of their affects on behaviour of pipeline crossing fault.

- i) Pipe Diameter: 0.25m, 0.5m & 1.0m.
- ii) Pipe Thickness: 0.01m, 0.015m & 0.02m.
- iii) Pipe Material: 1.6 e11 Pa, 1.8 e11 Pa & 2.01 e11 Pa.
- iv) Fault Displacement: 1m, 2m & 3m.
- v) Cover Depth: 1m, 2m & 3m
- vi) Soil Cohesion: 0 kPa, 5 kPa & 10 kPa.
- vii) Soil Friction Angle: 0°, 20°, & 35°.

Other than the parameter under study all other values were same as in Sec 3.1.

5.2 Modelling for Parametric Study

The pipeline-soil model remains essentially the same as in Sec.3.2 The difference lies in the values of the real constants or imposed value of the displacements. For most cases the soil spring specifications vary and a special purpose program which was written for this purpose. Thus all the stiffness values were calculated using this program based upon the equations as outlined in Sec. 2.5. During literature review it was found that many of these parameters weren't studied. Further the simplified beam model has so far not been exploited for this purpose. Certainly using the beam elements is much simpler in every respect then using shell elements. It is further a general observation that even in the parametric analysis that have been carried out so far its affect on the soil stiffness and the nonlinear behaviour of the soil has not been properly taken into account. Boundary conditions remain same as in Sec. 3.2 except for the case of varying fault displacement wherein the 1m values are replaced by corresponding value of displacement.

For different values of fault displacements, pipe thickness and pipe materials resistance of the surrounding soil will remain the same as depicted in Table 3.1. Thus same values were used for all three different values of each parameter.

Since the soil resistance to the pipelines will differ for different values of pipe diameters, cover depths, soil cohesion and soil friction angles they were computed using the formulae outlined in Sec.2.5. While considering different values of cover depth soil density was increased with the depth to model realistic situation. Thus soil densities used for 1m 2m & 3m cover depth were 1700 kg/m^3 , 1800 kg/m^3 & 2000 kg/m^3 respectively.

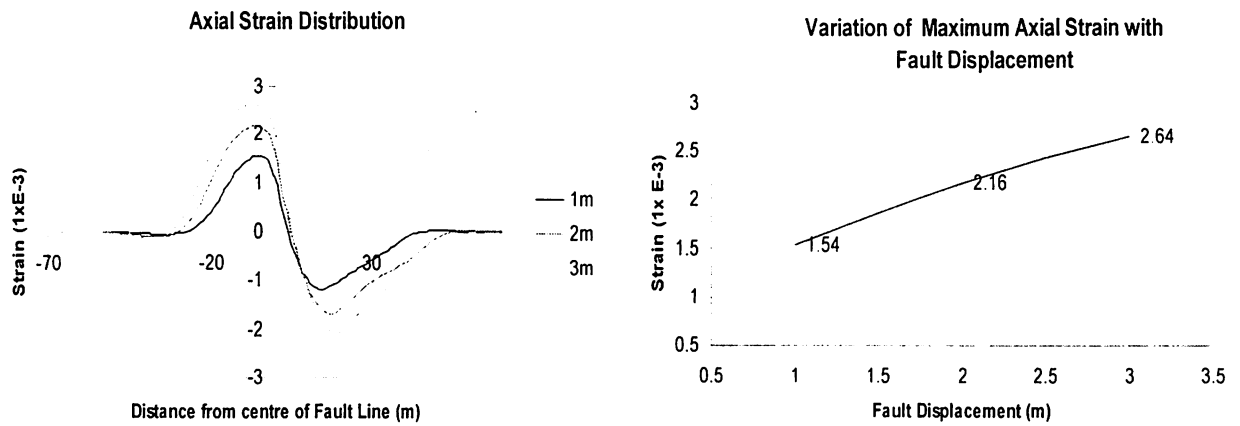
5.3 Results

Through the series of analysis it was found out that bending moment and the soil reaction forces followed the same pattern of variation i.e. nature of one can be used to predict the nature of the other. Thus based upon the discussions from previous analysis (Sec.3.3 & 3.4) following items (or parameters) were chosen for the current study for each parameter which was varied.

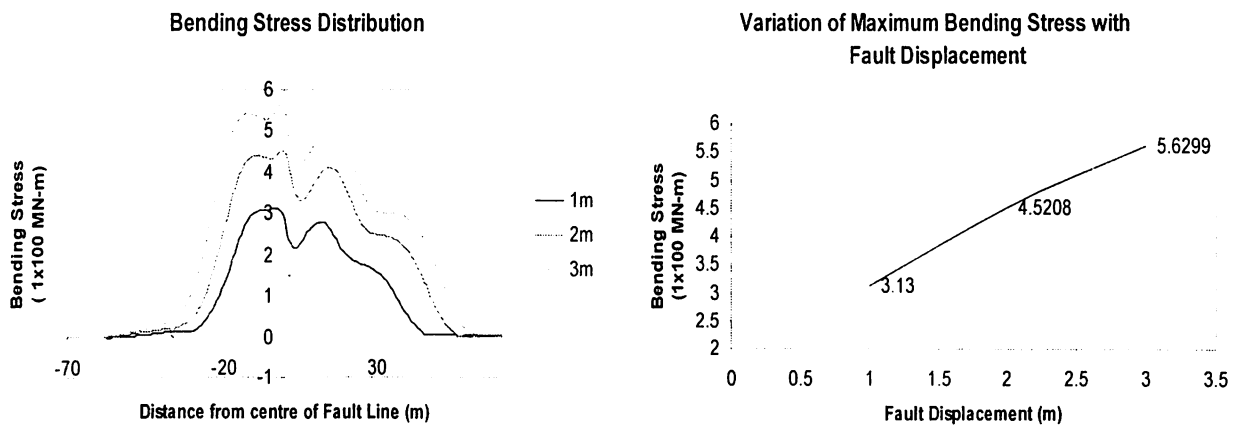
- i) Axial Strain at 45° to the vertical axis.
- ii) Bending Stress.
- iii) Soil reaction force in vertical direction.

Keeping in view that reaction forces can give additional information like length of affected pipe length and distance from the centre of fault line to which the soil is mobilized due to slipping it was chosen as one of the items instead of bending moment.

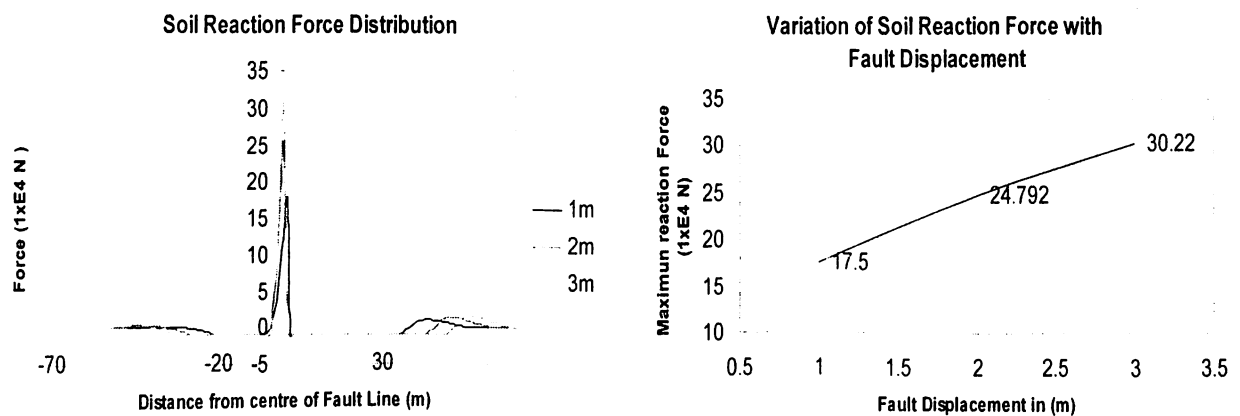
All the elemental definitions and the terminologies are identical to the one outlined in Sec. 3.2.1



(a)

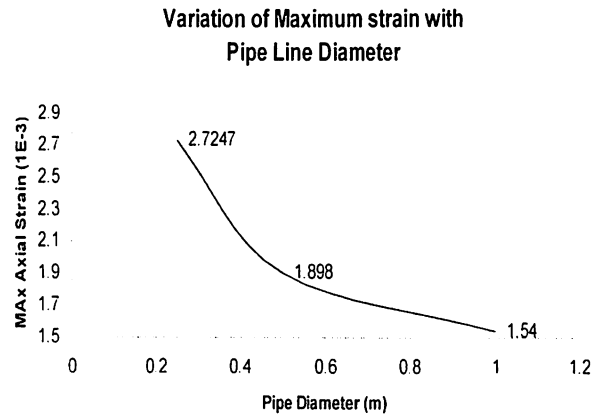
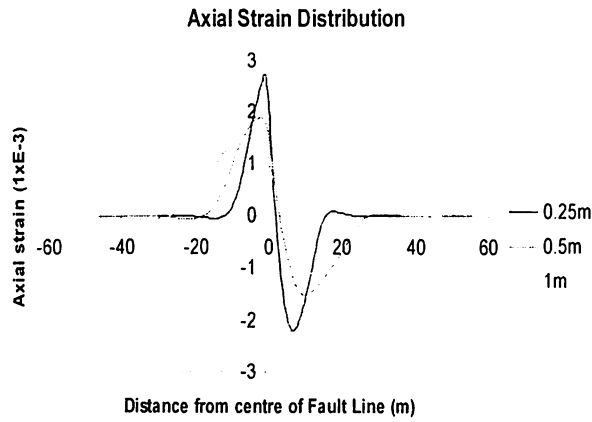


(b)

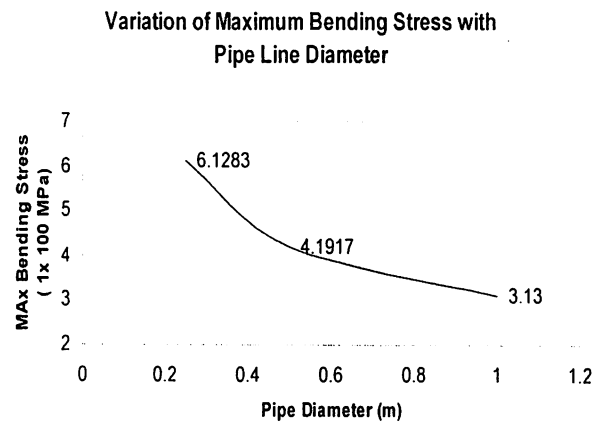
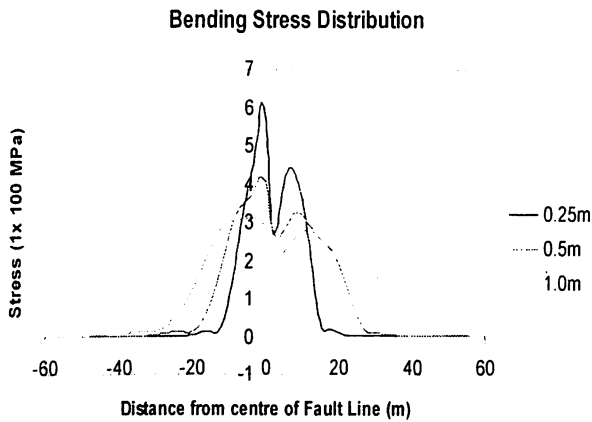


(c)

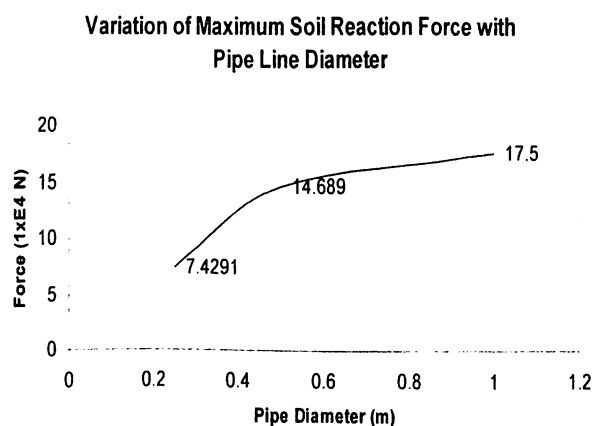
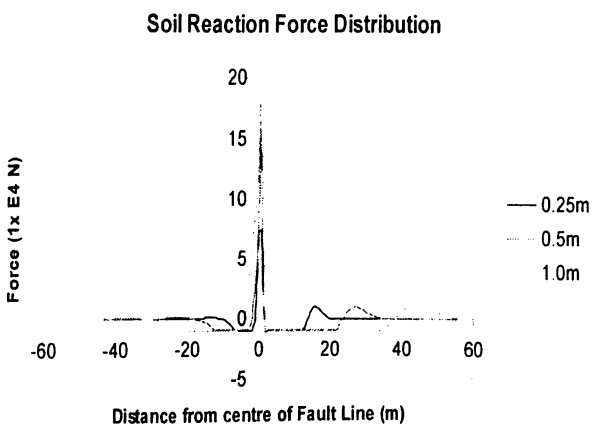
Fig. 5.3.1 *Affect of Fault displacement on (a) Axial Strain (b) Bending stress (c) Soil Reaction Forces*



(a)

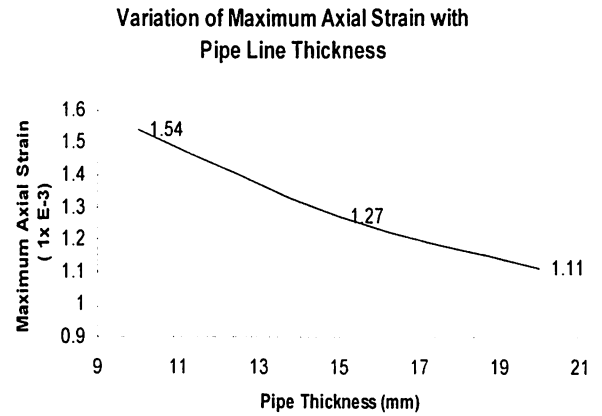
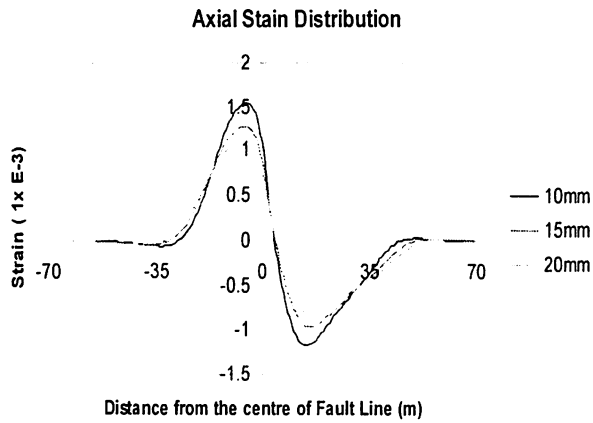


(b)

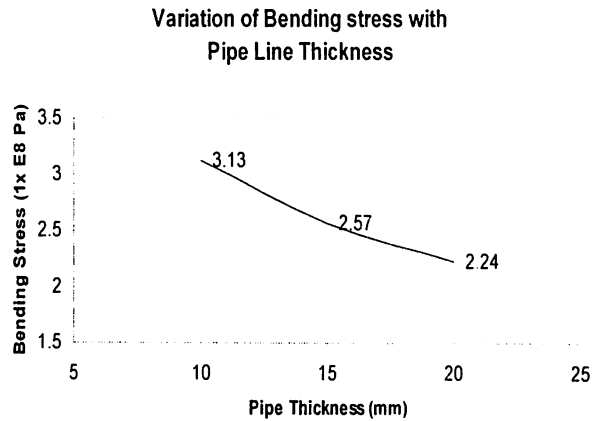
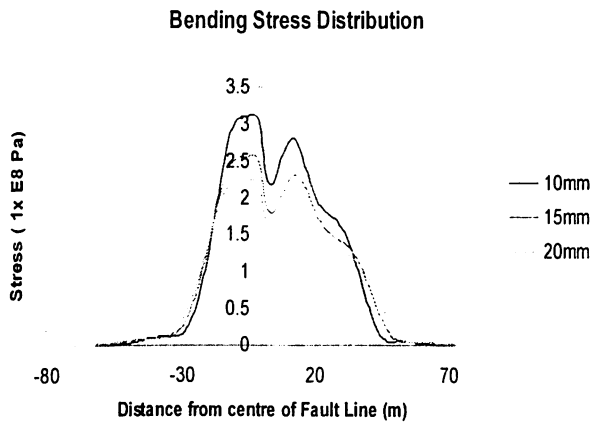


(c)

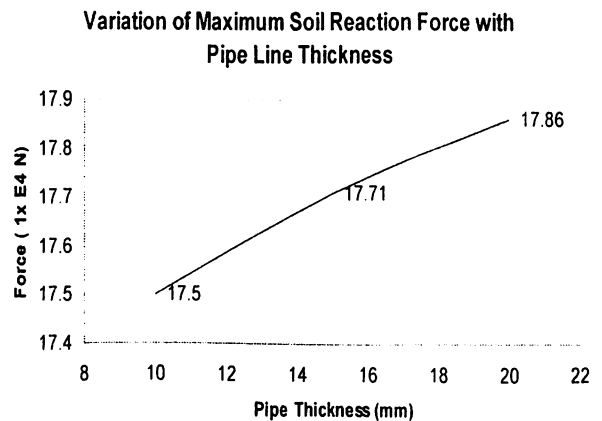
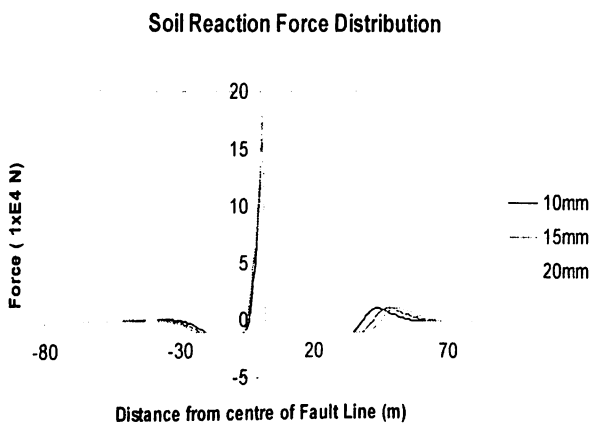
Fig. 5.3.2 Affect of Pipe Diameter on (a) Axial Strain (b) Bending stress (c) Soil Reaction Forces



(a)

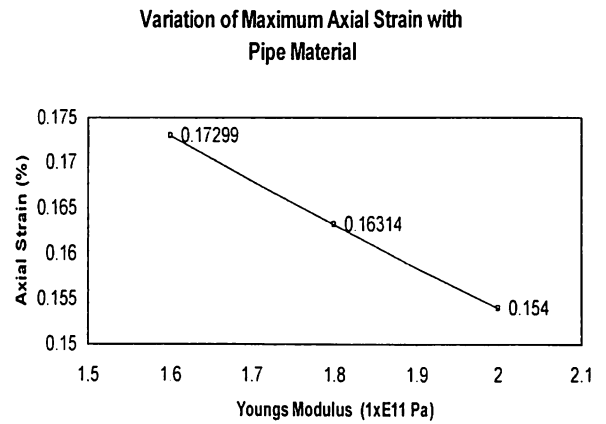
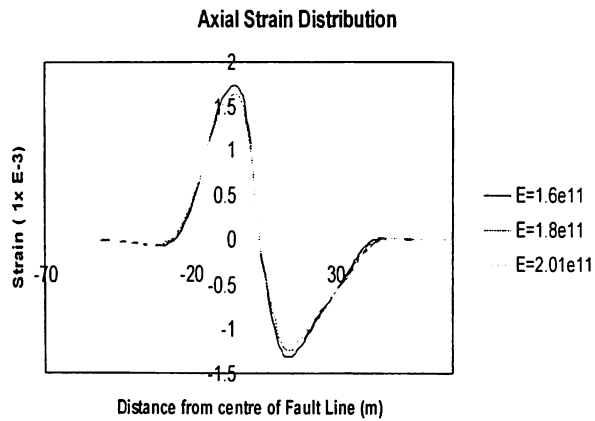


(b)

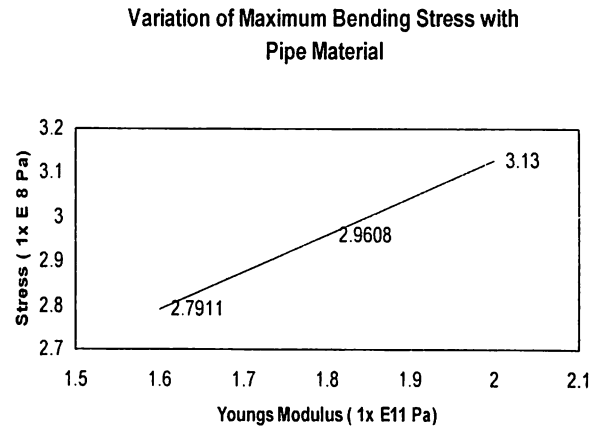
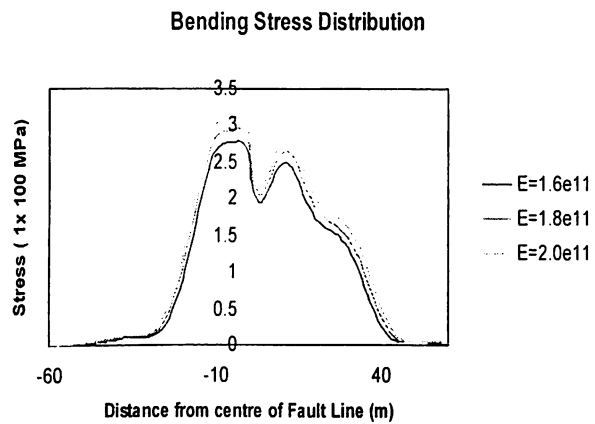


(c)

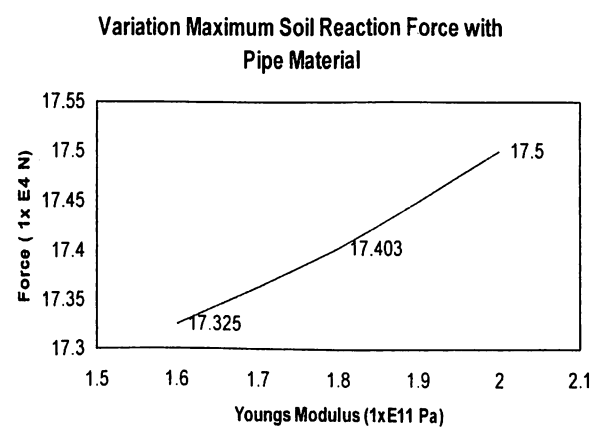
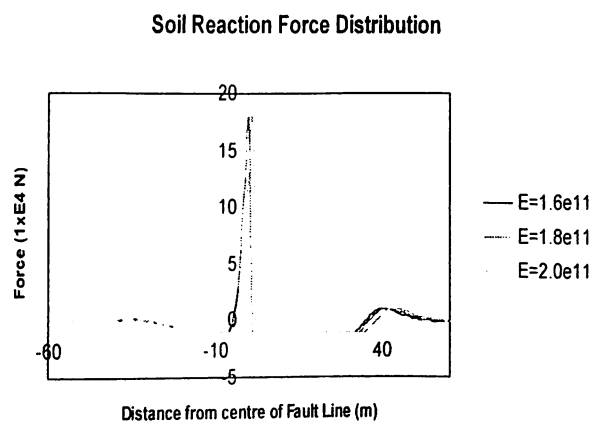
Fig. 5.3.3 Affect of Pipe Thickness on (a) Axial Strain (b) Bending stress (c) Soil Reaction Forces



(a)

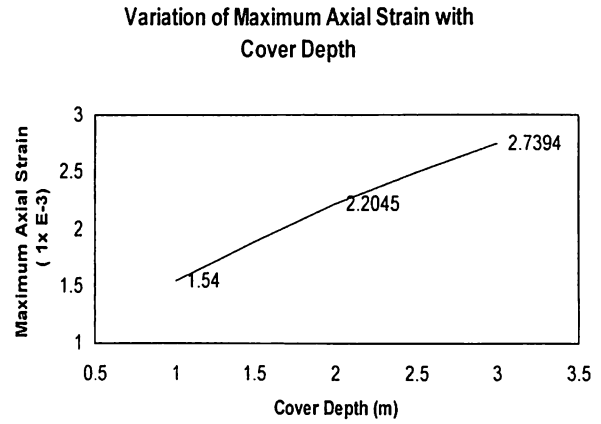
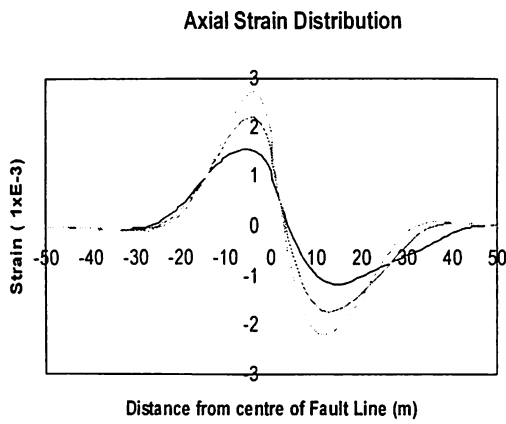


(b)

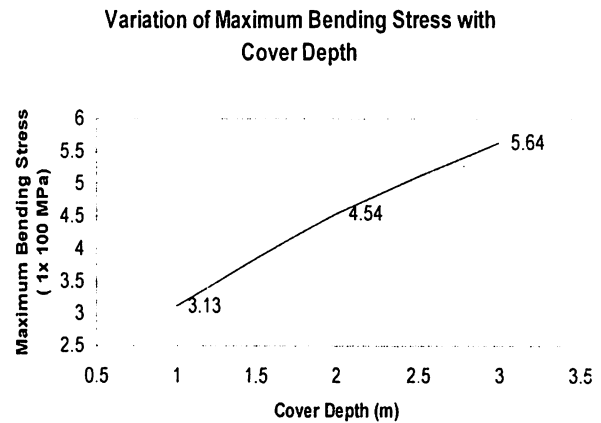
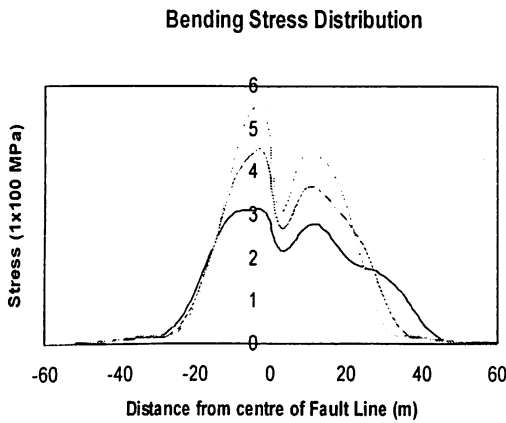


(c)

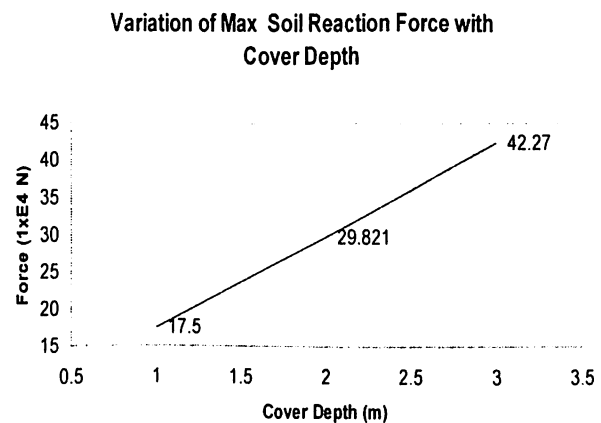
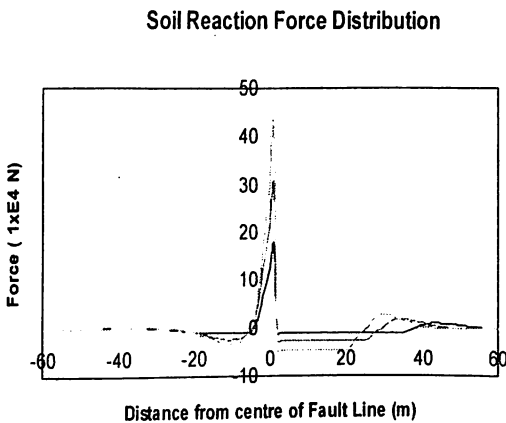
Fig. 5.3.4 Affect of Pipe Material on (a) Axial Strain (b) Bending stress (c) Soil Reaction Forces



(a)

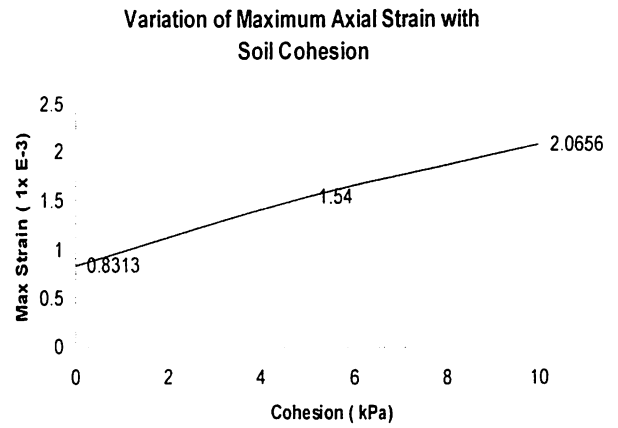
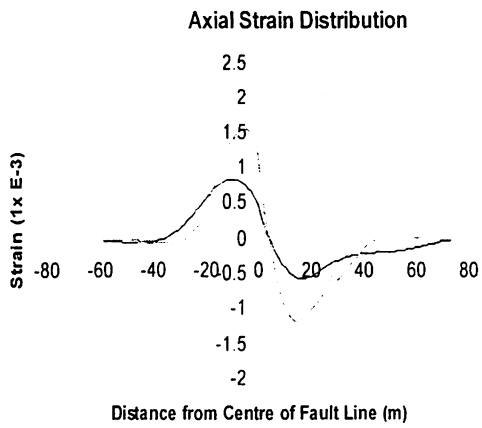


(b)

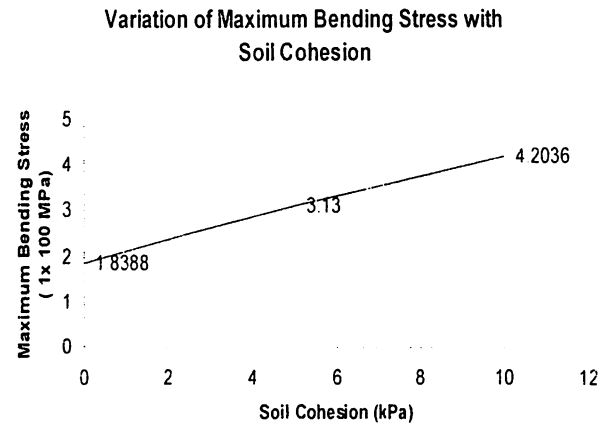
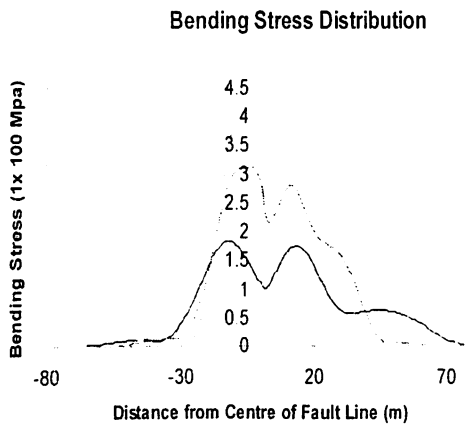


(c)

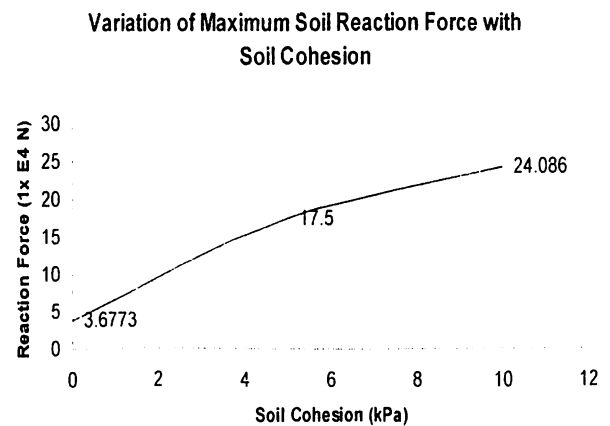
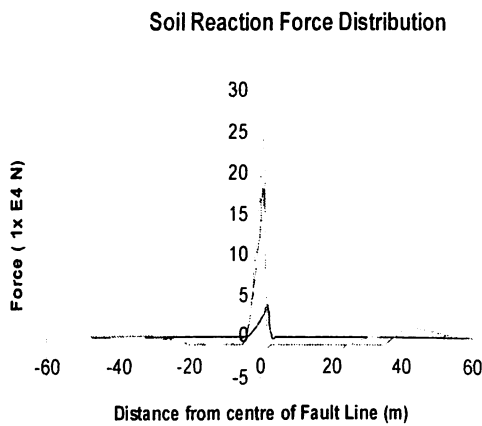
Fig. 5.3.5 *Affect of Cover Depth on (a) Axial Strain (b) Bending stress (c) Soil Reaction Forces*



(a)

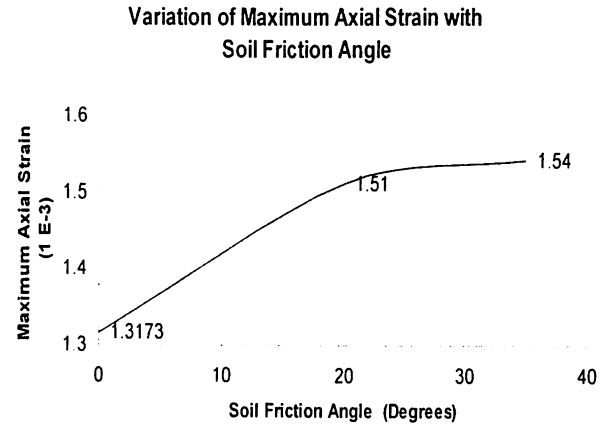
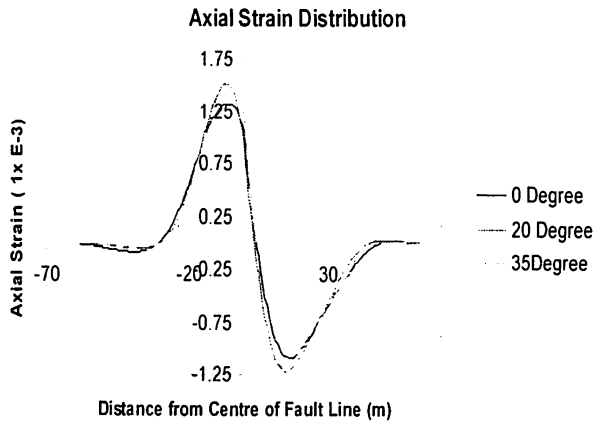


(b)

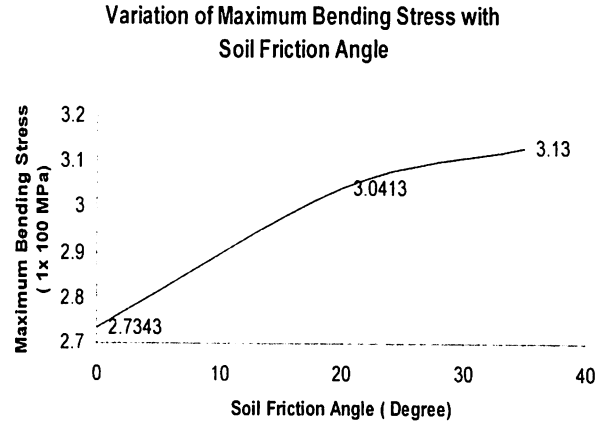
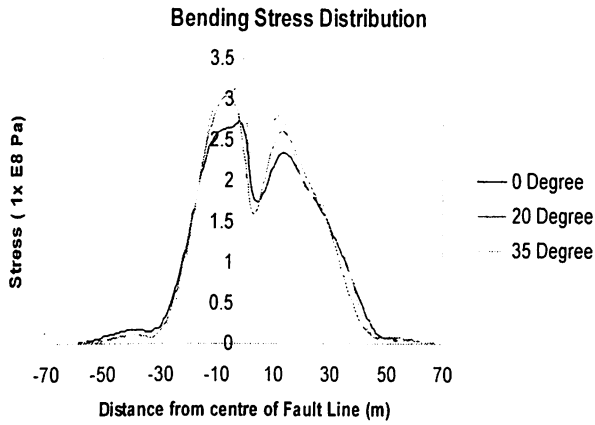


(c)

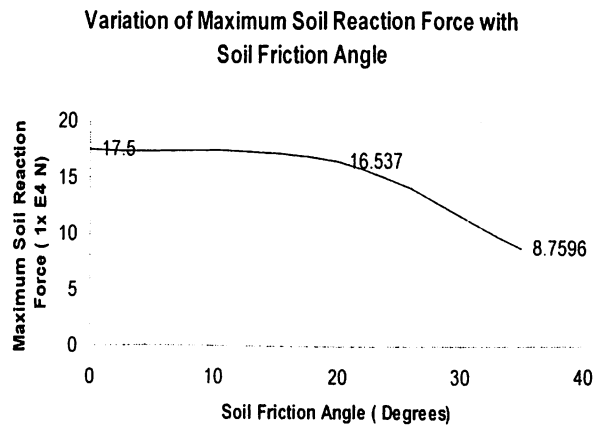
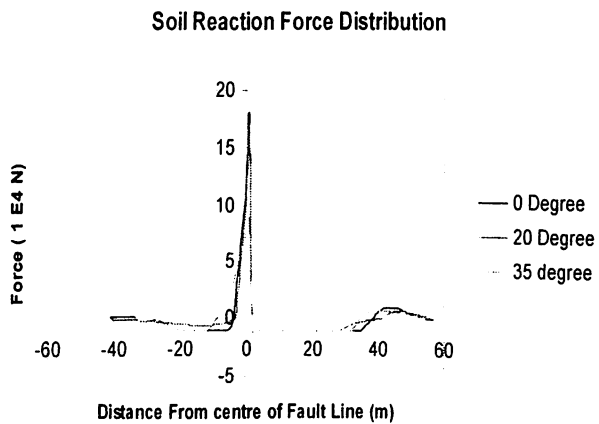
Fig. 5.3.6 *Affect of Soil Cohesion on (a) Axial Strain (b) Bending stress (c) Soil Reaction Forces*



(a)



(b)



(c)

Fig. 5.3.7 Affect of Soil Friction Angle on (a) Axial Strain (b) Bending stress (c) Soil Reaction Forces

6.1 Design criteria for Buoyancy due to liquefaction :

When the liquefaction of the soil around the pipeline occurs, buoyancy forces are exerted upon pipeline and must be resisted by anchors and the drag forces imposed by the liquefied soil as the pipeline begins to elevate.

Buoyancy effects are probably of greatest concern in areas such as flood plains and estuaries where massive liquefaction could take place in a large earthquake. When the surface liquefies, the pipe keeps uplifting at most to a position where a portion of pipe is at ground surface near the centre of the liquefied zone. However, when a non-liquefied soil layer is present as a cover over liquefied layer, the pipe come to rest at the interface of the non-liquefied and liquefied layer.

6.2 Buoyant force on pipeline :

The net upward force on unit length of pipeline is:

$$F_b = \frac{\pi D^2}{4} (\gamma_{sat} - \gamma_{content}) - \pi D t \gamma_{pipe} \quad (8)$$

Where

- F_b = Upward force due to buoyancy per unit length of pipe
- γ_{sat} = Saturated unit weight of soil
- $\gamma_{content}$ = Unit weight of pipe content
- γ_{pipe} = unit weight of pipe material
- D = Diameter of the pipe
- t = Thickness of the pipe

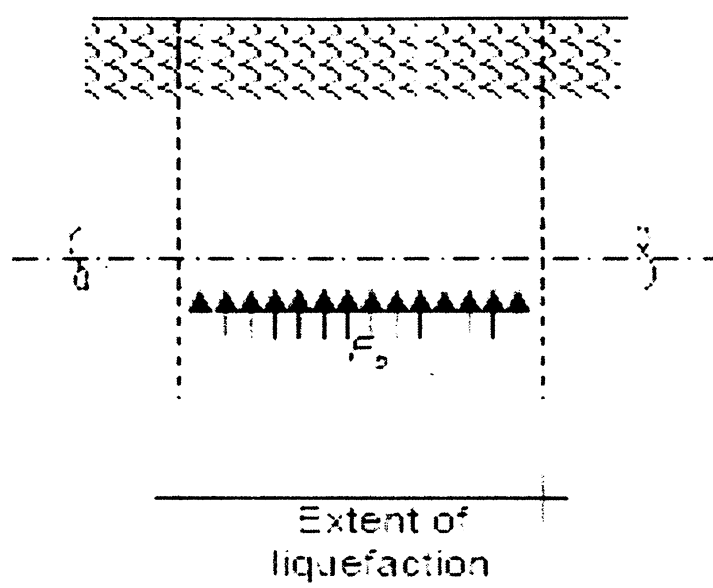


Fig 6.2.1 Longitudinal section of the pipeline showing the force upon it due to buoyancy (ALA, 2001)

6.3 Bending strain in the pipe due to buoyancy:

The bending strain in the pipeline due to uplift force may be approximated as:

$$\epsilon_b = \pm \frac{F_b L_l^2}{3\pi E t D^2} \dots\dots\dots(9)$$

Where,

E = Modulus of elasticity of pipe material

t = Thickness of the pipeline

Ll= Length of the pipe subjected to liquefaction

While calculating the bending strain, the pipe is considered as a stiff beam restrained due to non-liquefied soil beyond the margins of liquefied zone.

6.4 Let us analyze the effect of buoyancy on different size and thickness of pipelines under same operating conditions.

Example :

Four pipelines of different diameters as 12", 18", 24" and 30" which are operating under the same pressure of 75 Kg / cm²

The buoyancy due to liquefaction of the surface layer over a pipe length of 100m, where the saturated unit weight of the soil is 19.5kN/m³

The pipes are of API X-65 grade and with different thickness depending upon the class zone like class II, class III, class IV.. etc.

The table shows the thickness of the pipes used for various classes .

| D = 12" | D = 18" | D = 24" | D = 30" |
|------------|------------|------------|------------|
| t = 6.4 mm | t = 8.7mm | t = 11.1mm | t = 14.3mm |
| t = 7.1mm | t = 10.3mm | t = 14.3mm | t = 17.5mm |
| t = 12.7mm | t = 12.7mm | t = 17.5mm | t = 20.6mm |

Solutions :

Due to the liquefaction of upper soil layer, the net upward force on unit length of pipeline is:

$$F_b = \frac{\pi D^2}{4} (\gamma_{sat} - \gamma_{content}) - \pi D t \gamma_{pipe}$$

Where,

F_b = Upward force due to buoyancy per unit length of pipe

γ_{sat} = Saturated unit weight of soil = 19500 N/m³

$\gamma_{content}$ = Unit weight of pipe content = 0 Is the pipe empty?

γ_{pipe} = unit weight of pipe material = 76977.1 N/m³

The bending strain in the pipeline due to uplift force may be approximated as:

$$\epsilon_b = \frac{F_b L^2}{3 \pi E t D^2}$$

Where

E = Modulus of elasticity of pipe material

t = Thickness of pipeline

L = Length of pipe subjected to liquefaction

The allowable strain in compression = ϵ_{cr-c}
 = 0.175 (t/R) (O'Rourke, X.Liu, Raul Berrones, 1995)

Where

t = thickness of the pipe

R = radius of the pipeline

Results:

Fig 6.4.1

Strain Vs Thickness for 12" Pipeline

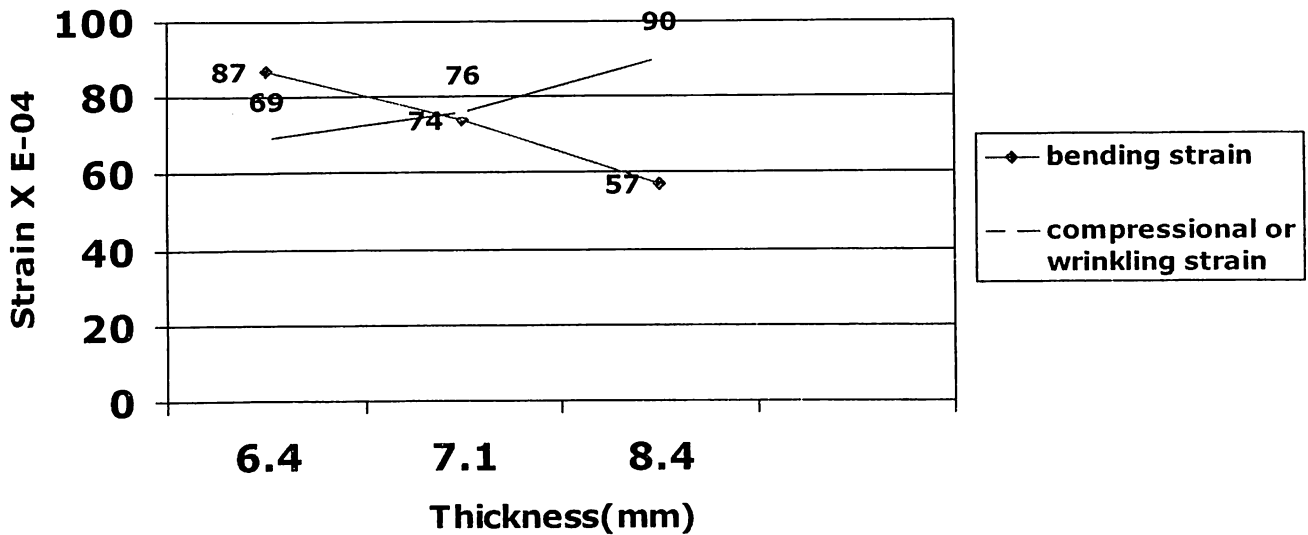


Fig 6.4.2

Strain Vs Thickness for 18" Pipeline

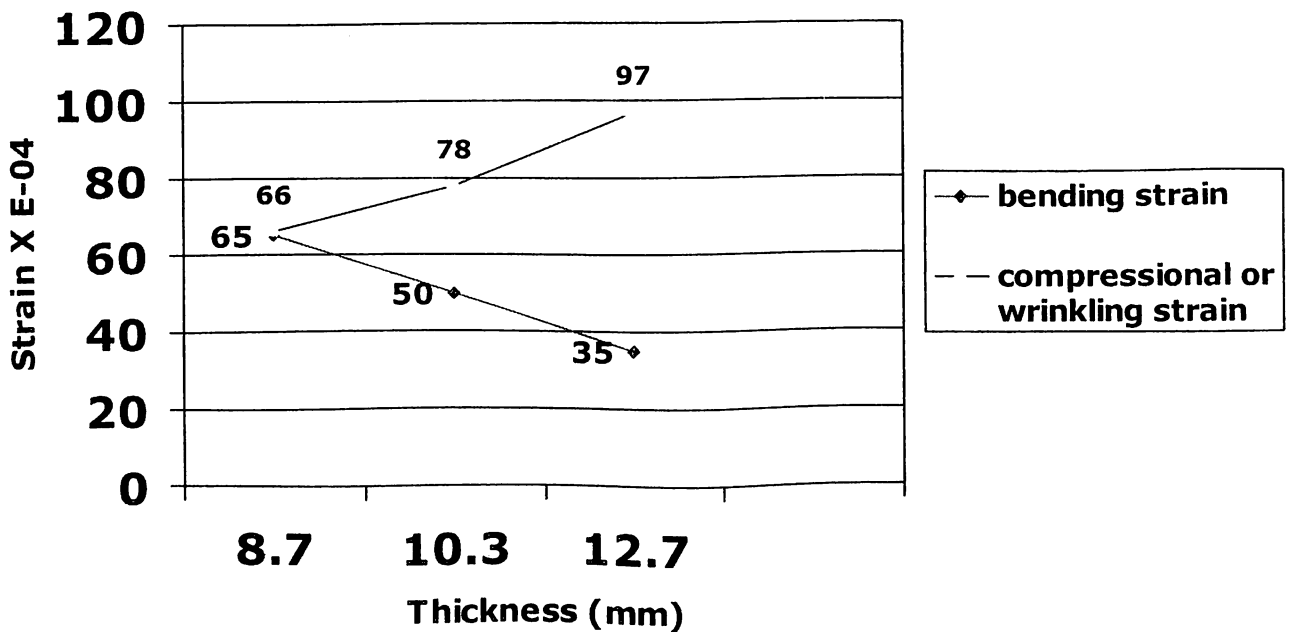


Fig 6.4.3

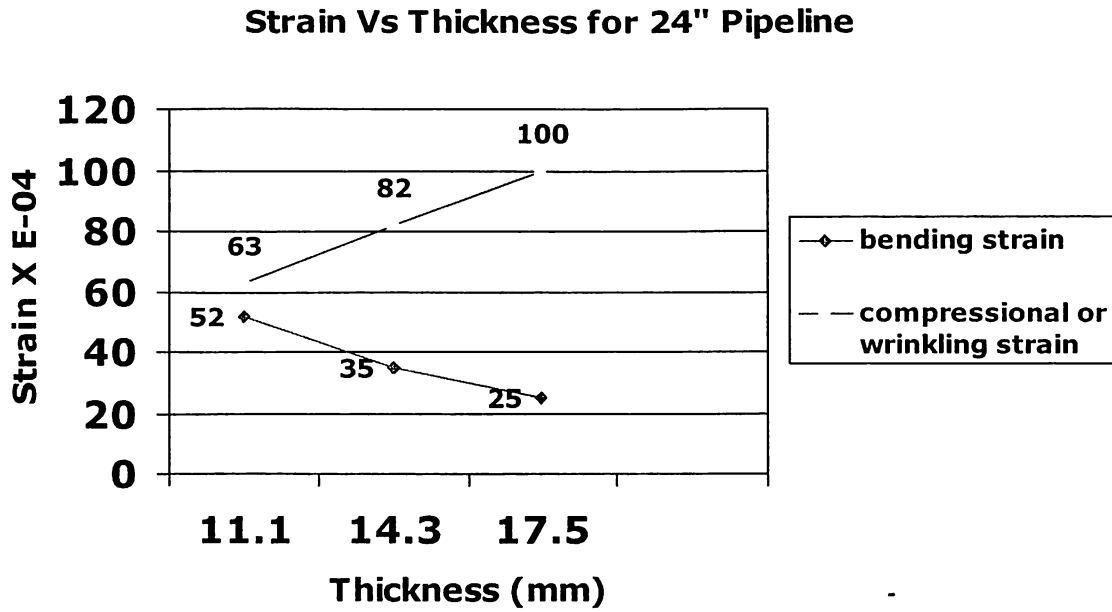


Fig 6.4.4

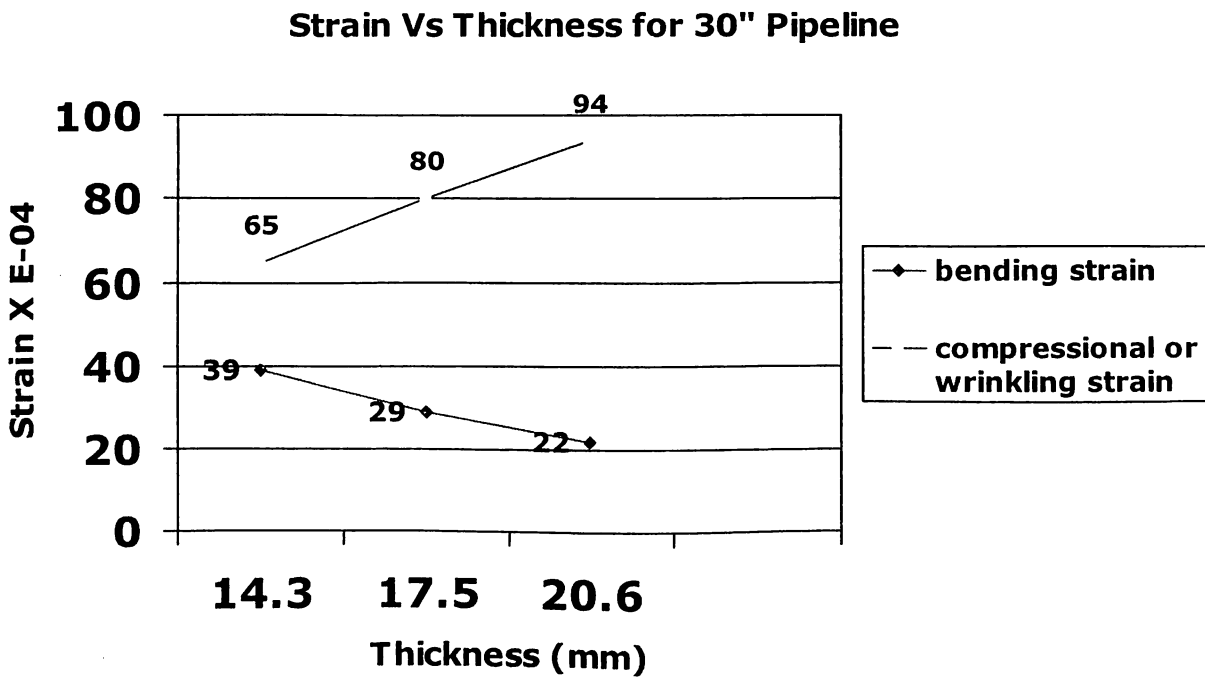
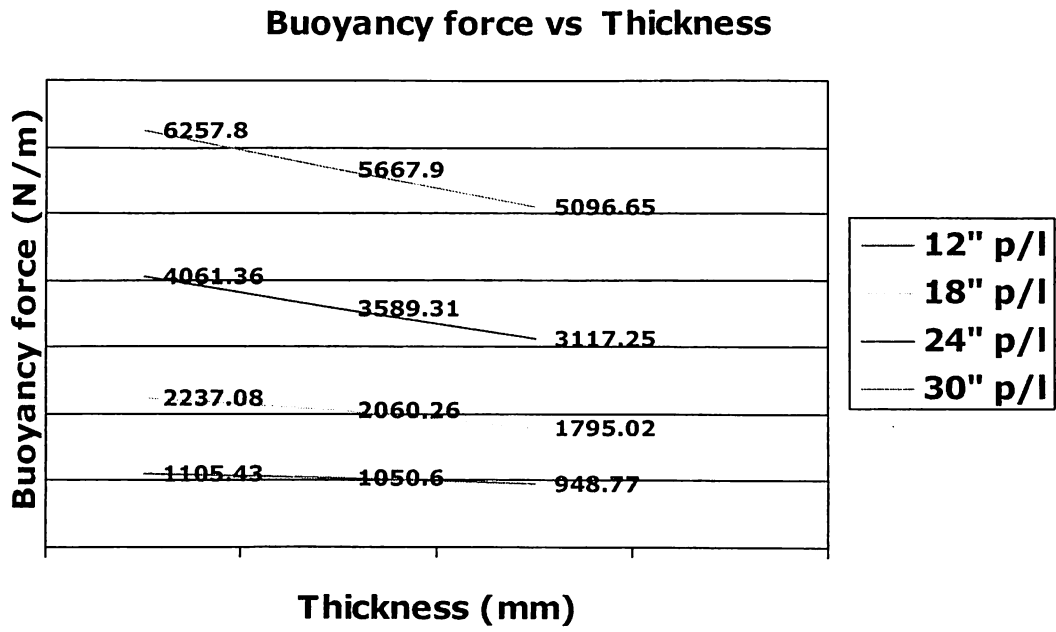


Fig 6.4.5



7.1 Discussion from Fault Crossing Modeling

Following were the observations and conclusions arrived at through the results obtained:

- 1) The difference in uplift and bearing stiffness has clearly affected the pipe behaviour in vertical direction. From Fig.3.3.3 it is observed that most of the displacement of pipe has occurred in the region where it has to just over come the uplift resistance. This is so because the soil yields at much lower values of displacement in uplift then in bearing. In the case of lateral movement pipe shows a symmetric behaviour on account of symmetric nature of stiffness of the lateral springs. Had the modeling been done exploiting seeming symmetric nature of the problem, this fact would not have been observed. This kind of difference in lateral and vertical displacement profile has been observed in reality and is outlined by *Kennedy et al.* [10]
- 2) It is noteworthy point that maximum displacement in both the lateral and vertical direction is slightly more, 1.0193m & 1.0311m respectively, than the actual fault displacement imposed. Further the location point where it occurs is a little away from the fault centre line (in this case it occurs at 24m and 12m from fault centerline in lateral and vertical directions respectively).
- 3) From the graphs of reaction forces in two directions it is observed that as one approaches near the fault the reaction forces gradually increase to a maximum value that can be offered by the soil till it causes yielding/slipping. The flat portions of the curves represent this phenomenon. Owing to high bearing resistance such a phenomenon is not observed in portions where bearing reaction is being offered to the pipeline.
- 4) The nature of the displacement profile & soil reaction forces in vertical direction are exactly of the same nature as obtained in *Guidelines for the Design of Buried Steel Pipe* [17]. Guideline neglects the lateral resistance and considers vertical subsidence alone on a nonlinear pipe material. This indicates that even elastic model of the pipeline captures in essence the behaviour of the pipeline under fault movement. Further it can be seen that imposing the lateral fault offset simultaneously with vertical offset has not altered nature of

any of the parameter (soil reaction force, strain, displacement profile etc.) corresponding to vertical direction.

- 5) The bending moments in a particular direction is representative of the forces encountered in an orthogonal direction. Thus bending moment in Y direction shows that pipe is subjected to symmetric loading in the transverse direction. The profile in Z direction representing the loading in Y direction is well in accordance with the ones obtained by *Barros et al.* [16]. Such a profile is of importance to decide upon the capacity and the spacing of the joints (flexible or bellow) while designing against fault movement. For a given fault displacement the distance between the two opposite peaks will govern the recommended value of spacing between two joints in the fault region.
- 6) From the study of stress profiles it can be seen that maximum equivalent stress distribution follows closely the distribution of the bending stress. Thus just the bending stress profile is representative of both the bending moments and the equivalent stresses encountered by the pipeline.
- 7) Further from the comparison of all the graphs it is observed that bending stress profile gives the largest value for the extent of pipeline that has been influenced by the fault line. This value is roughly 65-67m from centre of the fault line.
- 8) From study of strain profiles it can be ascertained that maximum axial strain is encountered at 45° to the vertical axis. Further looking at the strain profiles in y and z direction it can be concluded that the resultant equivalent strain profile will be similar to the profile obtained at 45° to the vertical axis.
- 9) It was observed that length of 400m of the pipeline is sufficient enough to model only about 0.25m of axial displacement when applied symmetrically. For study of the affect of fault crossing angle and fault movement along the axis of pipeline still higher length of pipeline has to be modeled. Otherwise the soil springs in axial direction slip pass the pipeline over its entire length.

7.2 Discussion from Parametric Modeling

- 1) An increase in the imposed guillotine settlement (Fault Displacement) shows an increase in the distance where the maximum values of axial strain occurs apart from expected increase in magnitude of strain itself. All the items under study i.e. axial strain, bending stress and soil reaction force increases with the Fault displacement. From the reaction force distribution it can be seen that the distance from fault-line up to which the soil slips pass the pipe also increases substantially with the fault displacement
- 2) While the soil reaction (and thus the moment) is higher for pipeline of larger diameter, the bending stress and axial strains are lower. With diameter although the pipe stiffness increases the effective soil resistance also increases owing to higher contact area. Lateral extension of the diagram indicates that larger pipelines deform to larger distances from the fault, which can be explained by their better capability to adapt and recover from imposed deformations. The vertical uplift soil forces are greater for larger diameter pipelines, since they have a better capability to adapt and recover from imposed deformations, resulting in larger lengths of yielded soil around the fault. Thus pipe with larger diameter perform better.
- 3) The increase in thickness of the pipeline shows the same nature as that of the increase in diameter but the extent of affect is smaller. Unlike the case of increase in diameter. Increase in thickness in no way increases the soil stiffness. Yet there is marked increase in soil reaction forces. This can be accorded to the increase in pipe stiffness, the only affect of increasing the thickness of the pipeline. Because of this increased stiffness the pipeline tries to push over the same soil more then before resulting in increased reaction forces. Thus pipes with higher thickness perform better.
- 4) Of all the parameters under study the affect of varying the pipe material was the least prominent. Nonetheless, both the bending stress and soil reaction forces increase while the axial strain itself decreases with the increase in young's modulus of the pipe material. This is again primarily due to increase in pipe stiffness. Thus ductile material with higher initial modulus performs better under fault crossing.
- 5) The reaction forces for higher depths indicate that more the soil is stiffer (greater depths) the larger are the internal forces, since the pipeline will have lower capabilities to adapt and recover from the imposed settlement. It can be noted that bearing capacity was never reached

at any point along the pipeline. Due to the greater flexibility of soil for lower depths of the pipeline layout, the soil would yield along larger areas.

- 6) The depth influence on the forces is not exactly because of the same reasons as the diameter influence. Unlike what occurs by increasing the diameter, an increase in depth leads to a deformation in closer areas to the fault settlement location. Although for higher depths the reaction forces are higher, these occur closer to the fault location than for lower depths. The most relevant difference in increasing the pipeline diameter and its depth, is that in the first case pipe stiffness increases and in the second soil stiffness increases. In both cases the soil reaction forces increase.
- 7) Since soils with higher soil friction angle are stiffer, it means that the greater this parameter is, the lesser the pipeline adapts and recovers from the imposed deformations, resulting in higher internal forces. Hence all the items under study increase with increase in soil friction angle. The soil bearing resistance forces are greater for higher soil friction angles. The affect of friction angle in that sense is similar to the affect of cover depth although the extent of the influence is lower. Hence, it is clear that softer site soil is better for pipe crossing fault. Practically this nature of pipe-soil behaviour explains why the pipeline laid with lighter backfill will perform better under fault crossing.
- 8) With the increase in cohesion of the surrounding soil although the stresses and the strains increase the imposed soil reaction and thus the moment itself decreases. Further the affect of cohesion is less pronounced than the affect of soil friction angle. It can be ascertained from the graphs that sandy soil will perform better than cohesive soils.
- 9) Results for affect of variation in pipe material and pipe diameter on maximum strain developed are very well in matching with those obtained by *Guo et al.* [15] using full 3-D shell analysis. Further the affect of pipeline diameter, soil friction angle and cover depth on the bending moment diagram are in accordance with the results obtained by *Barros et al.*[16] This shows that considering the affect of material nonlinearity and elaborate shell modeling are not necessary to capture the parametric behaviour of the pipelines.

8. SUMMARY AND CONCLUSIONS

1. From past seismic performance of pipelines it can be concluded that there are number of seismic hazards which pose high threat to the proper functioning of the pipelines. The damage caused by any of them is of severe nature and results into number of direct and indirect losses. Further the most catastrophic of all the seismic hazards, as far as buried pipelines are considered, is the one posed by fault crossing.
2. From the review of analytical work that have been carried out so far it was observed that simple beam model of the pipeline has not been used to explore the parametric behaviour of pipelines.
3. A simplified finite element model of pipeline soil system crossing an active fault was developed in ANSYS software and results were obtained in terms of displacement profiles, soil reaction forces, bending stress, equivalent stresses and axial strain distributions. These values were obtained at different circumferential locations and compared.
4. It was observed that in response to lateral strike slip the displacement was symmetric in its profile about the fault line. In response to vertical uplift, the most of the displacement was accommodated in the region which is at lower elevation. This behaviour has been observed in past earthquakes. The lower value of soil stiffness in uplift then bearing is attributed to be the cause of such behaviour.
5. From the study of stress profiles it was observed that maximum equivalent stress distribution follows closely the distribution of the bending stress. Thus the bending stress profile in case of pipelines under fault crossing are representative of equivalent stresses encountered by the pipeline too.
6. From study of strain profiles it was ascertained that maximum axial strain is encountered at 45° to the vertical axis. Further looking at the strain profiles in y and z direction it could be concluded that the resultant equivalent strain profile will be similar to the profile obtained at 45° to the vertical axis.

7. The nature of the displacement profile & soil reaction forces in vertical direction were exactly of the same nature as obtained in *Guidelines for the Design of Buried Steel Pipe* [17] which considered nonlinear pipe material. This indicates that even elastic model of the pipeline captures in essence the behaviour of the pipeline under fault movement. Further it was noted that imposing the lateral fault offset simultaneously with vertical offset has not altered nature of any of the parameter (soil reaction force, strain, displacement profile etc.) corresponding to vertical direction.
8. Parametric analysis was then carried out for different values of fault displacements, pipe material, pipe diameters, pipe thickness, depths of cover soil, soil cohesion and soil friction angles. Same model as used earlier was modified as per requirement for the analysis. Different values of parameters were chosen based upon the observed nature of variation in reality. All the soil springs were re calculated to take into account the affect of parameters on soil resistance.
9. An increase in the imposed guillotine settlement (fault displacement) showed an increase in the distance where the maximum values of axial strain occurs apart from expected increase in magnitude of strain. All the items under study i.e. axial strain, bending stress and soil reaction force increased with the fault displacement. From the reaction force distribution it was concluded that the distance from fault-line up to which the soil slips pass the pipe also increases substantially with the fault displacement.
10. Lateral extension of the diagram indicated that larger pipelines deform to larger distances from the fault, which can be explained by their better capability to adapt and recover from imposed deformations. The vertical uplift soil forces were greater for larger diameter pipelines and have larger lengths of yielded soil around the fault. Thus pipe with larger diameter perform better. The increase in thickness of the pipeline showed the same nature as that of the increase in diameter. Thus pipes with higher thickness perform better. Both the bending stress and soil reaction forces increase while the axial strain itself decreases with the increase in young's modulus of the pipe material. Thus ductile material with higher initial modulus performs better under fault crossing.
11. The reaction forces for higher depths indicate that more the soil is stiffer (greater depths) the larger are the internal forces, since the pipeline will have lower capabilities to adapt and recover from the imposed settlement. Thus pipelines at shallow depth perform better.

12. Since soils with higher soil friction angle are stiffer, it means that the greater this parameter is, the lesser the pipeline adapts and recovers from the imposed deformations, resulting in higher internal forces. Hence, it is clear that softer site soil is better for pipe crossing fault. Practically this nature of pipe-soil behaviour explains why the pipeline laid with lighter backfill will perform better under fault crossing. With the increase in cohesion of the surrounding soil although the stresses and the strains increase the imposed soil reaction and thus the moment itself decreases. Further the affect of cohesion was observed to be less pronounced than the affect of soil friction angle. From the strain distribution profiles it was clear that sandy soil will perform better than cohesive soils.
13. Results for affect of variation in pipe material and pipe diameter on maximum strain developed are very well in matching with those obtained by *Guo et al.* [15] using full 3-D shell analysis. Further the affect of pipeline diameter, soil friction angle and cover depth on the bending moment diagram are in accordance with the results obtained by *Barros et al.* [16] This shows that considering the affect of material nonlinearity and elaborate shell modeling are not necessary to capture the parametric behaviour of the pipelines.
14. The Model was then modified to study the affect of considering nonlinear material behaviour of steel (pipeline material). Stress-strain values were used to define the material characteristics and plastic beam element was used for modeling the pipeline. Pipe was modeled to be governed by Von-Mises yield criteria and isotropic work hardening was assumed.
15. Significant difference was observed in results of elastic and plastic analysis. Thus material nonlinearity with yield criteria and large deformation affect must be considered for any analysis like this. It was observed that the same trend or pattern of variation was observed with change in parameters as was obtained by considering elastic material properties. Difference was that maximum values or the point where they occurred were now different. Another interesting point noted from strain distribution curves was that while in elastic limits the tensile strains were dominant; in plastic analysis compressive strains are much more dominant. It was noted that the affected length of the pipeline in both the cases is almost the same.
16. The nature of the axial strain distribution and bending moment distribution curves now matched with those obtained in *Guidelines for the Design of Buried Steel Pipe* [17] which considered material nonlinearity.

17. Finally the affected length of the above pipeline was modeled once again using shell elements and the cross-sectional deformations were studied. The shell elements near the fault region underwent a severe deformation and the phenomenon of ovaling and distortion of the initial cross-section of the pipe was observed. It was noted that deformed shape of cross sections at various locations near fault region closely matched with the field observation of. Thus shell analysis is useful to understand the behaviour of the pipeline in detail.
18. The strain results obtained from the shell analysis (0.201%) were in close approximation with the results obtained from equivalent beam model (0.1997%). Further the deformation pattern shown by the shell model was captured by the equivalent beam model to a close extent. Even the soil reaction forces were of exactly same nature as was depicted by beam model. It was observed that the analysis with shell model, particularly with the nonlinearities of soil springs and pipe material, frequently encountered convergence problems. Thus it was concluded that until unless the analysis is specialized for capturing the deformation pattern of the cross-section the beam analysis is good enough to capture the essence of behaviour.

9.Recommendations

9.1 Recommendations may be followed to reduce the risk of pipeline subjected to faulting:

- The pipelines crossing fault line should be oriented in such a way to avoid compression in the pipeline. The optimum angle of fault crossing will depend upon the dip of the fault plane and the expected type of movement. And it should be within 90 degree
- Pipeline ductility should be increased in fault-crossing region to accommodate large fault movement without rapture.
- Abrupt changes in wall thickness or other strain concentrators should be avoided within fault zone.
- In all areas of potential ground rapture, pipelines should be laid in relatively straight section avoiding sharp changes in direction and elevation.
- To the extent possible, pipelines should be constructed without field bends, elbows , and flanges that tend to anchor the pipeline to the ground.

Example: **APPENDIX** , **APPENDIX**

- If longer length of pipeline is available to conform to fault movement, level of strain gets reduced. Hence, the points of anchorage should be provided away from the fault zone to the extent possible in order to lower the level of strain in the pipeline.
- A hard and smooth coating on the pipeline such as an epoxy coating may be used in the vicinity of the fault crossing to reduce the angle of friction between pipeline and soil.

Example: Three layer of epoxy coating

- The burial depth of pipeline should be minimized within fault zones in order to reduce soil restraint on the pipeline during fault movement.

Example : New Dimension for Trenching **APPENDIX**

If the expected fault displacement is very large then it is advised to take the pipeline above ground and design with sliding supports to sustain the expected level of ground displacement.

Example : TAPS **APPENDIX**

- While crossing the faults for which the movement is horizontal, TAPS design can be used. But in case of vertical movement of the fault the shock absorbing polymers as a backfill materials can be used to accommodate the displacement of the pipeline in the vertical direction.

Example : Shock absorbing polymers as a backfill **APPENDIX**.

9.2 Recommendations to minimized the buoyancy effect upon pipeline due to Liquefaction:

- Pipeline may be encased in concrete pipes to reduce the buoyancy effects, but the increase diameter will also increase lateral drag forces on the pipe.

Example : Guniting (APPENDIX)



Fig: 9.2.1

Concrete coated pipeline before welding .



Fig: 9.2.2 *Concrete coated Pipeline after welding*

- Concrete weights or gravel filled blankets can be utilized to provide additional resistance to buoyancy.
- The buoyancy effect can also be minimized by shallow burial of the pipeline above the ground water level.
- Where uplift is the main concern, one may provide anchors at a spacing of up to 150 m to prevent uplift
- It has been shown in the example that is due to the increase of thickness for the same diameter of pipe the wrinkling due to compression also increases.
- Use of shutoff valves may be increased to protect the pipeline of gas leakage in case of any severe damages.
- Distance between SV (Sectionizational valve stationals, basically ball valves) stations is 8 km, 16 km, 24 km and 32 km as per ASME code for gas pipeline for class I, II, III and IV zones. But to minimize the effect of any damage due to leakage or full bore rupture of the pipeline , these distances between the SV stations can be minimized to 8 Km for the entire zone.

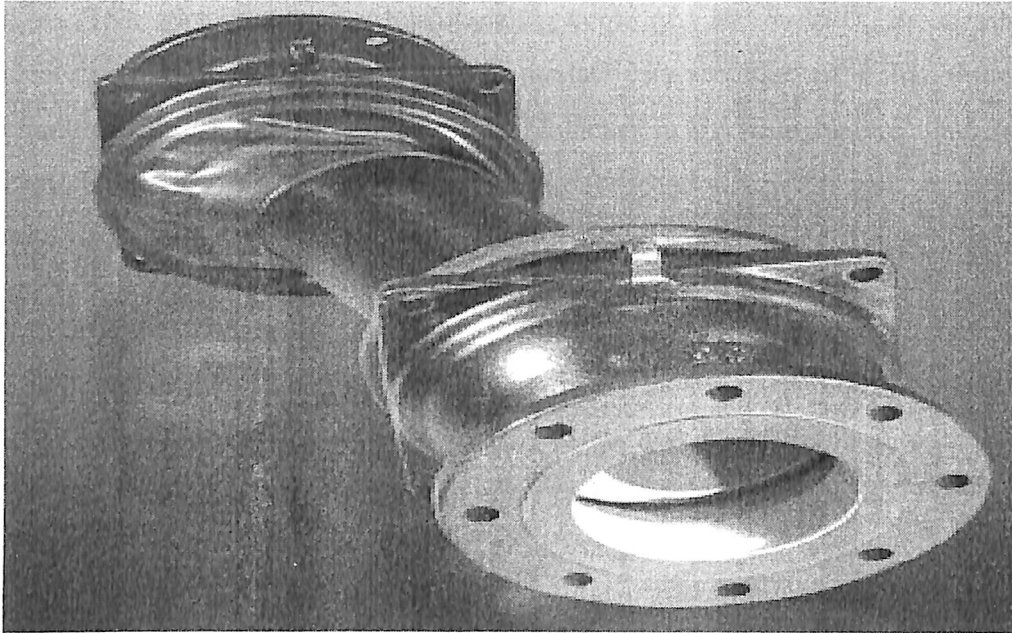
- As there is no such code for the distance between the SV stations for the oil pipelines , it is recommended that to minimize the effect of oil spill due to leakage or rupture in the pipeline the distance between the SV stations can be taken as 8 Km for that zone.

References

1. Wells, D.L., and Coppersmith, K.J., 1994, Updated empirical relationships among magnitude, rupture length, rupture area and surface displacement, Bulletin of the Seismological Society of America.
2. Ferritto, J.M., 1997, "Seismic design criteria for lifelines," Naval Facilities Engineering Service Center Port Hueneme, California.
3. O'Rourke, M.J., and Ayala, G., 1993, "Pipeline damage to wave propagation," Journal of Geotechnical Engineering, ASCE, Vol. 119, No. 9, 1993.
4. Zhou, J., 2003, "Arctic Pipelines: Opportunities and challenges for technology," New Construction, Materials and Welding Research & Development Forum, Washington, D.C.
5. Katayama, T. and Lian, W., 1983, "Recent research on seismic behavior of buried pipelines in China," Bulletin of Earthquake Resistant Structure Research Centre, No.17, pp.33-66.
6. Guo, E., Wang, D., Lu, M., and Shao, G., 2002, "Damage to lifelines during Ms 8.1 earthquake near Qinghai-Xinjiang border", Earthquake Engineering and Engineering Vibration, 6, Vol.22, No.3, pp77-81.
7. Eidinger, J., 2001, "Performance of thames water 2.2 meter diameter steel pipe at north Anatolian fault crossing," G&E Report 48.01.01.
8. Takada, S. *et al.*, 2001, "A new proposal for simplified design of buried steel pipes crossing active faults," Journal of Earthquake Engg. and Structural Dynamics, No.30, pp. 1243-1257.
9. Newmark, N.M. and Hall, W.J, 1975, "Pipeline design to resist large fault displacement." Proceedings, U. S. National Conference on Earthquake Engineering, EERI, an Arbor CA, pp. 416-425.
10. Kennedy, R.P. *et al.*, 1977 "Fault movement effects on buried oil pipeline." Transportation Engineering Journal, ASCE, 103: 617-633.
11. Wang, L. L. R. *et al.*, 1998, "Parametric study of buried pipelines due to large fault movement." Proceedings, Third China-Japan-US Trilateral Symposium on LEE, Kunmin, China, pp.165-172.
12. Liu, A.W., Hu, Y.X. *et al.*, 2000, "Responses of buried pipelines in large fault movements." Proceedings, Sixth International Conference of Seismic Zonation, EERI.
13. ANSYS, Reference Manual, v 7.0, Ansys Inc.
14. Ivanov,R., 2004, "Analytical assessment of the vulnerability of the underground jointed pvc pipelines to fault displacements," 13th World Conference on Earthquake Engineering, Vancouver, B.C., Canada. Paper No.195
15. Guo, E., 2004, "Numerical study on damage to buried oil pipeline under large fault displacement," 13th World Conference on Earthquake Engineering, Vancouver, B.C., Canada. Paper No.2876
16. Barros, R.C., 2004, "A parametric study on the comprehensive analysis of pipelines under generalized actions," 13th World Conference on Earthquake Engineering, Vancouver, B.C., Canada. Paper No.2311
17. Guidelines for the Design of Buried Steel Pipe, 2001, ASCE.
18. IS : 4948, IS: 269, IS: 383, IS: 456.

APPENDIX:

FLEXIBLE JOINTS:



The Romac FlexiJoint™ is a flexible, ductile iron joint, developed to accommodate pipeline forces that could result in damage or loss of service. The FlexiJoint compensates for expansion, contraction, rotation, bending and settlement of your pipeline all at the same time, with one fitting. FlexiJoints are available with flanged or Mechanical Joint style ends. When properly installed the FlexiJoint can be used at working pressures up to 350 psi. Sizes range from 3 inches to 24 inches. The following technical data shows why the FlexiJoint is the best solution for pipeline protection in the areas that are subject to movements.

No Bolts

The casing of the FlexiJoint is one piece and requires no threaded fasteners for assembly. This unique design feature eliminates flanged assembly connections. The resulting monolithic casing construction is an essential element that achieves restraint capabilities of 8.4d1 tons of force for all sizes. By eliminating unnecessary components, the compact design allows a lightweight assembly for ease of installation.

Accommodates Bending and Offset of Pipelines:

A single FlexiJoint ball end is able to provide a bending angle of up to $\pm 15^\circ$ to $\pm 20^\circ$ (depending on size). This corresponds to a total bending angle of $\pm 30^\circ$ to $\pm 40^\circ$. By varying the length of the sleeve, the FlexiJoint will also accommodate lateral offset of 4 to 20 inches. When special conditions demand, a FlexiJoint of 3 to 12 inches in size can accommodate an additional bending angle. Please contact Romac Industries, Inc. for assistance when your application requires special consideration.

Reacts to Torsion

The design of the FlexiJoint will allow rotation or torsion of the pipeline components. This freedom of movement prevents damage to flanges, valves and other structures associated with the pipeline. The FlexiJoint allows this movement while still accommodating bending and offset of the pipeline.

Superior Corrosion Resistance

FlexiJoint components, including the stainless steel lock ring, are lined and coated with fusion bonded epoxy powder, meeting the requirements of AWWA2 C2133 . Each component of the FlexiJoint is holiday tested. This coating provides superior corrosion resistance and meets the requirements of NSF4 Standard 615 .

Watertight

The seals of the FlexiJoint are specially molded rubber gaskets. These gaskets are used in the casing to allow deflection and in the ball to allow expansion and contraction. A casing cover is provided to assure contamination free operation.

1 Where "d" is in inches.

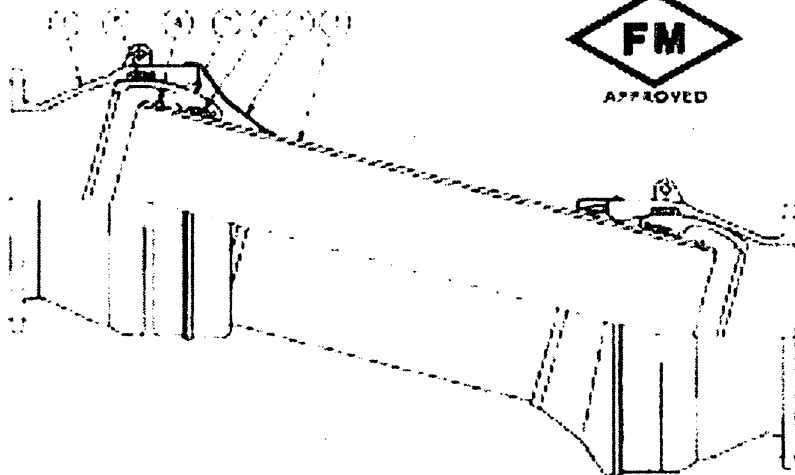
2 American Waterworks Association, 6666 West Quincy Ave., Denver, CO 80235.

3 AWWA Standard for Fusion-Epoxy Coating For The Interior And Exterior Of Steel Water Pipelines.

4 NSF International, PO Box 130140, Ann Arbor, MI 48113-0140, USA.

5 NSF Standard 61: Drinking Water System Components – Health Effects. .

Flexijoint™



| No. | Name of Parts | Materials |
|-----|---------------------|------------------------|
| 1 | Casing | ASTM A536 ¹ |
| 2 | Ball | ASTM A536 |
| 3 | Sleeve | ASTM A536 |
| 4 | Lock Ring | Type 410 SS |
| 5 | Ring Gasket, Casing | EPDM ² |
| 6 | Ring Gasket, Ball | EPDM ² |
| 7 | Casing Cover | EPDM ² |

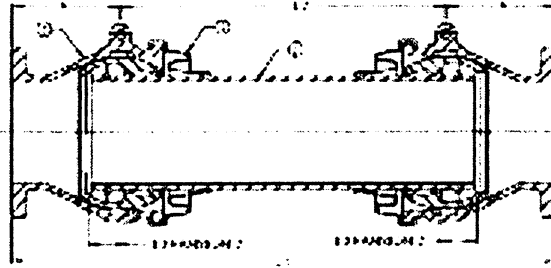
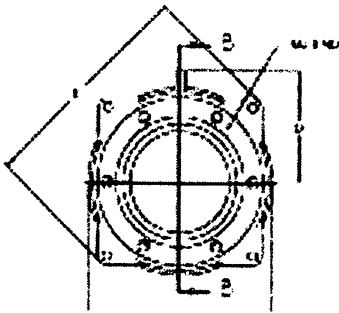
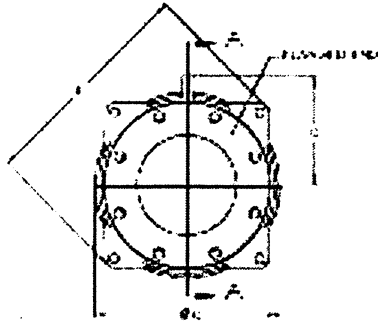
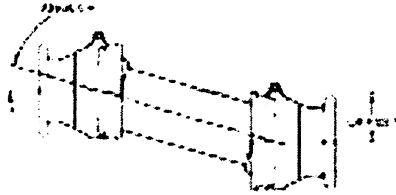
¹ASTM A536 Ductile Iron, Grade 65-45-12

²EPDM: Ethylene Propylene Diene Rubber

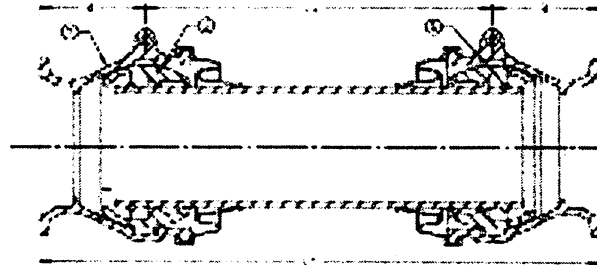
Flexijoint



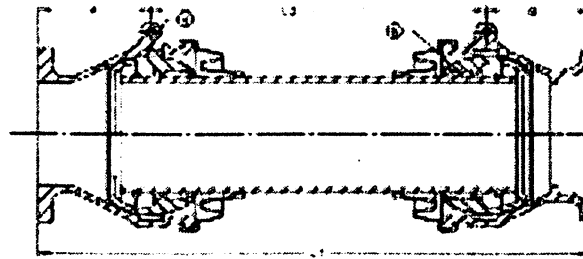
3" - 24" Dimensions
 NOTE: Measurements are in inches



SECTION A-A
 FLANGE X FLANGE



SECTION B-B
 MJ X MJ

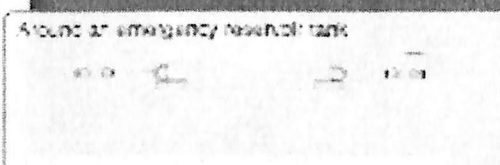
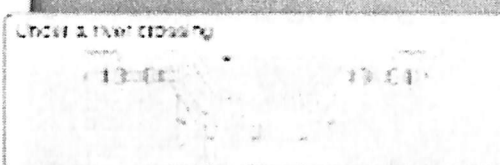
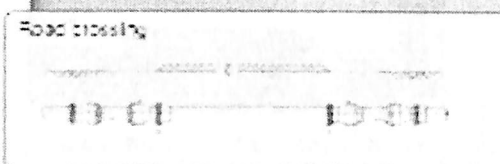
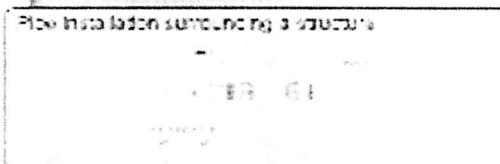
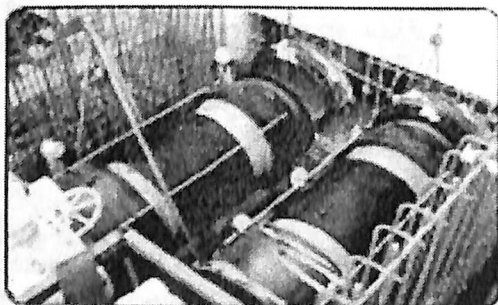
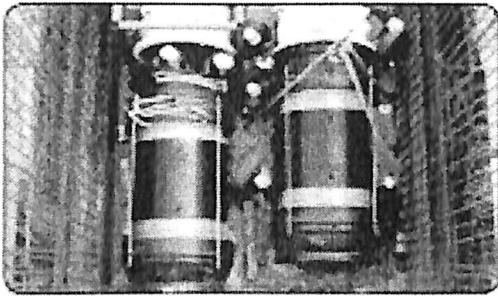


SECTION C-C
 FLANGE X MJ

Flexijoint

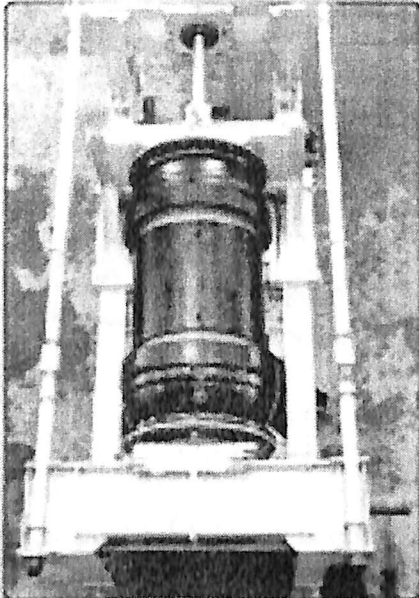
Applications

The Flexijoint was designed to excel in a diverse range of critical applications.

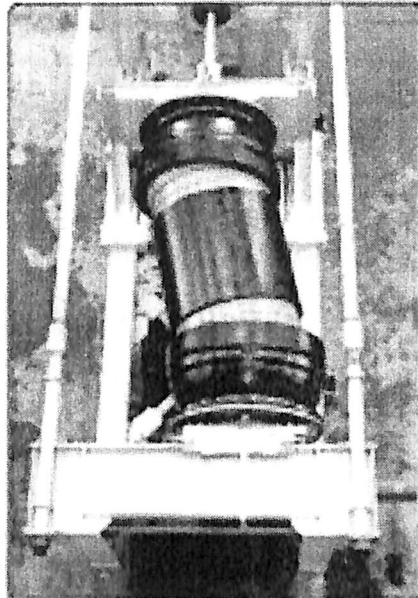


Flexijoint™

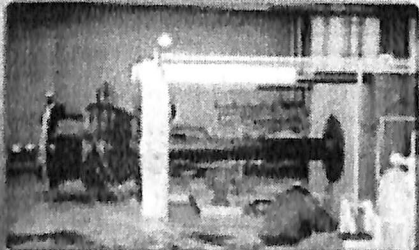
Performance Tests



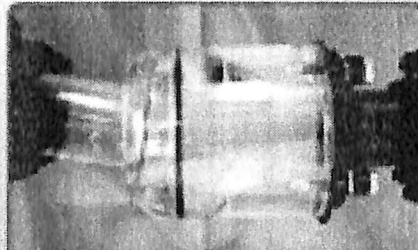
Testing Integrity of Flexijoint at the straight and horizontal position. Test also confirms function of Flexijoint during cyclic loading.



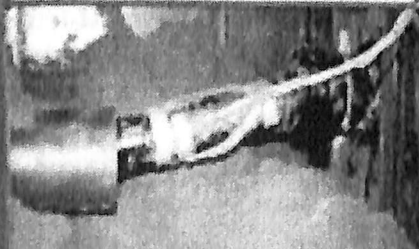
Testing integrity of Flexijoint at the offset position. Test also confirms function of Flexijoint during cyclic loading.



Testing restraint capability of Flexijoint.



Testing water flow through of Flexijoint.
Flow speed 2.63m/sec



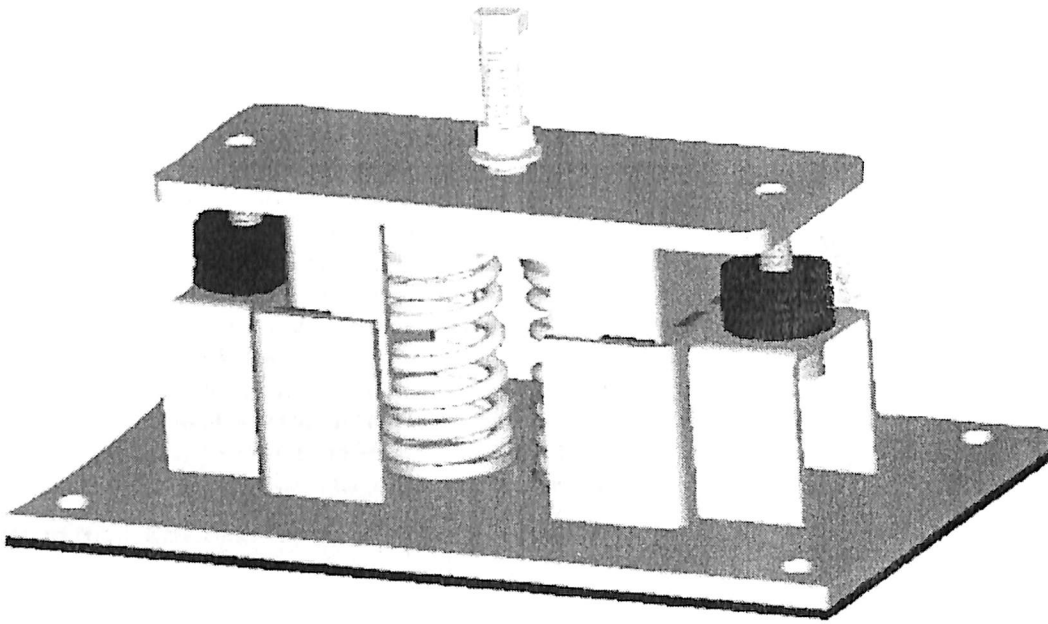
Testing earthquake resistance of outside Flexijoint.
Sh. offset.



Determining water head loss of Flexijoint.

APPENDIX :

Seismic Isolators:



Features

The design of Silex isolators optimizes both vibration isolation efficiency and cost efficiency because the springs are interchangeable within the same housing.

Application

The Silex Seismic Isolators are specially designed for use on stationary generator sets.

Other uses include:

- Engine drive compressor sets
- Engine and motor driven pumps
- Utility sets
- Reciprocating compressors
- Refrigeration machines

Springs — Oil Tempered and Chrome Silicon Steel is used on the standard springs.

Internal Dampening — All Silex isolators incorporate internal neoprene-shear rubbersided dampening. This dampening limits the machine vibration while the engine passes through the start-up resonant frequency.

Silex Sound Pad — To provide a non-skid surface and to increase isolation efficiency, the Silex Sound Pad is installed on all isolators.

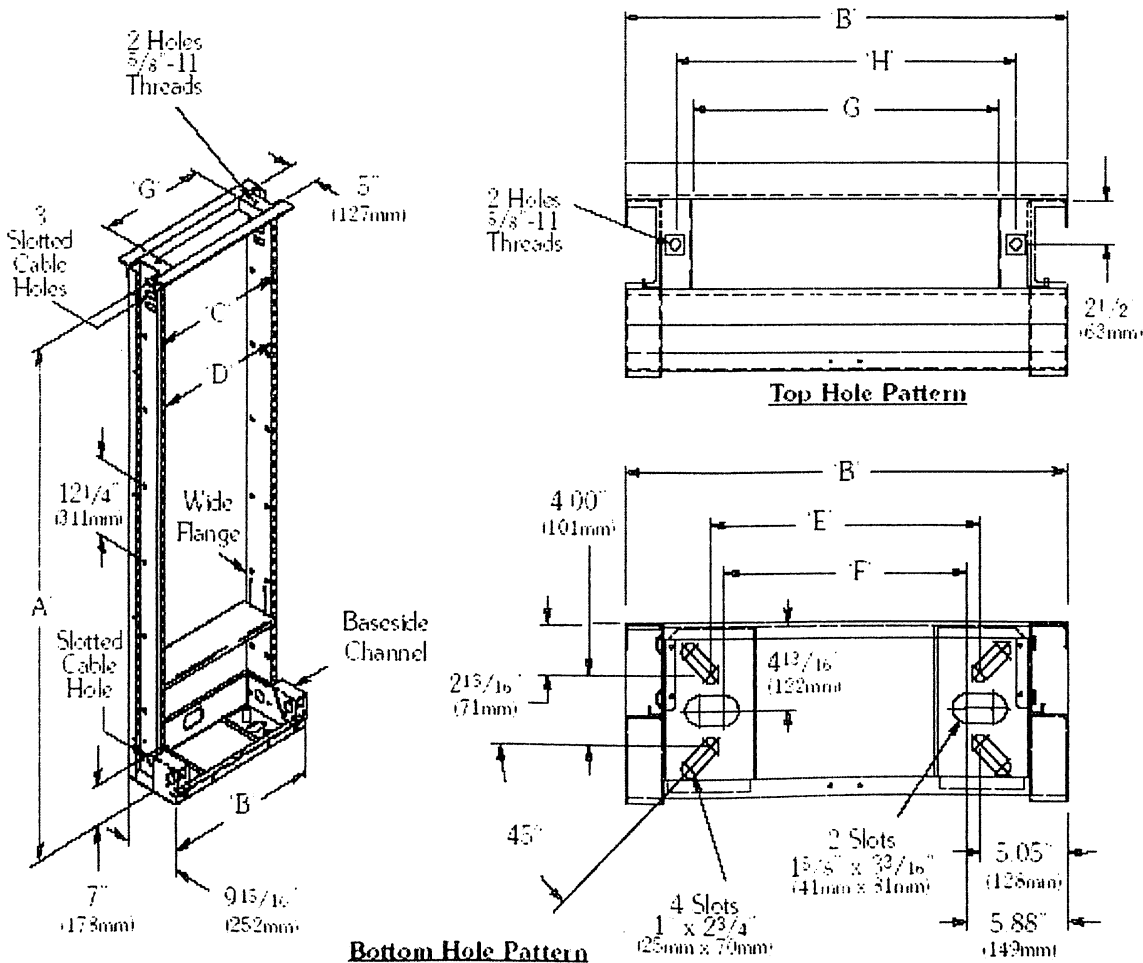
Side Snubber — Side snubber is standard .

Level Adjusting Bolt — All Silex isolators have an external adjustment that is long enough to accommodate a 2" base channel

APPENDIX :

Seismic Zone 4. Open Duct Unequal Flange Rack - Open Throat Style

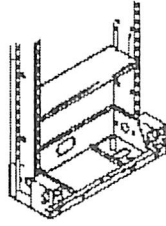
- Use to mount electronic switching equipment in seismic environments.
- Certified to ANSI T1.329-2000 and Telcordia NEBS GR-63-CORE for seismic zone 4 installation [84" (2133mm) only].
- Removable base cover plate for easier anchor and cable installation.
- Heavy duty welded construction, ideal for central office installations.
- Open top for easy cable access.
- Includes: Anchor plates, shims and seismically approved concrete anchors.
- Conformance to EIA-310-D (except inside clearance).
- Double-Side 1 3/4" (44mm) panel mounting spacing [1 1/4" (32mm), 1 1/2" (38mm) hole spacing]
- Double heavy duty 2" (51mm) x 2" (51mm) top angles for added rigidity.
- #12-24 panel mounting holes.
- Accessory mounting holes provided in base, uprights and top.
- Integrated cable grounding strip available on 84" (2133mm) rack (contact factory).
- Material: 11 Ga. (3mm) ASTM A1011SS structural steel
- Finish: Telco Gray Powder Coat (TG), other finishes available.
- U.S. Patent No. 5,284,254 - Canada Patent No. 2,099,081



See page 140 for cable support bar quantity required

Continued on page 143

Seismic Zone 4, Open Duct Unequal Flange Rack - Open Throat Style



Cover Plate
Included

See page 146 for guard rail covers

| | | Dimensions | | | |
|---|---------------------|------------------------------------|--------|------------------------------------|--------|
| | | 19" (482mm) Rack Width | | 23" (584mm) Rack Width | |
| | | In. | mm | In. | mm |
| A | Overall Height | 84" | (2133) | 84" | (2133) |
| B | Overall Width | 21 ¹⁵ / ₁₆ " | (557) | 25 ¹⁵ / ₁₆ " | (653) |
| C | Panel Mounting | 18 ⁵ / ₁₆ " | (465) | 22 ⁷ / ₁₆ " | (567) |
| D | Usable Inside Width | 17 ¹ / ₂ " | (444) | 21 ¹ / ₂ " | (546) |
| E | Angle Slot Spacing | 11 ²⁷ / ₃₂ " | (300) | 15 ²⁷ / ₃₂ " | (402) |
| F | Center Slot Spacing | 10 ³ / ₁₆ " | (259) | 14 ³ / ₁₆ " | (360) |
| G | Throat Opening | 13 ¹⁵ / ₁₆ " | (354) | 17 ¹⁵ / ₁₆ " | (453) |
| H | Top Hole Spacing | 16" | (406) | 20" | (508) |

1³/₄" (41mm) Panel Mounting Spacing
1¹/₄" (32mm), 1¹/₂" (13mm) Hole Spacing

| Part Number | A Height | | Mtg. Spaces | Weight | |
|-------------------------------|-------------|--------|----------------|--------|--------|
| | In. | (mm) | | Lbs. | (kg) |
| 23" (584mm) Rack Width | | | | | |
| SB-6066-084 | 84" | (2133) | 43 | 106 | (48 D) |
| 19" (482mm) Rack Width | | | | | |
| SB-6061-084 | 84" | (2133) | 43 | 95 | (43 D) |

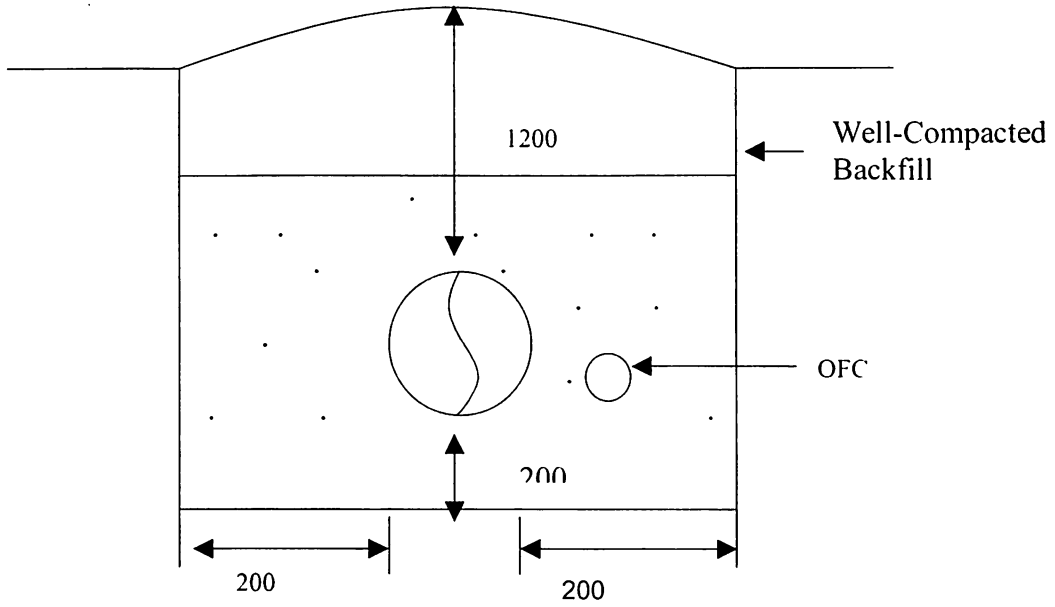
For EIA Universal Spacing [5/8" (16mm), 3/8" (10mm),
1/2" (13mm)] add -U suffix to part numbers.

Example: SB-60(66 or 61)-084-U

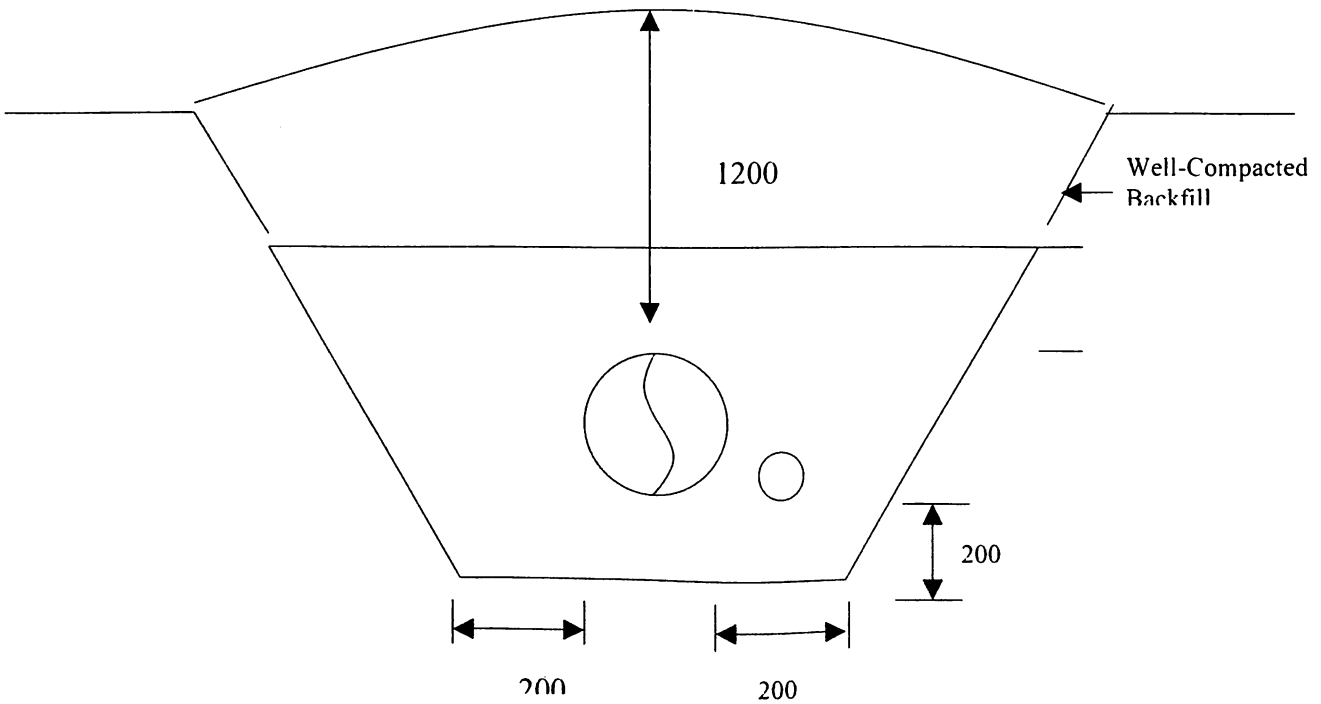
APPENDIX

Old Trench Dimension for the Buried Pipelines :

For Rocky Strata/Gravel Area:

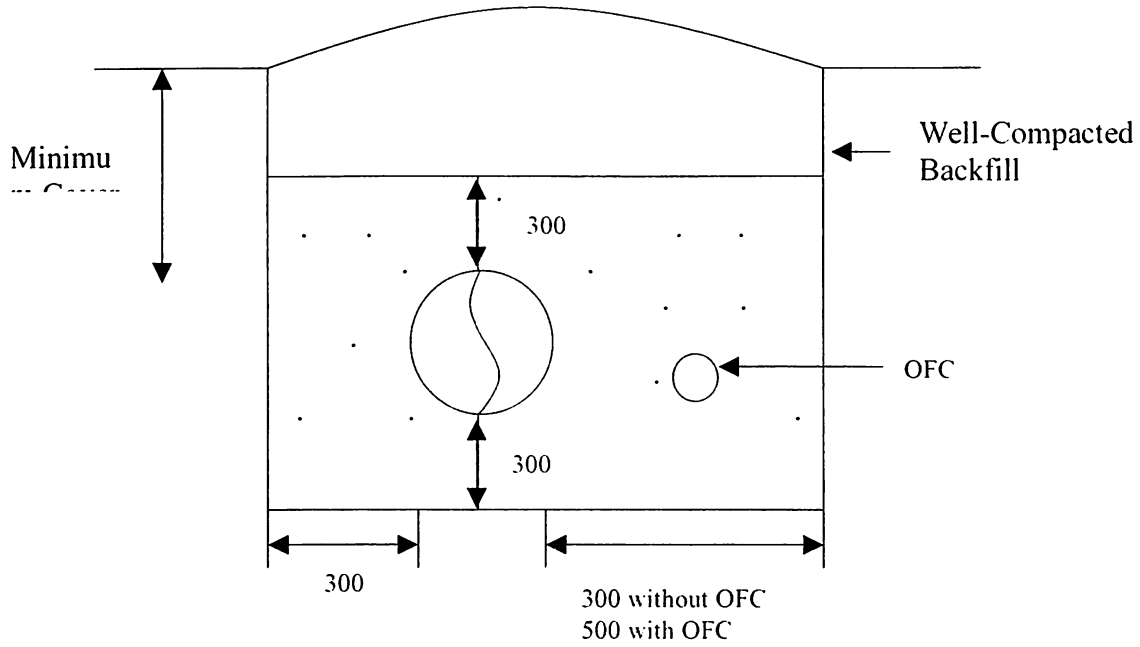


For Clay Soil:

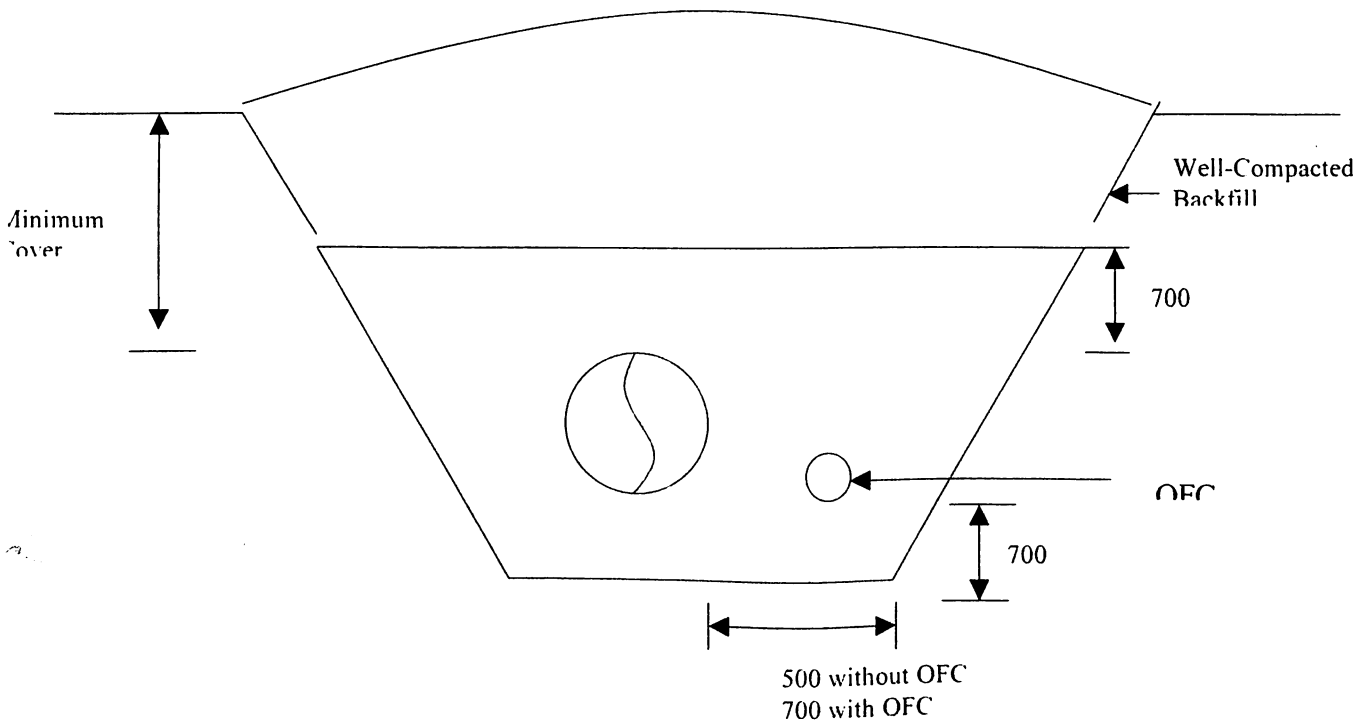


New Trench Dimension for the Buried Pipelines in the Seismic Zone:

For Rocky Strata/Gravel Area:



For Clay Soil:



APPENDIX

Instrumentation :

Lessons from the Monitoring Program

Approach to Monitoring. The best approach to monitoring includes identifying the hazard, evaluating the risks of the hazard, designing the monitoring program as an element of mitigation, implementing trigger levels and contingency plans, and reviewing data regularly. Instruments should be placed where maximum changes in displacement or stress are expected. A knowledge of the local geology, such as the boundaries, depth, and relative stability of landslides, can guide the placement of instruments and also helps in the interpretation of results.

Landslide Instrumentation

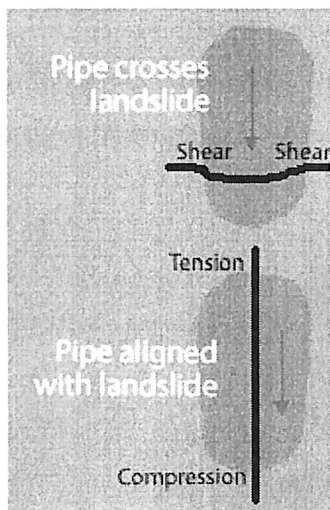
Inclinometer:

Inclinometers are useful for detecting the onset of movement. They also reveal the precise depth of the slip plane and whether multiple slip planes are present. When installed close to the pipeline, inclinometers show displacements similar to that of the pipe.

Preliminary geotechnical studies at Douglas Pass identified the boundaries and approximate depths of the individual landslides in the area. This information was used to select suitable locations and depths for the inclinometers. The bottom of the inclinometer casing must be anchored in stable ground below the slip plane of the landslide so that movements can be referenced to a stable point.

Inclinometer surveys were obtained about once a month during periods of low activity and more frequently during the spring, when wet weather reactivated the slides and increased the rate of movement.

Landslide movement eventually pinches the inclinometer casing, preventing further surveys with the inclinometer probe. Two or three inches of movement across a narrow slip plane can close the casing. However, it is possible to extend use of the casings by converting them to simple wire extensometers.



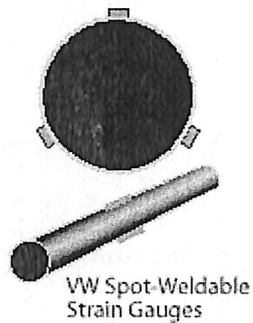
Wire Extensometers

Wire extensometers are useful for monitoring large movements. Substantial movements generally occur before pipeline failure, so the reduced accuracy of these extensometers is not a serious limitation. To convert inclinometer casings to wire extensometers, company engineers attached a wire to an anchor and pushed the anchor into the casing to a depth below the slip plane. The other end of the wire exits the top of the casing. Landslide movement is monitored by measuring the length of wire that is pulled into the casing. As reported above, one of the wire extensometers measured movement of 10 feet.

The depth of the slip plane is determined by the inclinometer, so it is best to start with inclinometer surveys and then convert the casing to an extensometer as required. When large deformations are anticipated, it is advisable to convert the inclinometer to an extensometer soon after the slip plane is located.

Piezometer:

Standpipe piezometers are used to monitor pore-water pressure and the effectiveness of drainage measures. Rising pore-water pressure is a useful indicator of impending landslide activity.



Standpipe piezometer measurements are obtained with a water level indicator or with a VW wire pressure transducer. Although the pressure transducer is more expensive, it can be connected to a data acquisition system for unattended readings.

Surface Surveys

Surface surveys are used at the most active sites to monitor movement of monuments installed in the ground or survey targets welded to the buried pipe. Survey costs can be high and it is not always easy to relate surface movements to pipeline integrity.

Pipeline Instrumentation

When the pipeline crosses a landslide, it is subjected to shearing forces at the lateral edges of the slide. This can result in bending and subsequent rupture of the pipe. When the pipeline is aligned with the landslide, it will be subjected to compressive and tensile stresses by the downward moving soil. Compressive stresses cause buckling and rupture. Tensile stresses rarely cause failures.

VW Spot-Weldable Strain Gauges

VW strain gauges are used to monitor strain in the pipe. At each monitored location, three strain gauges are mounted 120 degrees apart and oriented to measure strain in the longitudinal axis of the

pipe. The distribution of tensile and compressive strains reported by the three gauges reveals how the pipe is being deformed.

Strain gauges should be installed on new pipe or pipe that has been effectively stress-relieved by excavation or cutting. This provides baseline readings for later calculations of stress in the pipe. The maximum strain in the pipe is calculated from the three measurements and can be substantially higher than the individual strain readings.

Trigger levels for stress relief or other mitigation measures are based on allowable longitudinal stress. This provides a safety margin to account for such uncertainties as initial stress condition, future deformation of the pipe, corrosion effects, and the fact that the strain gauges may not be located at the point of maximum strain.

Good applications for strain gauges are monitoring pipelines affected by slow-moving landslides and for monitoring the effectiveness of mitigation measures. Strain gauges are not appropriate for monitoring fast-moving hazards such as mudflows or rockfalls.

Mitigation by Trenching

A variety of measures are available to protect the pipeline from a landslide. The most expensive and time consuming measures are stabilizing the landslide or relocating the pipeline. The size and number of landslides at Douglas Pass made such measures unfeasible.

Trenching is a reliable mitigation measure that can be completed quickly at modest cost. It involves excavating a trench along the upslope side of the pipe, when the alignment of the pipeline is perpendicular to the direction of ground movement. Trenching provides rapid relief, as documented by strain gauge monitoring. The effect is also visible: the pipeline shifts upslope in the trench by several feet immediately after trenching.

Trenching is less effective when the pipeline is aligned with the direction of landslide movement, and it is not effective at all for rapid, catastrophic landslides. However, landslides of this character are always preceded by significant increases in the rate of deformation. If the area is properly instrumented and monitored, the landslide can be predicted, and emergency measures can be undertaken prior to the failure.

APPENDIX

- **Use of FRC as a joint coating material:**

The experimental investigation of the use of fiber reinforced composites for the strengthening of welded slip joints against seismic attack has been shown to be an effective and economic solution to this ever-present problem. The experimental results shown by Cornell University is that the improvement of performance, with FRC retrofit, for the 12 inch diameter pipe with ¼" wall thickness to be approximately 30% under compressive loading. The next series of tests, Phase 2 and Phase 3, will investigate the real-time cyclic tension-compression loading of the retrofitted pipes at D/t ratios of 50 and 250.

Thus, the research program is moving into the typical large diameter pipe geometries that are used by large municipalities, such as the Los Angeles Department of Water and Power. It is expected that as the D/t ratio increases, the as-built capacity of the welded slip joint will decrease with respect to the prismatic section capacity. It is also expected that as the D/t ratios increase, the net enhancement of capacity of the FRC retrofitted welded slip joint will increase to nearly 100%, to near prismatic section capacity.

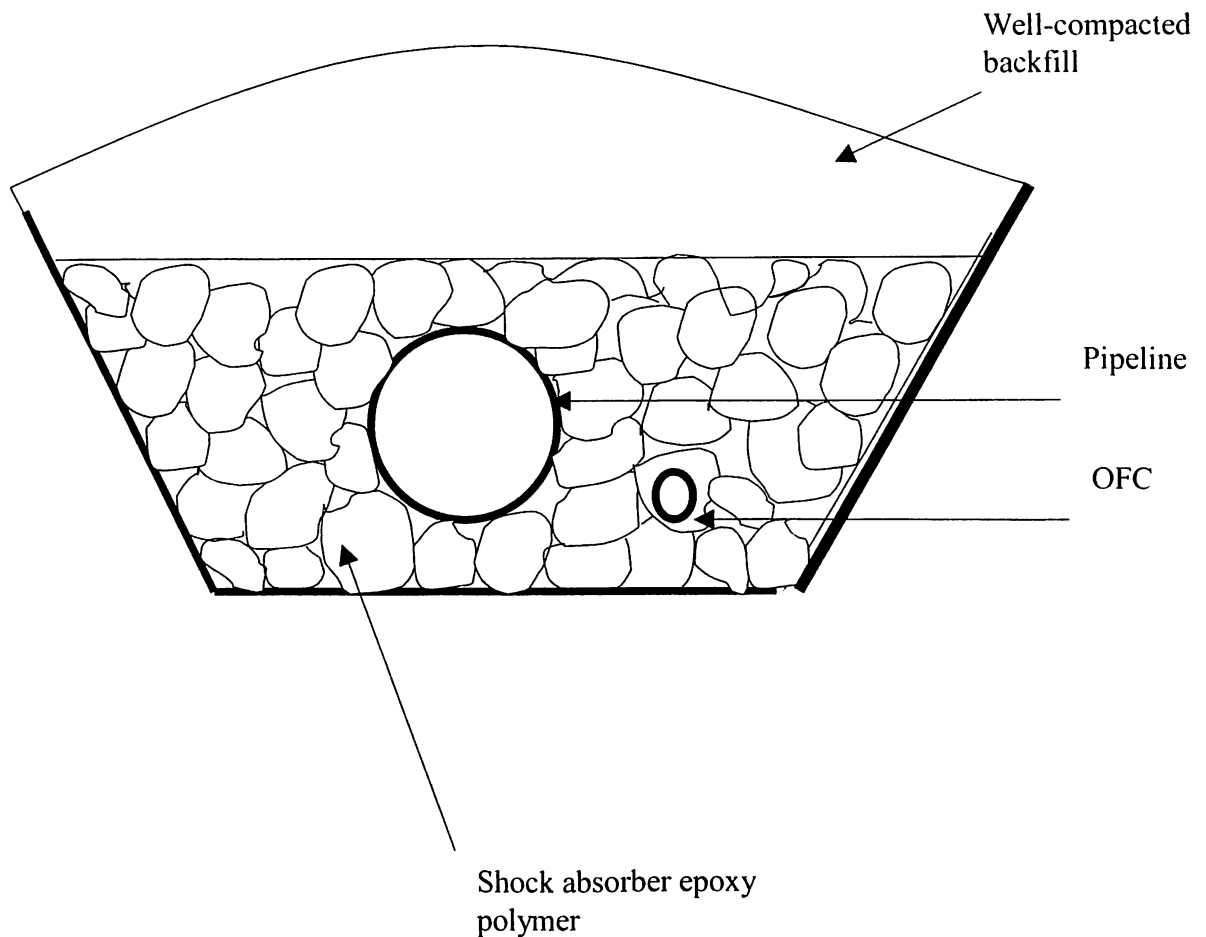
APPENDIX

- **Use of Seismic Shut off Valves**

Earthquake sensitive gas shut-off valve is designed to close in the event of an earthquake, preventing gas flow into a structure where earthquake damage may have occurred. Reduces the potential for fire or explosion due to the release of gas into a structure. Valve is designed to remain closed until manually reset. Not intended for replacing upstream manual shutoff valves. The trip mechanism is factory set and sealed. A sight glass is provided so that the Open or Closed indicator can be seen, and the trip mechanism status of the valve can be easily determined.

APPENDIX

Use of expandable epoxy polymer as a backfill in case of vertical movement of fault:



In case of vertical movement of the fault the TAPS sliding attachment cannot be used. To accommodate the vertical displacement of the pipeline in the trench, a shock absorbing epoxy polymer backfill is suggested in place of soil backfill.

If this polymer is not available or costly then the pieces of tyre can be used for the specific zones. These materials will allow the pipeline to move freely in the vertical direction and will also absorb the shockwaves to some extent. Thus will be providing a cushioning effect to the line pipe.

APPENDIX

Location Classes for Design and Construction: (ASME B 31.8-1999 Edition, Chapter 840.22)

- (a) *Location class 1:* A location Class 1 is any 1-mile section that has 10 or fewer buildings intended for human occupancy. A Location Class 1 is intended to reflect areas such as wasteland, deserts, mountains, grazing land, farmland, and sparsely populated areas.
- (1) *Class 1, Division 1.* This Division is a location Class 1 where the design factor of the pipe is greater than 0.72 but equal to or less than 0.80 and has hydrostatically tested to 1.25 times the maximum operating pressure. (See Table 841.114B for exceptions to design factor.)
- (2) *Class 1, Division 2.* This Division is a location Class 1 where the design factor of the pipe is greater than 0.72 but equal to or less than 1.1 times the maximum operating pressure. (See Table 841.114B for exceptions to design factor.)
- (b) *Location class 2:* A location Class 2 is any 1-mile section that has more than 10 but fewer than 46 buildings intended for human occupancy. A Location Class 1 is intended to reflect areas where the degree of population is intermediate between Location Class 1 and Location Class 3 such as fringe areas around cities and towns , industrial areas, ranch or country estates , etc.
- (c) *Location class 3 .* A location Class 3 is any 1-mile section that has 46 or more buildings intended for human occupancy except when a Location Class 4 prevails. A Location Class 3 is intended to reflect areas such as suburban housing developments, shopping centers, residential areas, and other populated areas not meeting Location Class 4 requirements.
- (d) *Location class 4.* A location Class 4 includes areas where multistory buildings are prevalent, where traffic is heavy or dense, and where there may be numerous other utilities underground. Multistory means four or more floors above ground including the first or ground floor. The depth of basements or number of basement floors is immaterial.

APPENDIX

TAPS

Prior to construction of the Trans-Alaska Pipeline System (TAPS), a geologic study and field survey was conducted to identify active surface faults crossing the proposed route of the pipeline. Three potentially active fault zones were identified: Denali, McGinnis Glacier, and Donnelly Dome. In addition, over half of the route traverses areas of thaw unstable permafrost necessitating an above-ground mode on piling supports. A special design utilizing long grade beam supports was utilized within the Denali Fault zone.

The magnitude 7.9 Denali Fault earthquake produced ground motions that slightly exceeded the TAPS seismic criteria at periods longer than about 1.0 second and generally approached design criteria at shorter periods. The duration of shaking was approximately 100 seconds, with violent shaking in the near fault region of the pipeline. In near proximity to the Denali Fault crossing, large fault movements occurred.

The long period nature of the ground motion, produced a maximum ground velocity of approximately 114 cm/sec (45 in/sec) coupled with violent near fault movement

in the above-ground segments. The event tested the ability of the fault crossing design to withstand fault rupture displacements approaching design level with respect to pipe movement on the at-grade sliding supports and pipe stress. There was no evidence of damage to the pipeline in the form of wrinkling or buckling of the pipe, but there was some support damage as described later in this paper. Realignment of a limited number of supports in the fault zone was required following the event to restore the fault movement response capacity of the pipeline to an additional 1.7 m of strike slip. This allowance accounts for early estimates of further fault displacements that may reasonably be expected if additional faulting occurs in the short term. The standard above-ground pipeline segments immediately north and south of the fault crossing zone were also inspected and support damage was repaired as described in Sorensen et al. (2003). Subsequent smart pig runs verified this observation.

This paper provides an overview of the field reconnaissance conducted in proximity to the Denali Fault, observations of movement and damage resulting from the violent lurching motion induced by the earthquake, and a discussion of the methodology used during early adjustments to the special grade beam design for the Denali Fault.

TAPS Design Background

Seventy five percent of the TAPS route was originally underlain by permafrost, necessitating a unique above-ground design that accommodates potentially unstable, ice-rich permafrost conditions. The below-ground pipeline is a conventional buried design used in thawed soils and in permafrost soils that are defined as thaw stable. A deep burial mode (below unstable surficial soils) and a refrigerated insulated burial mode (thick non-thaw stable soils) are used in some areas. Over half the pipeline (676 km) is constructed above ground and the remainder (611 km) is buried.

Both above and below-ground designs are affected by the extreme seismic activity of Alaska. (The magnitude 9.2 Prince William Sound subduction zone earthquake of 1964 is the second largest earthquake ever recorded.) TAPS traverses a wide range of geotechnical conditions that directly affect design and operation of the pipeline and related facilities. The goal of the original

geotechnical design was to provide a stable foundation for pipeline elements, both statically and dynamically, so that the system can operate for the long term in an effective and safe manner without undesirable consequences to the public or environment. Alyeska Pipeline Service Company (Alyeska) conducted extensive seismological and engineering studies during the design of the pipeline to develop seismic structural design criteria, characterize active faults crossing the pipeline, and mitigate the potential affects of geohazards such as soil liquefaction and landslides.

Faulting that results in surface rupture is an important consideration for pipelines because pipelines crossing fault zones must deform or move longitudinally in response to axial compression or tension forces and laterally in response to bending and shear forces to accommodate ground surface offsets. Three potentially active faults were identified that crossed the pipeline in central Alaska. Alyeska carried out fault studies to characterize fault length, expected rupture slip, fault zone width, and slip recurrence interval (Cluff et al., 2003). Estimated ground displacements associated with these faults are shown in Table 1.

Table 1. Design Displacements at Active Fault Crossings.

| Fault | Milepost | Max Credible Slip (m) | | Design Slip Value (m) | |
|--|----------|-----------------------|----------|-----------------------|----------|
| | | Strike Slip | Dip Slip | Strike Slip | Dip Slip |
| Donnelly Dome | 556 | 9.1 | 2.1 | 6.1 | 1.5 |
| McGinnis Glacier | 587 | 4.0 | 3.0 | 2.4 | 1.8 |
| Denali | 589 | 1.5 | 4.6 | 0.9 | 10.0 |
| Note: Displacements were originally specified in units of integer feet | | | | | |

During the November 3, 2002 magnitude 7.9 event, the Denali Fault ruptured over a distance of 336 km. The epicenter occurred near the newly discovered Susitna Glacier thrust fault, approximately 90 km to the west of the pipeline. The fault intersects TAPS at Milepost 589 in central Alaska. Average slip on the fault is estimated to be 5.5 m near the pipeline crossing with maximum slip of almost 9 m occurring 120 km to the east of the pipeline crossing.

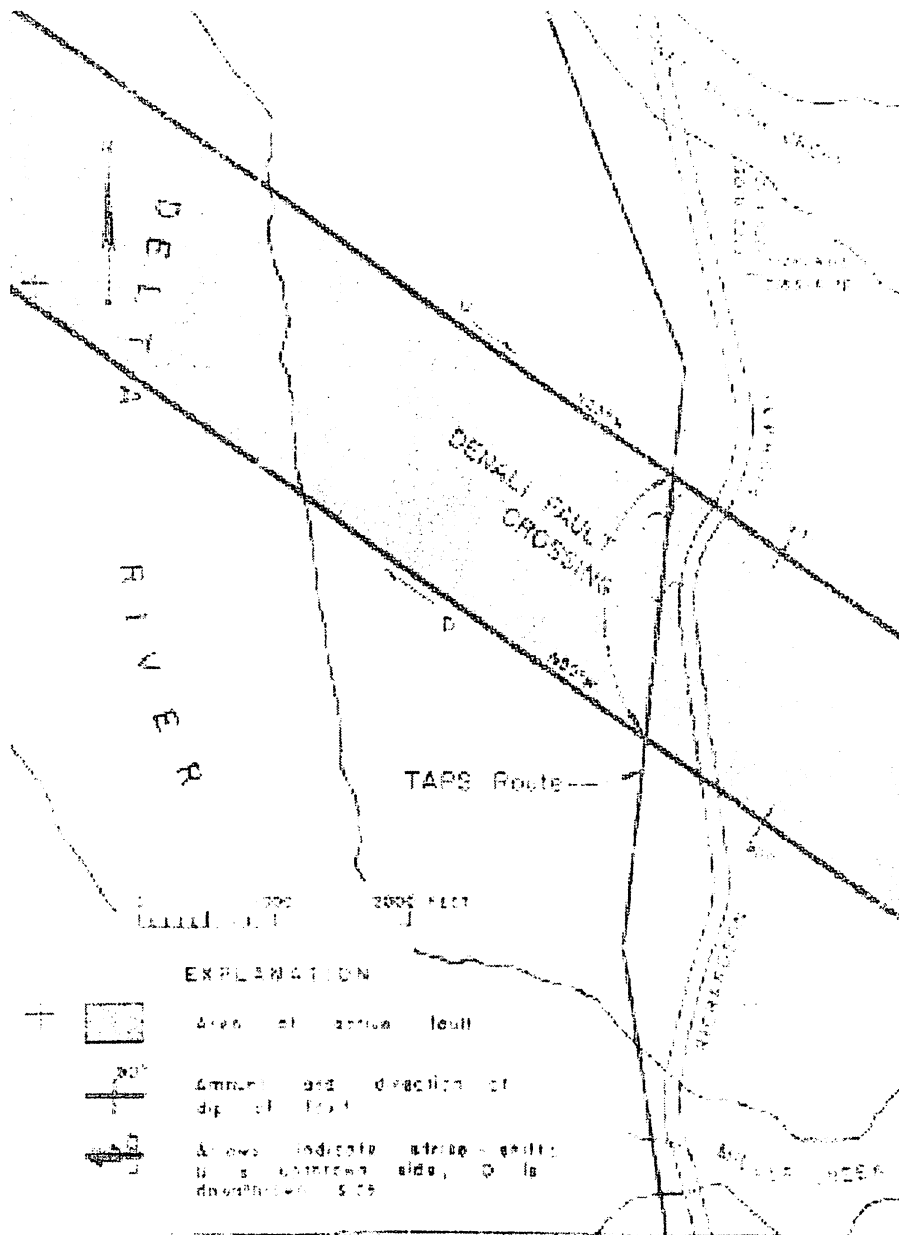
Special Above-Ground Configuration at Denali Fault Crossing

The Denali Fault extends east to west more than 650 km through the Alaska Range. It is a right-lateral strike-slip fault with a normal-slip component. The fault plane is nearly vertical, and the up-block is to the north. The pipeline crosses the Denali Fault zone between Lower Miller Creek and

Miller Creek near MP 589. The width of the fault zone used in design was 579 m, which implies that a surface rupture was possible anywhere within this zone. The limits of the fault zone were established between pipeline as-built Stations 31082+00 and 31101+00 (feet). The fault strike at the pipeline crossing is N55°W. Since the pipeline bearing is N6°32'E at the fault crossing, the fault crossing intersection angle is 61°32' counterclockwise with respect to the pipe survey centerline as shown in Figure .

The area is predominately a level outwash plain composed of thawed fluvial gravels and glacial till material overlaying bedrock at an undetermined depth. However, the northern 61 m of the fault zone is a relatively steep hill composed of silty gravelly glacial till and granite bedrock.

During the course of pipeline design, it was determined that the warm crude oil pipeline would be above-ground in the Denali Fault area because of the presence of thaw unstable permafrost soil. Due to the magnitude of the design fault displacements, conventional above-ground construction was judged impractical at the Denali Fault crossing. Instead, at-grade beam construction on which the pipe is free to slide was selected to provide support for the pipeline across the fault zone because it can accommodate relatively large displacements without significant pipe deformation. This low-to-the-ground construction mode has the added benefit of limiting damage to the pipeline if, for any reason, the pipe unexpectedly slips off the

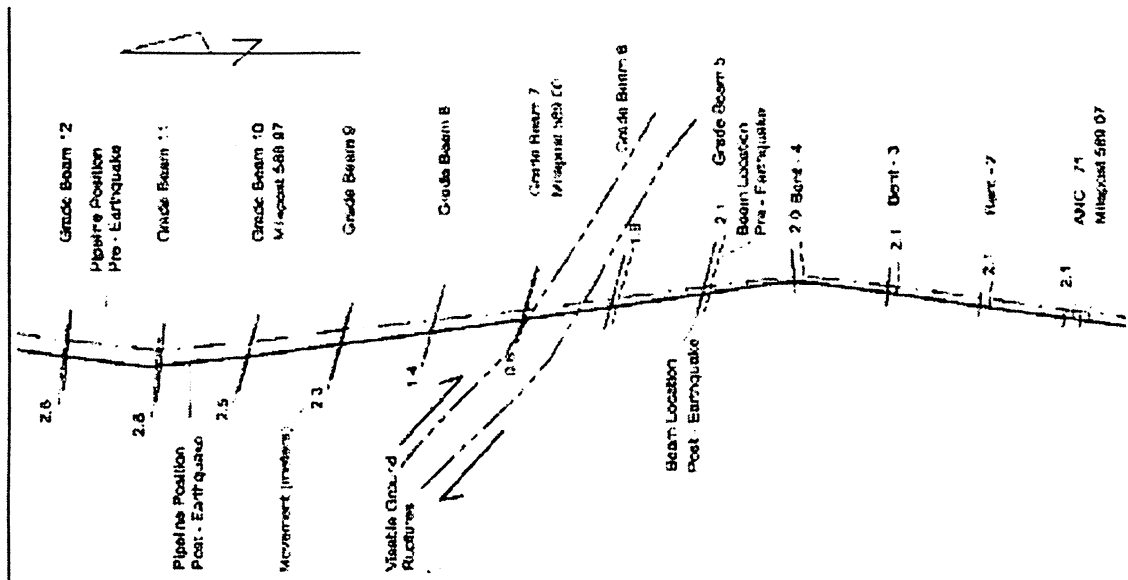


support beam during a seismic event. The pipeline was designed to accommodate a right lateral strike slip of 6 m and a vertical slip of 1.5 m with the north block up. The dip plane was assumed to be vertical. The three-dimensional displacement components relative to the pipeline orientation (i.e., parallel to the pipeline bearing of N 6°32' E) are 2.9 m longitudinal 5.4 m transverse, and 1.5 m vertical.

At the Denali Fault crossing, the pipeline is supported on 33 steel box beams and concrete beams set on-grade, at approximately 18-m intervals over a distance of 579 m. The beams are approximately 12 m long. The location of some of these beams is shown as Grade Beam Numbers 5

through 12 (Figure 2) in the immediate vicinity of the fault. These beams were sized and arranged to accommodate a fault slip. Anchors in the typical above-ground configuration bound the special Denali Fault above-ground segment north and south of the fault crossing area.

The pipeline shoes were lengthened in the fault zone to accommodate the large longitudinal and lateral pipeline movements anticipated by the largest projected fault displacement and magnitude as shown in Figure 3. Close attention was paid to the sliding surface of the crossbeam and the material lining the bottom of the pipe shoe. The pipe shoe base consisted of a 0.63-cm thick steel plate to which was bonded a



Teflon pad. The crossbeam surface was sand blasted and painted with zinc rich epoxy paint. The coefficients of friction values of 0.10 static and 0.05 dynamic were specified by design and confirmed through testing.

Performance of Special Fault Crossing Configuration

As expected, significant pipeline and pipeline support movements occurred during the November 3, 2002 fault rupture. The trace of the rupture was clearly visible between grade beam supports 6 and 7 near the southern end of the special

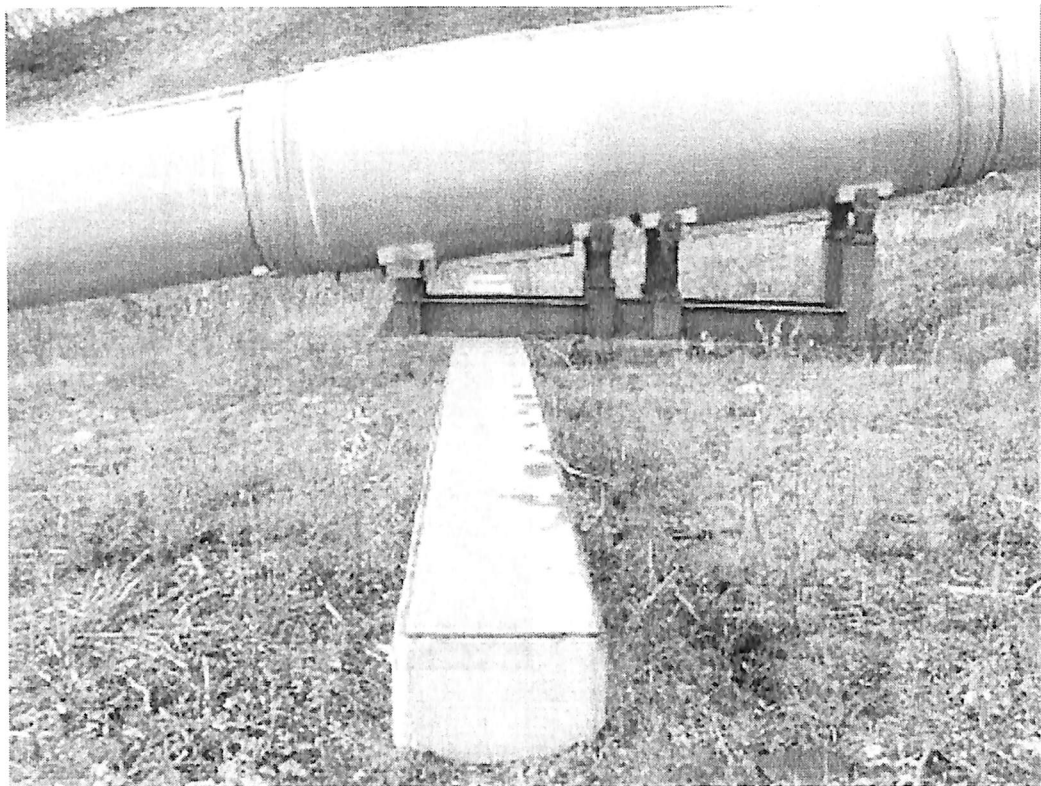


Figure . Typical special configuration bent on a concrete grade beam: Note offset shoe position by design to accommodate pipe movement in this case to the left. configuration shown schematically in Figure 2. A range of potential locations of fault surface rupture was analyzed during design. From these design studies, the most severe effect on the pipeline was determined to be when surface rupture was postulated at grade beam 7, which is only one bent away from the observed fault trace. Therefore, this event actually represented the near maximum expected movement for the design, as was indeed the observed result. The relative locations between pre-event and post-event pipeline and beam positions are shown in Figure

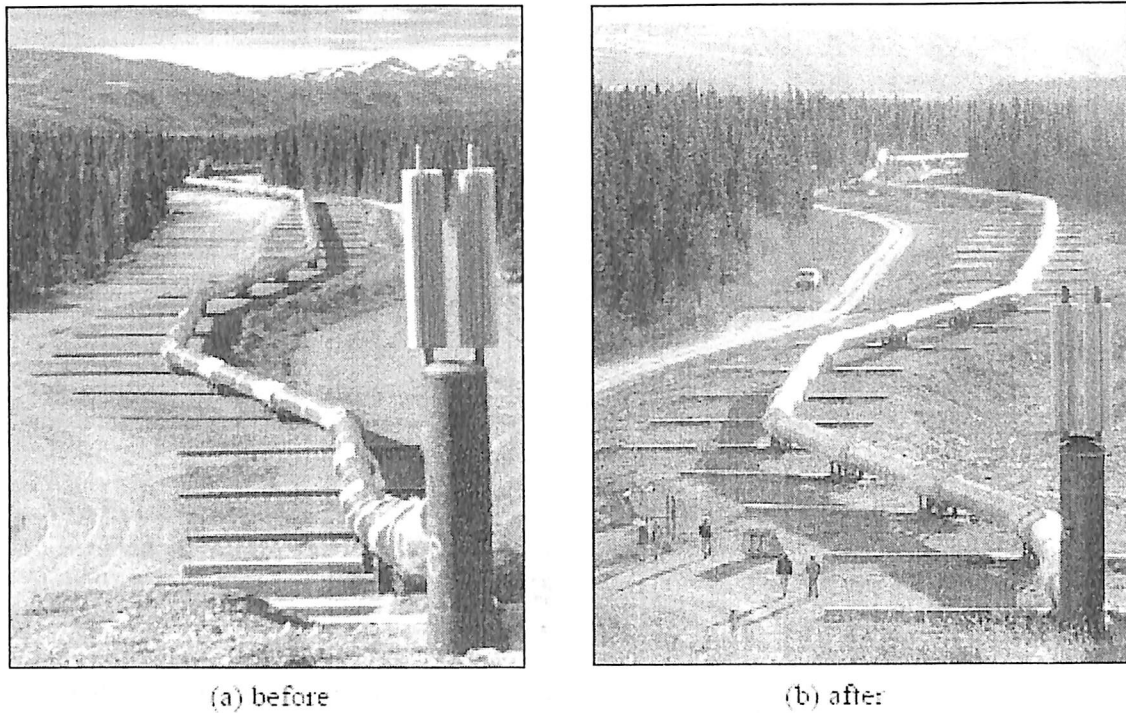


Figure 4. TAPS crossing of Denali Fault before and after fault slip, looking south. Note movement and bowed segment after fault displacement, which acts to compress the pipeline crossing segment.

Anchors are designed to control longitudinal movement of the pipeline through frictional resistance. Anchors begin slipping at an instantaneous force of 475 kN (105 kips). The anchors north and south of the fault crossing slipped longitudinally and experienced further movement through slippage between the anchor frame and support brackets on the VSMs. Some deformation of the anchor frames was observed via yielding of the slotted bolted connection on the frame itself, but not at the support bracket. During repair operations on the first anchor south of the Denali Fault, the pipe clamps connecting the anchor assembly to the pipeline were released. There was no observed movement of the pipe through the anchor clamps demonstrating that there was no residual compressive stress in the pipeline.

The pipeline support shoe at the first VSM bent (immediately south of the last grade beam configuration) was severely damaged (see Figure 5). This was probably due to the vertical faulting and concurrent violent dynamic shaking both vertically and horizontally. The shoe was replaced during the field repairs after the event, and the pipe was thoroughly inspected. Based on documented inspection reports, the pipe itself had no observable damage in this region.

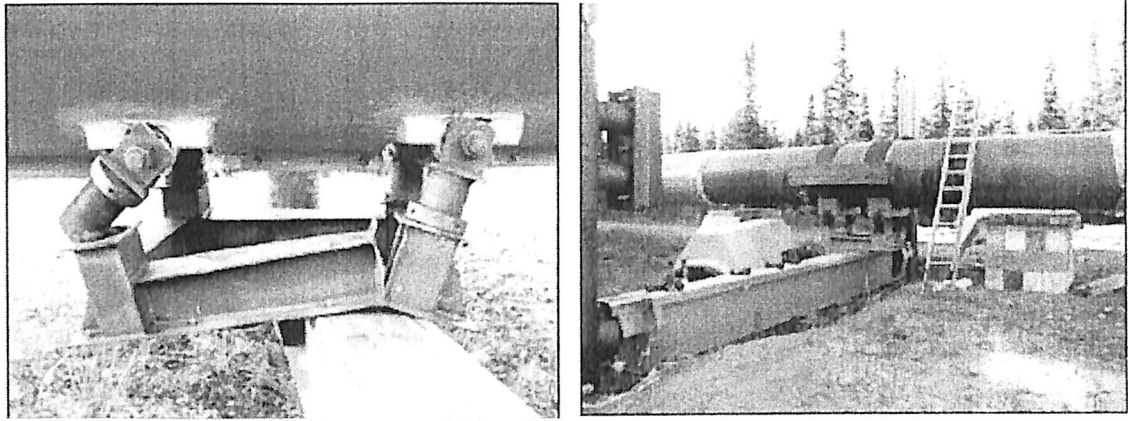


Figure 5. Post-event shoe damage (left) and pre-startup repair (right) on the seismic bent immediately south of the Denali Fault. Note the temporary shoring beneath the pipe used during repairs (right side of picture), the bumper beam on the pipe clamp (center), and the impact absorber on the VSM (far left side of the picture)

At special configuration locations, ground movement at the grade beams was evident, although no damage to the grade beams, pipe support shoes or the pipe itself was observed (see Figure 6). Slip marks caused by the pipeline shoe sliding across the crossbeams and grade beams during faulting and associated shaking were observed throughout the fault crossing. Some of the grade beams in the near fault area exhibited evidence of minor ground plowing, probably through inertial forces in the beam and/or as a result of sliding friction resistance between the shoe and beam. Pipe shoe movement was often more than the estimated ground fault displacement, and occurred well back from the rupture trace line due to compression and pipe flexure. The final “set” of the pipeline results from friction resistance between the shoe and the cross beam, producing the illusion of residual compression. The observed movement was expected and predicted by the design analysis.

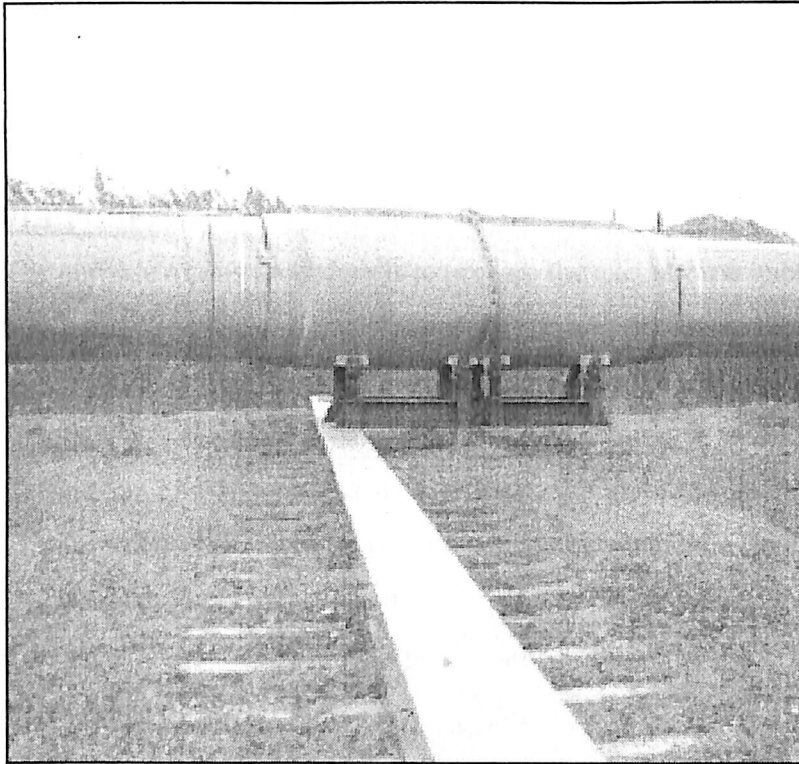


Figure . Post-earthquake shoe location on grade beam prior to re-centering.

APPENDIX:

Guniting :

PURPOSE:

The purpose of this procedure is to prepare the execution sequence involved for concrete coating (Guniting) to the exterior surface of pipes. Compressors and Hoppers are used for this purpose.

MATERIALS:

Cement:

Cement shall be of approved source / Manufacturer.

Conforming to IS: 269 MTC of each consignment shall be submitted to the Client company or consultant company and one lot of cement shall be tested in approved lab .

Cement shall be tested in lab as per IS: 269.

Fine Aggregates:

Fine Aggregate will be procured from quarries located at nearby area or any other Suitable quarries / vendors approved by consultant company.

Water:

Water will be used from consultant's approved Bore well or from any other sources for guniting work and curing & shall confirm to IS 456: 2000.

Welded Steel Wire Mesh:

Welded steel wire mesh of 2 X 4 inches of 13gauge will be procured from vendors approved by consultant company.

Method.

- The protective coating of each pipe length shall be carefully inspected before placing of welded steel wire mesh; if damages are found they shall be repaired before start of the work.
- Foreign matters, if any , shall be removed from the surface of the protective coating.
- The welded steel wire mesh shall be placed over the surface of pipe by providing the spacers.
- Circular and longitudinal joints of wire mesh shall be lapped & binding with 1.5mm diameter steel wire shall do attachments.
- One layer of wire mesh shall be provided for 50mm thick and two layers of wire mesh for thickness of 50mm. & above.

- Cement & dry sand of approved proportion shall be mixed manually on a clean platform by volume with a measuring box.
- The mixed dry cement mortar shall be placed on the hopper manually and shall be injected at high velocity against the exterior surface of pipe through compressed air to produce a hard, tight-adhering coating of desired thickness.

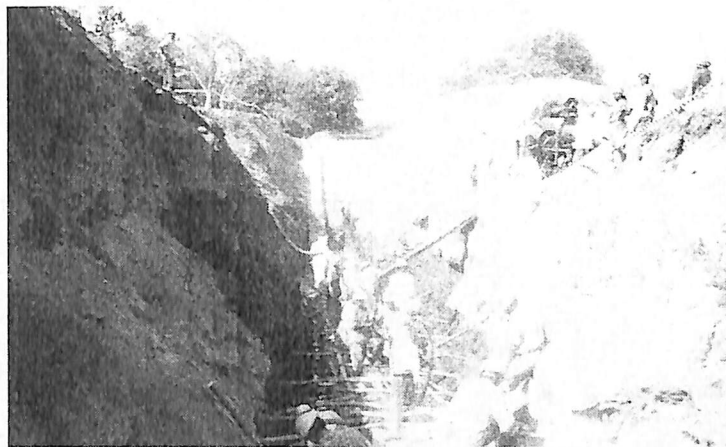


Fig: *In situ concreting*

- After completion of gunniting work and final setting of mortar , curing shall be performed in accordance with IS: 456 by wrapping wet Hessian cloth or with curing compound for a period of 7 days.

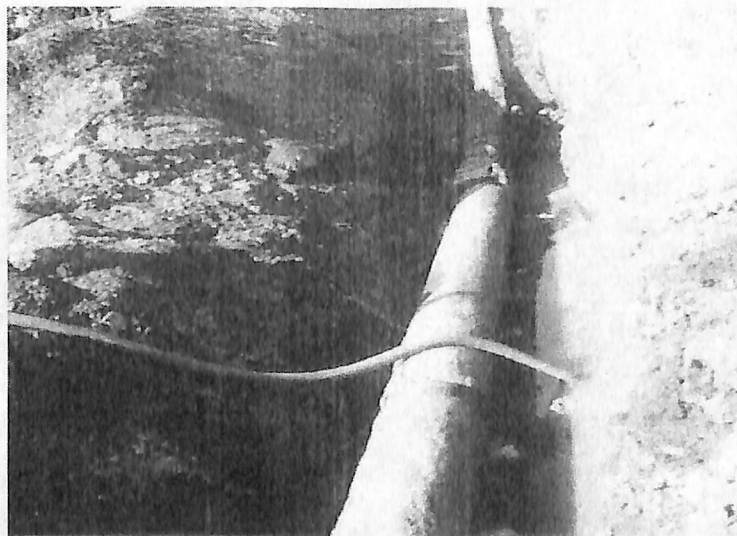


Fig: *Curing of in situ concrete coated pipeline*

TOLERANCES:

It shall be taken as per tender & IS specifications

A simple example on the calculation of Gunninging can be taken from Indian pipeline industry:

Example :

Calculate the thickness of concrete coating for the 18" diameter pipeline subjected to buoyancy due to liquefaction of soil . consider the density of pipe material to be 7800 kg/m^3 and that of concrete material is 2500 kg / m^3

Solution :

Weight of the sinker per linear meter prior to application of a protection

$$G_L = \frac{\pi}{4} \{0.457\}^2 \times 1000 \text{Kgf / m}^3 = 164 \text{Kgf} = 1608.88 \text{N} = 1.608 \text{KN}$$

Weight of the concrete coated pipe:

$$G_B = G_1 + G_2$$

$$= \text{Weight 1 (Steel pipe + P.E.coating) + Weight 2 protection}$$

Nominal thickness has to be more than 35 mm.

$$G_1 = \frac{\pi}{4} (0.457)^2 \times 7800 \text{Kgf} = 1279.6 \text{kgf} = 12.55 \text{kN}$$

$$G_2 = \frac{\pi}{4} (\phi_B^2 - 0.457^2) \times 2500 \text{kgf} = 19.256 (\phi_B^2 - 0.457^2) \text{kN}$$

$$\frac{G_B}{G_L} > 1.3$$

$$\therefore \frac{19.256 (\phi_B^2 - 0.457^2)}{1.608} > 1.3$$

$$\therefore \phi_B > 526 \text{mm (approx)}$$

$$\therefore t = \frac{\phi_B - 457}{2}$$

$$\therefore t > 35 \text{mm}$$

Where, f_B = average outer diameter of the pipe after the application of the protection (based on at least 5 measurements)

f_L = coated steel pipe.

So, as per document and safety t is taken as 100 mm for all the diameter pipes in this region for every project.